KINETIC FACADES FOR MAXIMIZING HUMAN COMFORT AND INCREASING SPACE USE EFFICIENCY IN HIGHLY GLAZED BUILDING INTERIORS

A THESIS SUBMITTED TO
THE GRADUATE SCHOOL OF NATURAL AND APPLIED SCIENCES
OF
MIDDLE EAST TECHNICAL UNIVERSITY

BY

ILGIN BÜKE ULULAR

IN PARTIAL FULFILLMENT OF THE REQUIREMENTS
FOR
THE DEGREE OF MASTER OF SCIENCE
IN
BUILDING SCIENCE IN ARCHITECTURE

DECEMBER 2022

Approval of the thesis:

KINETIC FACADES FOR MAXIMIZING HUMAN COMFORT AND INCREASING SPACE USE EFFICIENCY IN HIGHLY GLAZED BUILDING INTERIORS

submitted by **ILGIN BÜKE ULULAR** in partial fulfillment of the requirements for the degree of **Master of Science** i**n Building Science in Architecture, Middle East Technical University** by,

Prof. Dr. Halil Kalıpçılar
Dean, Graduate School of **Natural and Applied Sciences** ________________

Prof. Dr. Fatma Cana Bilsel
Head of the Department, **Architecture** ________________

Prof. Dr. Soofia Tahira Elias-Ozkan
Supervisor, **Architecture, METU** ________________

Examining Committee Members:

Assist. Prof. Dr. Mehmet Koray Pekeriçli
Architecture, METU ________________

Prof. Dr. Soofia Tahira Elias-Ozkan
Architecture, METU ________________

Prof. Dr. İdil Ayçam
Architecture, Gazi University ________________

Assist. Prof. Dr. Ayşegül Tereci
Architecture, KTO Karatay University ________________

Assist. Prof. Dr. Rukiye Çetin
Architecture, Yıldırım Beyazıt University ________________

Date: 02.12.2022

I hereby declare that all information in this document has been obtained and presented in accordance with academic rules and ethical conduct. I also declare that, as required by these rules and conduct, I have fully cited and referenced all material and results that are not original to this work.

Name Last name: Ilgın Büke Ulular

Signature :

ABSTRACT

KINETIC FACADES FOR MAXIMIZING HUMAN COMFORT AND INCREASING SPACE USE EFFICIENCY IN HIGHLY GLAZED BUILDING INTERIORS

Ulular, Ilgın Büke
Master of Science, Building Science in Architecture
Supervisor: Prof. Dr. Soofia Tahira Elias-Ozkan

December 2022, 154 pages

Environmental problems are one of the major concerns for the present time, and the building construction sector has a significant impact on the environment. So, existing buildings should be evaluated for efficient use. In public buildings where people can choose seats, efficient space use can decrease because of discomfort. Facades are significant to provide these conditions. Kinetic facades can be considered as an efficient option with their technological systems. In the literature, few studies are related to improving thermal and visual comfort in public buildings with large glazed areas.

This research investigates the impacts of thermal and visual comfort affecting space use in a case study building with glazed facades and the possible enhancements of applying kinetic facades. The research is based on a case study-building analysis. Climate graphs of Ankara were taken from Climate Consultant. Temperature data was collected by TESTO 405-V1. According to these results, the most uncomfortable section was selected as the focus study. The illuminance data was collected by RO 1335 lux-meter for one of the floors, and the simulations were calibrated with Velux Daylight Visualizer according to the actual results. A fixed shading and two different kinetic facades were proposed to enhance the thermal and visual comfort conditions. Kinetic morphologies were selected from the literature and optimized by Galapagos according to the illuminance data. All simulations were conducted by Ladybug and Honeybee. Operative temperature, illuminance, daylight factor, and useful daylight illuminance were simulated for all scenarios. The best result was achieved with the kinetic façade with square modules on the ground floor, with a 63% improvement in illuminance. Eventually, it was determined that the proposed kinetic morphologies have different effects on diverse floors; however, they can offer the most effective solution to improve visual and thermal comfort conditions in all scenarios.

Keywords: Kinetic facade, Thermal Comfort, Daylight Performance, Visual Comfort, Space Use

ÖZ

CAM ORANI YÜKSEK CEPHELİ BİNALARIN İÇ MEKANLARINDA İNSAN KONFORUNU EN ÜST DÜZEYE ÇIKARMAK VE MEKAN KULLANIM VERİMLİLİĞİNİ ARTIRMAK İÇİN KİNETİK CEPHE KULLANIMI

Ulular, Ilgın Büke
Yüksek Lisans, Yapı Bilimleri, Mimarlık
Tez Yöneticisi: Prof. Dr. Soofia Tahira Elias-Ozkan

Aralık 2022, 154 sayfa

Günümüzdeki en büyük endişelerden birisi çevresel sorunlardaki artıştır. İnşaat sektörünün bu konuda büyük bir etkisi olduğu görülmektedir. Bu nedenle, mevcut binalar verimli kullanım açısından değerlendirilmelidir. İnsanların oturma yerlerini seçebilecekleri kamu binalarında, konforsuzluk nedeniyle verimli alan kullanımı etkilenebilmektedir. Cepheler bu konuda önemli rol oynamaktadır. Kinetik cepheler, teknolojik sistemleri etkili seçeneklerden biri olarak kabul edilebilmektelerdir. Literatürde, cam oranı yüksek cephelere sahip kamu binalarında ısıl ve görsel konfor koşullarının iyileştirilmesiyle ilgili az sayıda çalışma bulunmaktadır.

Bu araştırma, cam oranı yüksek cephelere sahip bir vaka çalışması binasında, mekan kullanımını etkileyen ısıl ve görsel konfor koşullarının etkilerini ve kinetik cephelerin bu koşullar üzerindeki olası iyileştirmelerini incelemektedir. Araştırma, vaka binası çalışmasına dayalıdır. Ankara'nın iklim grafikleri Climate Consultant ile oluşturulmuştur. Sıcaklık verileri TESTO 405-V1 ile toplanmıştır. Bu sonuçlara göre en konforsuz sıcaklık koşullarına sahip olan bölüm odak olarak seçilmiştir. RO 1335 lüksmetre ile katlardan biri için aydınlatma verileri toplanmış ve bu sonuçlara göre simulasyonlar Velux Daylight Visualizer ile kalibre edilmiştir. Isıl ve görsel koşulları iyileştirmek için sabit güneş kırıcı ve iki farklı kinetik cephe önerilmiştir. Kinetik morfolojiler literatürden seçilmiş, aydınlatma değerlerine göre Galapagos ile optimize edilmiştir. Simulasyonlar için Honeybee ve Ladybug kullanılmıştır. Tüm senaryolar için çalışma sıcaklığı, aydınlatma, gün ışığı faktörü ve faydalı gün ışığı aydınlatması simüle edilmiştir. En iyi sonuç %63 iyileştirme oranıyla, zemin katta kare modüllü kinetik cephe ile aydınlatma için elde edilmiştir. Sonuç olarak, önerilen kinetik morfolojilerin farklı katlarda farklı etkilere sahip olduğu tespit edilmekle beraber görsel ve ısıl konforu iyileştirmek için en etkili çözümü sunabildikleri görülmüştür.

Anahtar Kelimeler: Kinetik Cephe, Isıl Konfor, Gün Işığı Performansı, Görsel Konfor, Mekan Kullanımı

To my beloved family and my dearest Pıtır

ACKNOWLEDGMENTS

I would like to express my sincerest and deepest gratitude to my thesis supervisor Prof. Dr. Soofia Tahira Elias-Ozkan for all her support during my research journey and for giving me the opportunity to conduct my research under her guidance. She encouraged me to overcome all challenges during the research and motivated me to go through them. I could not accomplish this study without her valuable comments, vision, understanding, sincerity, and trust. I learned a lot from her. I am extremely grateful and would like to thank her for all her support during this journey.

I would like to extend my sincere thanks to my examining committee members, Assist. Prof. Dr. Mehmet Koray Pekeriçli, Prof. Dr. İdil Ayçam, Assist. Prof. Dr. Ayşegül Tereci, and Assist. Prof. Dr. Rukiye Çetin for their valuable contributions, and comments.

I also would like to thank the academicians of Building Science Department of METU for giving me the opportunity to attend their lectures.

Additionally, I would like to thank my manager in Saint-Gobain Rigips, Kubilay Büyüklü, for all his support and understanding during my research journey.

I am thankful to all my friends for their endless support and friendship. They were always with me during my challenges.

Finally, I would like to present my deepest thanks to all my family members. Special thanks to my beloved mother, Gülbin Fırat Ulular, and my beloved father, Melih Ulular. They encouraged and supported me in accomplishing this study with their endless love, patience, understanding, and friendship. This journey would not be the same without them.

TABLE OF CONTENTS

LIST OF TABLES

TABLES

LIST OF FIGURES

FIGURES

LIST OF ABBREVIATIONS

ABBREVIATIONS

PV	Photovoltaic
SMA	Shape Memory Alloy
IAQ	Indoor Air Quality
UDI	Useful Daylight Illuminance
METU	Middle East Technical University
EUDI	Exceeded Useful Daylight Illuminance
NA	Not Applicable
EPW	EnergyPlus Weather
NT	No Table
CIBSE	Chartered Institution of Building Services Engineers

CHAPTER 1

INTRODUCTION

This research will focus on the thermal and visual comfort that may affect the space use in a public building with a large, glazed facade and the application of kinetic facades as a solution for optimizing them. In this chapter, the background, research problem, research objectives, research questions, hypothesis, and disposition are presented.

1.1 Background

Environmental problems have been growing day by day. The building construction sector is one of the primary sources damaging the environment. New building constructions have increased in speed in recent years (Enshassi, Kochendoerfer, & Rizq, 2014; X. Li, Zhu, & Z. Zhang, 2010; Zolfagharian, Nourbakhsh, Irizarry, Ressang, & Gheisari, 2012). The environmental impact of constructing new buildings is massive, so existing buildings should be evaluated before new constructions.

It may be challenging to refurbish the existing buildings with green strategies; however, by refurbishment, indoor environmental quality and, as a result, occupants' satisfaction can be enhanced (Ardente, Beccali, Cellura, & Mistretta, 2011; Zhou, S. Zhang, Wang, Zuo, He, & Rameezdeen, 2016). In addition to that, refurbishment is less harmful to the environment in comparison with new construction (Alba-Rodríguez, Martínez-Rocamora, González-Vallejo, Ferreira-Sánchez, & Marrero, 2017; Hasik, Escott, Bates, Carlisle, Faircloth, & Bilec, 2019; Schwartz, Raslan, & Mumovic, 2018).

On the other hand, when refurbishing or designing a building, providing comfort conditions is necessary for a healthy indoor environment. In the four aspects of comfort conditions, thermal, visual, acoustic, and respiratory comfort, occupants prioritize thermal comfort (Frontczak & Wargocki, 2011; Song, Mao, & Liu, 2019). Therefore, it may affect the efficiency of space use and the building’s utilization.

Besides all these, as a regulator and interface between the interior and exterior environment, facades are essential building elements (Nady, 2017; W. T. Sheikh & Asghar, 2019; Zuk & Clark, 1970). Kinetic facades can respond to different climatic conditions; therefore, they can provide maximum occupant comfort in a more energy-efficient way (Shahin, 2019). Hence, instead of using static facade systems, kinetic facades with their moveable elements can be helpful to improve thermal and visual comfort by responding to different environmental and climatic conditions; therefore, it may enhance the building's utilization (Elmokadem, Ekram, Waseef, & Nashaat, 2018; Mahmoud & Elghazi, 2016; Matin & Eydgahi, 2019; Nady, 2017; Nielsen, Svendsen, & Jensen, 2011; Zuk & Clark, 1970).

1.2 Problem Statement

In buildings with functions that allow users or occupants to choose their place in a space, they will avoid spots where they are not comfortable in terms of thermal and visual comfort. As a result, the building's space efficiency decreases; thus, the building's maximum utilization regarding space use cannot be achieved.

With the development of technology, kinetic facades can be considered one of the efficient options that can now be designed, evaluated, and implemented with the help of advanced computer systems and intelligent building technologies. Instead of static facade systems, kinetic facades, with their moveable elements, can improve thermal and visual comfort by responding to different environmental and climatic conditions.; therefore, they may enhance the building's space utilization efficiency. There are many studies related to the energy efficiency of kinetic facades and visual comfort in office buildings in the literature. However, few are related to improving thermal and visual comfort in public buildings with large, glazed areas, such as restaurants or cafeteria buildings.

1.3 Research Objectives

In the literature, research shows that kinetic facades are energy-efficient systems. In addition, they can also help provide thermal and visual comfort to occupants for more practical space use. In large public buildings with glazed facades, they can effectively provide these comfort conditions and enhance space use with the building's efficient utilization. This research aims to detect the thermal and visual discomfort conditions that may impact space use in a case study building with glazed facades and the possibility of kinetic facades to improve it.

1.4 Research Questions

According to the objectives previously mentioned, one main question and in relation to it, five sub-questions are stated in this research as given below:

Main Question:

i. What are the effects of kinetic facades on improving indoor conditions in terms of thermal and visual comfort in buildings with glazed facades?

Sub-Questions:

i. What is the ratio of glazing of the facades?
ii. Which floor levels are more uncomfortable in terms of thermal and visual comfort in the case study building?
iii. What are the orientations of the most uncomfortable spaces?
iv. What potential effect does the kinetic facade have on improving thermal and visual comfort?

v. Which morphology of the kinetic facade has the best performance for such buildings?

1.5 Hypotheses

In non-residential buildings with large glazed facades, such as cafeterias, where people have a choice of seating locations, the thermal and visual comfort may impact these preferences; therefore, the space use of buildings. Kinetic facades, with their advanced technology, can provide a solution to improve these conditions affecting space use. In this scope, this research has two hypotheses as below:

i. Hypothesis 1

H_0: There is no relationship between the application of kinetic facades and thermal and visual comfort improvement.

H_1: Kinetic facades are useful to improve thermal and visual comfort.

ii. Hypothesis 2

H_0: There is no relation between the morphology of kinetic facades and thermal and visual comfort improvement.

H_2: Different facade morphologies have an impact on the thermal and visual comfort results.

These hypotheses are tested by measuring current thermal and visual comfort conditions, and the facade morphology selected from the literature is simulated using appropriate software.

1.6 Dispositions

This study consists of five chapters.

In the first chapter, after brief background information, the research problem, research objectives, research questions, and hypothesis are explained.

The second chapter presents an overview of the construction industry's environmental impacts and the comparison of building refurbishment and new construction. Afterward, the comfort aspects are introduced, and two focus aspects of this study, thermal and visual comfort, are explained. Then, the kinetic architecture and its evolution are covered. Finally, the kinetic facades are discussed with their functions and performance, environmental factors for the design, and evaluation.

In the third chapter, the research materials and methodology are discussed. The current comfort conditions are analyzed as an initial step. Afterward, facade morphologies in the literature are investigated for implementing the modules. The design case is proposed according to these investigations, and simulations are run accordingly. Since the methodology is mentioned in this chapter, the software used for the simulation and models is also indicated.

The fourth chapter presents and discusses the results of TESTO 405-V1 and simulations. Six dining halls are simulated for thermal and visual comfort. Furthermore, the evaluation of the applied kinetic facade morphology is compared with the base case scenarios of six dining halls, and improvements in comfort conditions are discussed.

The fifth chapter shows the conclusion of the study. The important derivations and future study recommendations are presented.

CHAPTER 2

LITERATURE REVIEW

This chapter focuses on the existing publications in relation to the scope of this study. Firstly, the construction sector's environmental impact and the comparison of building refurbishment and new construction are presented. Then, the comfort aspects are introduced, and thermal and visual comfort are explained in more detail since they are the focus of this study. Afterward, kinetic architecture is illustrated. Lastly, discussed as an offer to improve thermal and visual comfort in the case building, kinetic facades are discussed.

2.1 Environmental Impacts of Building Construction

The building construction sector significantly impacts the environment by causing water, soil, air pollution and risky working areas. Public health, resources, and majorly 65-67.5% of the ecosystem's total impact are damaged by it (Enshassi et al., 2014; X. Li et al., 2010; Zolfagharian et al., 2012). This environmental damage is increasing day by day since new buildings are constructed countlessly (Zolfagharian et al., 2012).

Because of the considerations related to climate change and environmental problems, it is critical to convert the existing buildings to have more sustainable cities and countries (Lee, Wargocki, Chan, Chen, & Tham, 2020; Zhou et al., 2016).

2.2 Environmental Impact Evaluation of Refurbishment

Lee et al. (2020) claim that applying green strategies to an existing building can be challenging regarding physical, economic, and operational limits. As a result of their study, implementing “Green Marking Standards” to both existing and new buildings can be effective in improving indoor environmental quality, even though there is a challenge for existing buildings.

Improving the building envelope has one of the most significant retrofitting process outcomes (Ardente et al., 2011; H. M. Teamah, Kabeel, & M. Teamah, 2022). The study of Zhou et al. (2016) shows that users' satisfaction levels in thermal, visual, and acoustic conditions have been enhanced after the refurbishment of an office building.

Hasik et al. (2019) state that renovating a building is approximately three-quarters less harmful than constructing a new one in terms of environmental impact.

Refurbishment of a building can also provide a decrease in cost and environmental impacts simultaneously compared to the new construction and demolition. “Ecological Footprint” of refurbishing energy consumption is lower than the new construction, as seen in Figure 2.1 (Alba-Rodríguez et al., 2017).

Schwartz, Raslan, and Mumovic (2018) mention the difference between new construction and refurbishments in terms of carbon footprint instead of energy. Their research shows that even though some new buildings have a lower carbon footprint than refurbished ones, overall, refurbishing buildings perform better than constructing new ones (Schwartz et al., 2018; H. M. Teamah et al., 2022).

2.3 Comfort Aspects in Buildings

Comfort is a significant issue in the buildings’ indoor environmental quality. Buildings should be assessed according to comfort requirements to provide healthy and convenient spaces for occupants.

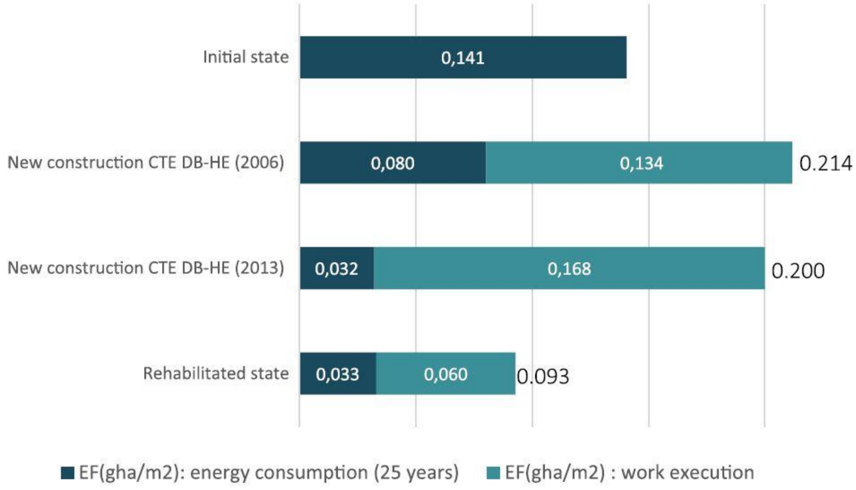

Figure 2.1. Environmental Impact Comparison of Refurbishment and New Construction in terms of Total Ecological Footprint (Alba-Rodríguez et al., 2017)

Comfort conditions can be related to both physical and chemical factors. It is also not only associated with physical parameters; it can also be subjective. However, in the literature, many studies show that environmental factors are influential in human comfort (Frontczak & Wargocki, 2011). There are four main comfort aspects in buildings which are thermal, visual, acoustic, and respiratory comfort, which can be seen in Figure 2.2 in relation to their corresponding environmental factors (Song, Mao, & Q. Liu, 2019).

Amongst these four comfort aspects, thermal and visual ones are explained in the below section since they are in the scope of this research.

2.3.1 Thermal Comfort

Thermal comfort is defined as “that condition of mind that expresses satisfaction with the thermal environment” (ASHRAE Standard 55-2017, 2017).

According to the research done by Frontczak and Wargocki (2011), indoor environmental quality is majorly affected by thermal comfort; hence, thermal comfort is one of the most significant factors for human satisfaction and should be a priority.

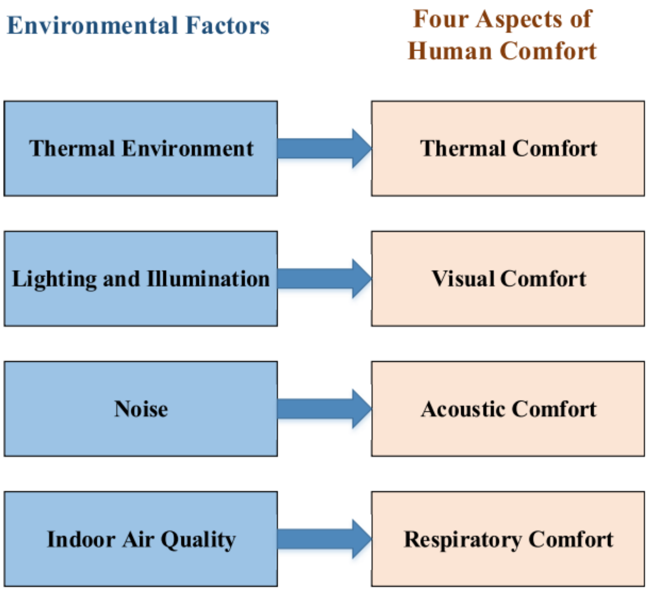

Figure 2.2. Comfort Aspects and Corresponding Environmental Factors (Song et al., 2019)

Building type and seasonal changes have an impact on thermal comfort. Since it is affected by building type, it should be considered specific to the building function to obtain a proper thermal comfort condition. Additionally, seasonal changes and temperature differences between different seasons should be observed, and the differences in a day (Frontczak & Wargocki, 2011).

According to the ASHRAE Standard 55-2017 (2017), for an acceptable thermal conditions in a building, there are six factors that should be taken into consideration as follows:

- Metabolic rate
- Clothing insulation

- Air temperature
- Radiant temperature
- Air speed
- Humidity

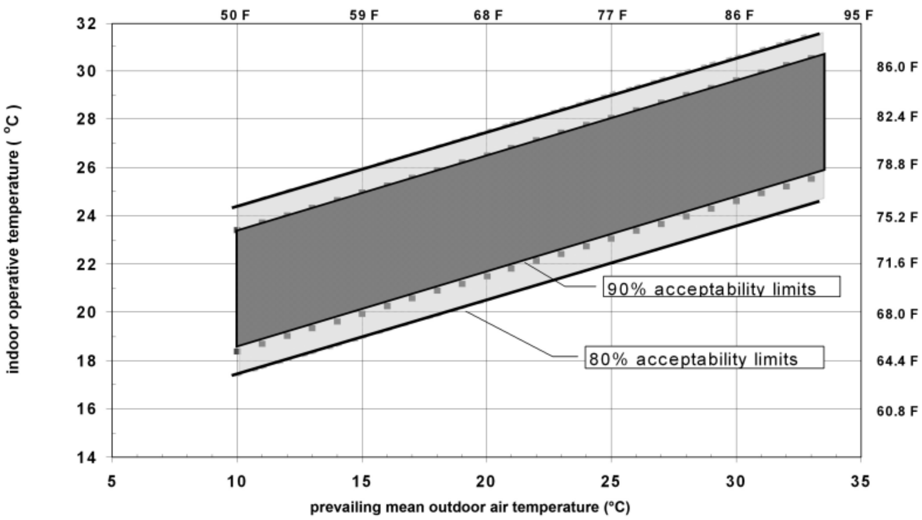

Figure 2.3 For the buildings that have natural ventilation, acceptable operative temperatures ranges (ASHRAE Standard 55-2017, 2017)

The acceptable range of operative temperatures for naturally conditioned buildings can be calculated according to the graphic shown in Figure 2.3. According to the representation, the standards explain that limit of %80 acceptability can be used to detect the proper indoor operative temperature value (ASHRAE Standard 55-2017, 2017).

The operative temperature has a definition for the acceptable thermal conditions as a range to define a zone that is comfortable for people (ASHRAE Standard 55-2017, 2017). The operative temperature range should be 24.5 °C ± 1.5 °C, as stated in ISO 7730 (2005).

2.3.2 Visual Comfort

EN 12665 defines visual comfort as "a subjective condition of visual well-being induced by the visual environment" (Frontczak & Wargocki, 2011). There are three human needs to determine lighting conditions: visual comfort, performance, and safety. Luminance distribution, illuminance, glare, the directionality of light, color rendering, and color appearance of the light, flicker, and daylight are the parameters to detect the luminous environment (EN 12464-1, 2002).

Distance to the glazed area and the window configuration affect the occupant's visual comfort and satisfaction in the interior space; thus, visual comfort should be considered accordingly (Kong, Utzinger, Freihoefer, & Steege, 2018; Korsavi, Zomorodian, & Tahsildoost, 2016).

Useful daylight illuminance (UDI) is a parameter under realistic sky conditions. Meteorological datasets produce UDI based on absolute value time series over a year (Nabil & Mardaljevic, 2005). The research conducted by Nabil and Mardaljevic (2005) analyzed published field works and surveys to observe the efficient UDI range. The results show that 500 lux to 2000 lux is an acceptable range. In addition, 100 lux is low, and people do not find it tolerable, while values above 2000 lux are uncomfortable (Nabil & Mardaljevic, 2005). In the literature, it is observed that some of the research related to UDI shows this metric can be considered as 50% of the year should be in the range of indicated threshold (Nabil & Mardaljevic, 2005; Shafavi, Tahsildoost, & Zomorodian, 2020).

According to the Chartered Institution of Building Services Engineers (CIBSE) Lighting Code (W. Wu & Ng, 2016), 300 lux should be the minimum value for the study areas. EN 12464-1 (2002) defines 200 lux as the minimum for a "self-service restaurant."

Daylight factor is a definition in percentage. It is a ratio between indoor and outdoor illumination that is horizontal. A continuously overcast sky is the condition of daylight factor (Müeller, 2013). Mehdizadeh, Ahadi, Masoumi, and Maleki (2014) claim that the daylight factor has different values according to UK Building Research Energy Conservation Support Unit. The acceptable range for a window to provide sufficient daylight is between 2% and 5%. Darker points occur if this factor is below 2%, which requires artificial lighting most of the time, while the amount of daylight is sufficient at a level that does not require much artificial lighting if it is above 5% (Mehdizadeh et al., 2014). Correlatively, 2% of daylight factor should be provided as the minimum value according to the Leadership in Energy and Environmental Design Certificate (United States Green Building Council, n.d.).

2.4 Comfort Conditions in Kinetic Architecture

“Architecture is not static, as has traditionally been the case, but one that has the capability of adapting to change through kinetics.” (Zuk & Clark, 1970, p. 4)

Architecture should provide safe shelter to humans. However, the needs of humans have changed. Therefore, buildings should also be adapted to this change, which means their function must not be limited to this definition. Since communities are dynamic, architecture should also be dynamic to respond to their needs, which can be achieved by implementing kinetics in architecture. Otherwise, it cannot be able to meet the requirements of society. The buildings' form should change their shape under different pressures to provide user satisfaction (Zuk & Clark, 1970).

Trubiano’s study (2013) (Elmokadem et al., 2018) also shows that rather than static forces, dynamic ones such as time, weather, functions, and human needs affect the buildings; hence, the buildings that can adapt themselves into climatic changes energy are needed.

Elmokadem et al. (2018) claim that the construction of buildings with transformative and automated components is the idea behind kinetic architecture. The buildings shift their shapes to respond to the needs of the people and adapt to the environment.

Since providing a comfortable place where humans can be protected from environmental conditions is the fundamental goal of architecture, the building envelope is the primary consideration in achieving this goal. Moreover, one of the most critical elements of the building is the facades (Nady, 2017).

2.4.1 Development of Kinetic Systems

Ramzy and Fayed (2011) claim that kineticism is not a very new term for architecture. However, kinetic architecture, as a concept, is newer. It has been a widespread discussion mostly in the last decades. The futuristic designs became a factor affecting the concept with their moveable, dynamic, and high-speed characteristics.

Elmokadem et al. (2018) argue that kinetic design was originally developed in 1908. Randl's study (2008) shows that in 1908 Rotary building was designed by Thomas Gaynor as an initial kinetic concept and Alter's study (2017) states that Villa Girasole was designed by Angelo Invernizzi in 1935 as another residence. Afterward, Emanuel (2016) points out that as a moveable architecture, "Spatial Town" was introduced in the 1950s by Yona Friedman, who also explained a manifesto called Mobile Architecture one year earlier Issues in Construction and Refurbishment (Elmokadem et al., 2018).

Dynamic concepts mostly caught attention in the 1960s and 1970s with the development of computer technologies and their integration into building technology. As a result, architecture evolved from a static structure to a dynamic one (Elmokadem et al., 2018). In the 1960s, Fun Palace, designed by Cedric Price, was the earliest and most important example in the field. Moveable spaces were introduced with this project (Alotaibi, 2015; Elmokadem et al., 2018). In 1967, moveable architecture, which is a city that can walk, was introduced by the team of Archigram (Alotaibi, 2015; Fortmeyer & Linn, 2014).

In the last half of the 20th century, since electronics and digital systems were developed, systems of kinetic architecture also gained further qualifications.

Afterward, with the development of artificial intelligence, dynamic systems became more advanced (Ramzy & Fayed, 2011).

Elmokadem et al. (2018) claim that kinetic architecture with high technology is constitutively developed in the twenty-first century. Many buildings in the kinetic concept were designed and constructed sin that century.

According to Shafaghat and Keyvanfar (2022), since moveable facades can reduce energy consumption and emissions, it becomes more significant with the latest commitments related to climate, such as Kyoto Protocol.

2.4.2 Kinetic Typologies in Architecture

According to Fox and Miles, *"One who puts in motion"* is the corresponding phrase for kinetic in Ancient Greek (Di Salvo, 2018).

Three typologies for kinetic systems Figure 2.4, which are embedded, deployable, and dynamic, are introduced by Fox and Kemp (Fox & Kemp, 2009).

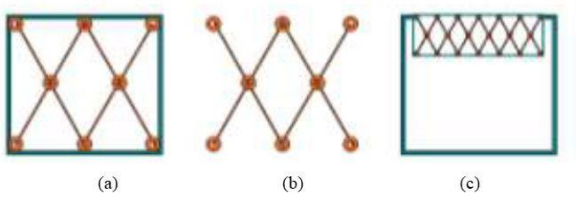

Figure 2.4. Kinetic typologies embedded (a), deployable (b), and dynamic (c) (Elmokadem et al., 2018)

The aim of embedded kinetic systems, which are fixed in a location and an essential component of a building, is to give a response to changes by regulating a larger system or a building. This type is a more developed system than the deployable and dynamic structures (Fox & Kemp, 2009).

The entire building's inherent flexibility can be provided by deployable systems, which are also a part of a larger architectural structure. Deconstruction and reconstruction are permitted by this system in a fixed structure (Fox & Kemp, 2009).

The most known typology of this classification is dynamic kinetic structures, which are also a part of a larger system like embedded and deployable kinetic systems. However, even if it is a part of an integral system, it does not act dependently in this context. Typical building elements, including escalators, doors, and windows, can exemplify this kinetic system. There are three subcategories of dynamic kinetic structures, which are mobile, transformable, and incremental systems (Fox & Kemp, 2009).

According to Fox and Kemp (2009), subcategories of dynamic kinetic structures can be defined as the following:

> Mobile systems would include all types that can be physically moved about within an architectural space to a different location. Transformable structures are those that can change to take on different spatial configurations and can be used for space saving and utilitarian needs. Incremental systems can be added to or subtracted from, like LEGO pieces, to create a larger whole out of discrete parts. (p.48)

2.4.3 Transformation Types

Facade panels can shift their shapes based on geometrical change and material deformation. As shown in Figure 2.5, four different changes are defined by Moloney (2011). The three geometric transformations in space are translation, rotation, scaling, and movement via material deformation." (Moloney, 2011, p. 7).

The first movement type is translation. It is defined as when the elements of kinetic facades move in a steady and horizontal direction. The movement occurs around a centerline, and it is the second typology, which is called rotation. The third one is scaling, which is a system that provides panel movement by expanding and shrinking. The last one is actualized by the flexibility and elastic properties of the selected material of the panels (Moloney, 2011).

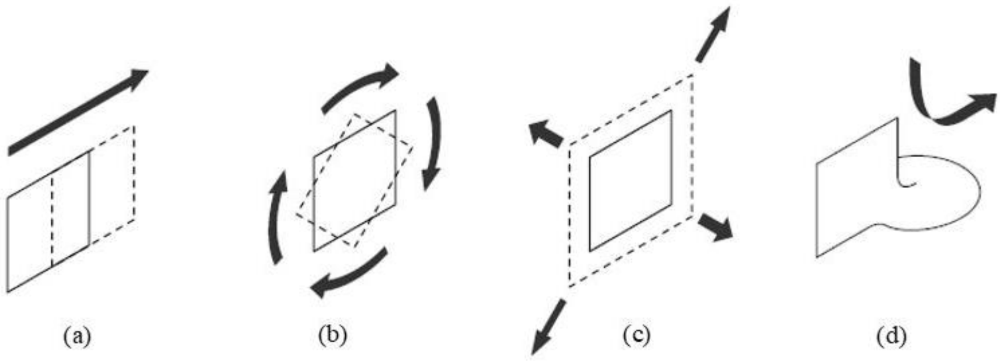

Figure 2.5. Transformation types which are translation (a), rotation (b), scaling (c) and material deformation (d) (Moloney, 2011)

2.5 Kinetic Facades

In buildings, facades are one of the crucial elements in order to enhance the performance of the building as a result of their function as an interface between the exterior and interior conditions (Nady, 2017; W. T. Sheikh & Asghar, 2019; Zuk & Clark, 1970). Facades have gained the ability to adapt their behavior and functions according to environmental conditions and user requirements by virtue of the implementation of developed technologies into their system (Matin & Eydgahi, 2019).

2.5.1 Environmental Factors Effect Design

i. Sun’s Position

The usage of elements such as dynamic louvers or overhangs can be effective in regulating the energy that is gained from the sun. By using these elements, solar radiation can be controlled automatically (Kensek & Hansanuwat, 2011).

Temperature is one factor in relation to the sun’s position. Formentini and Lenci (2018) express that in order to design a ventilated facade, kinetic panels can be used, which are activated by exterior temperatures. According to their research, the designed kinetic panel with SMA wires can respond to these environmental temperatures. As a result, kinetic panels are closed during winter to provide heating, while in summer, they are opened to provide cooling, as shown in Figure 2.6.

Another factor affected by the sun is the light conditions. Static elements for shading can be effective according to climate conditions. However, even if these can protect the interior of the building from excess daylight, their efficiency is limited (Kensek & Hansanuwat, 2011).

Research by Hosseini, Mohammadi, and Guerra-Santin (2019) shows that the sun's position can be a trigger for the movement of kinetic panels. The proposed facade system has a hierarchical structure that aims to provide visual comfort by combining daylight and user position, which can be seen in Figure 2.7. Direct sun radiation is also reduced as an inherent result of its shape, which provides self-shading (S. M. Hosseini et al., 2019).

The study by Fakourian and Asefi (2019) also shows that sunlight can be a factor for moveable panels to change their shapes.

Designed by Jean Nouvel in 1988, Institut du Monde Arabe is a leading example of a kinetic facade that moves according to light conditions. It has panels shaped like camera lenses with an opening and closing mechanism, as seen in Figure 2.8. By doing that, the amount of lighting coming into the building can be controlled by this dynamic facade system (Nady, 2017).

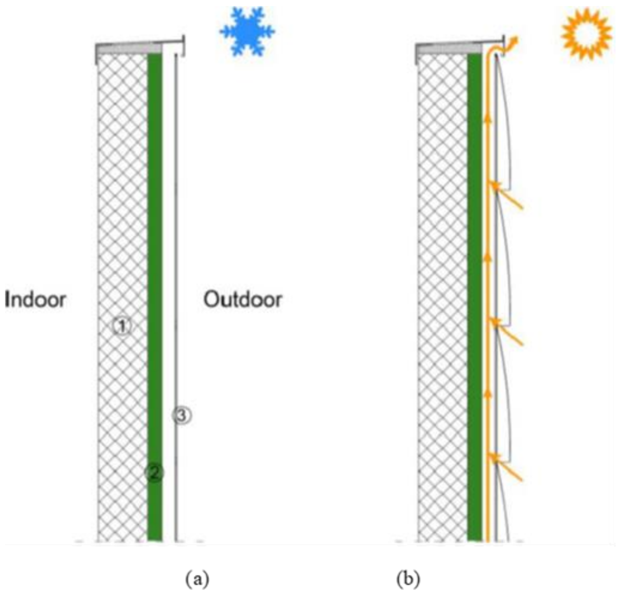

Figure 2.6. Schematic Illustration of the Designed Ventilated Facade of in winter, panel closed (a) and in summer, panels open (b) (Formentini & Lenci, 2018)

ii. Ventilation

Kinetic facades can also provide natural ventilation and night cooling with their movement mechanism. For example, as shown in Figure 2.9, in the facade of Al Bahar Towers, with the actuators of the kinetic facade mechanism, windows can open automatically for natural ventilation. The building can be cooled during the night by using this air movement (Alotaibi, 2015).

The wind is the critical factor in the kinetic movement for ventilation. Its direction is important, as well as its velocity. Since these two parameters cannot be foreseen, designing a moveable facade for ventilation can be more problematic than the ones for daylight or temperature (Kensek & Hansanuwat, 2011).

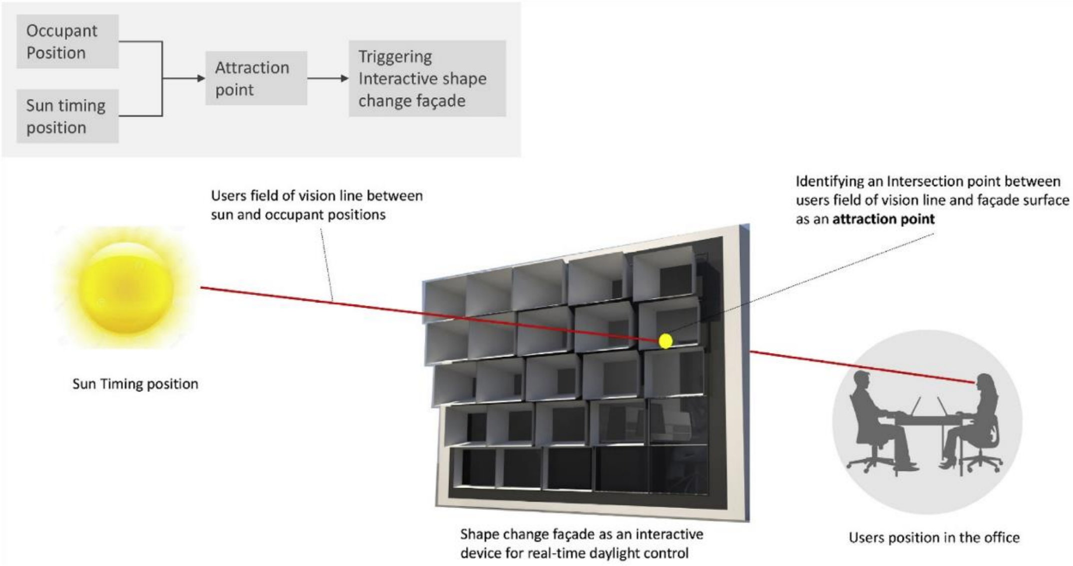

Figure 2.7. Sun position and user behavior as factors that affect shape changes (S. M. Hosseini et al., 2019)

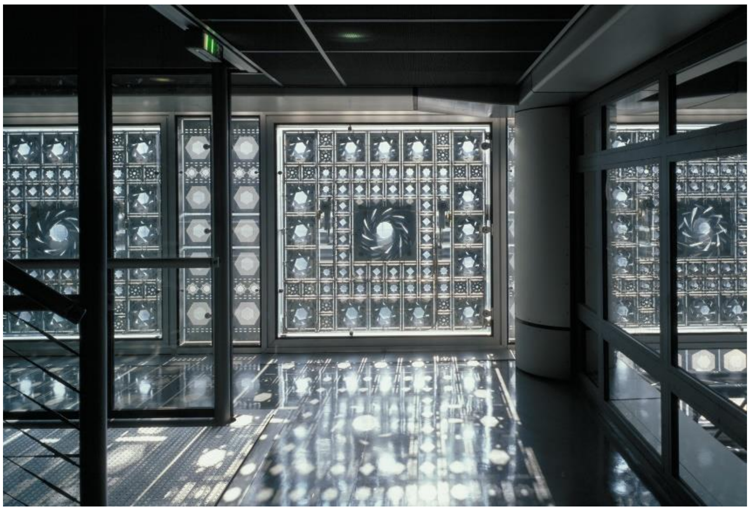

Figure 2.8. The facade system, like the camera lenses of Institut du Monde Arabe (Schielke, 2014)

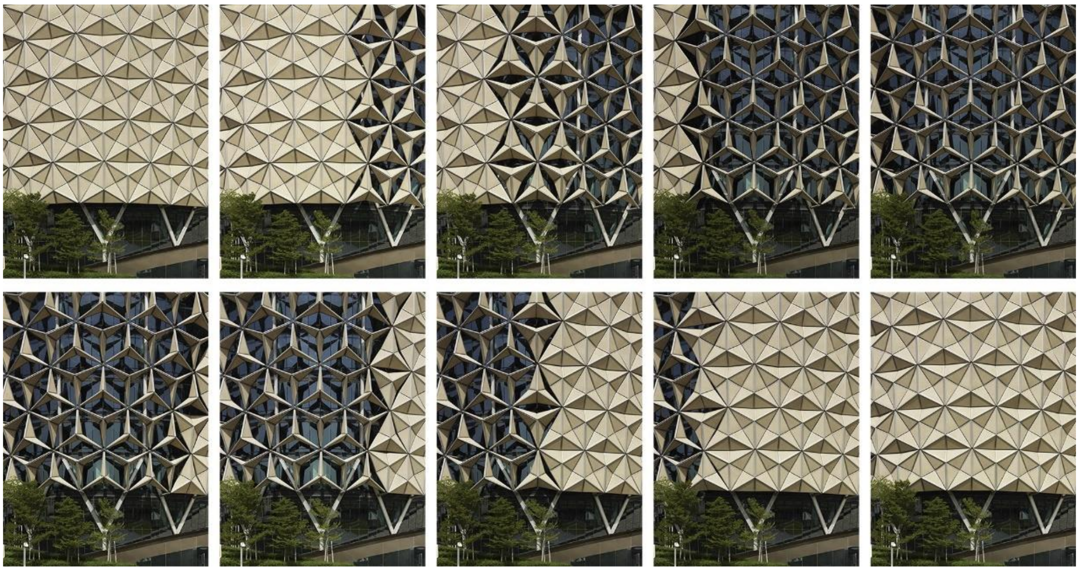

Figure 2.9. The facade system of Al Bahar Towers allowing ventilation with its opening and closing mechanism (Schielke, 2014)

2.5.2 Functions

The building envelope is significant due to the fact that it is the element of a building that interacts with the exterior conditions (Nady, 2017). Elmokadem et al. (2018) state that a building envelope's function is to regulate indoor climate conditions while sustaining internal comfort.

As an element of the building envelope, the facade is valued in terms of both aesthetics and performance. Since a building's skin is the part of a building that attracts attention, firstly, it should be designed considering that fact (Nady, 2017). On the other hand, the more advanced system a facade has, the more effective protection it will provide by filtering the exterior weather conditions. Providing occupant comfort should be the main goal of a dynamic facade. By achieving this goal, users can work more efficiently (Alotaibi, 2015).

Soyluk and Sarıcıoğlu (2015) state that kinetic facades can provide an aesthetic view with their different shapes from the outside of the building while they provide sound or thermal insulation for the interior with their dynamic structure.

Kinetic facades are able to give a response to environmental conditions such as temperature, light, and wind by collecting data from sensors and moving by using control switches and actuators (Dewidar, K., Mahmoud, A. H., Magdy, N., & Ahmed, 2010).

Matin and Eydgahi (2019) claim that facades have gained the ability to adapt their behavior and functions according to environmental conditions and user requirements by virtue of implementing developed technologies into their system.

According to the study by Fakourian and Asefi (2019), educational buildings have majorly wide glasses as a facade typology since the penetration of natural lighting is essential for classes and provides user comfort. On the other hand, using wide glass windows can cause a negative effect. This can be prevented by controlling natural lighting and ventilation with the design of kinetic facades. Kinetic panels can also be designed in different configurations, responding to different environmental conditions for each facade.

2.5.3 Performance and User Satisfaction

According to Fakourian and Asefi (2019), since both occupants' needs and designers' goals can be achieved more sustainably, the usage of dynamic facades systems is ever-increasing. For example, a comfortable indoor environment can be provided in educational buildings by designing an adaptable facade that controls heat and light (Fakourian & Asefi, 2019). However, since there is an interaction between interior and exterior spaces, providing optimized conditions for visual and thermal comfort, which conflict with each other simultaneously, is not easy (S. M. Hosseini et al., 2019). Nielsen et al. (2011) claim that thermal comfort and visual indoor environmental conditions simultaneously with occupant comfort can only be provided and qualified at a room-scale.

i. Thermal Comfort

Research by Fakourian and Asefi (2019) shows that penetration of the sun and temperature can be controlled in an educational building by kinetic panels with their opening and closing mechanism to provide occupants' comfort.

According to the study results by Kensek and Hansanuwat (2011), a kinetic facade with moveable shading elements independent of the shading system can perform 30% better than a system that has no shading in an office building.

ii. Daylight and Visual Comfort

Kinetic facades are significant in providing daylight and visual comfort simultaneously for occupants in an office building (Bakker, Hoes-van Oeffelen, Loonen, & Hensen, 2014; S. M. Hosseini et al., 2019). According to their research, three different facade systems based on daylight and occupants' engagement were designed to provide visual comfort, and their performance was assessed by computer simulations. As it can be seen in Figure 2.10, a plane window as a static facade, two-dimensional shape changes facade as an automatic facade, and three-dimensional shape changes facade as an interactive facade were compared after simulations. According to the simulation results, plain windows cannot efficiently provide visual comfort, while two-dimensional and three-dimensional changes provide better results. However, the difference between two-dimensional and three-dimensional shape changes is also remarkable. Since three-dimensional shape changes have both scaling and translating movement capability with their hierarchical configuration, they provide more useful daylight and enhanced visual comfort (S. M. Hosseini et al., 2019).

W. T. Sheikh and Asghar (2019) claim that designing a facade that is effective in reducing energy consumption can decrease visual comfort conditions in the interior space. However, they found that an adaptive facade with horizontal and vertical movement inspired by biomimicry in a highly glazed office building can effectively reduce energy consumption and simultaneously protect visual comfort. They are inspired by the Oxalis oregana leaf, as shown in Figure 2.11, tracking the sun's path and adapting itself accordingly.

Fakourian and Asefi (2019) also mention that kinetic facade systems are able to control the light that is coming from the sun; thus, comfort requirements for occupants can be achieved by their moveable mechanism. A kinetic system with vertical louvers can work 55% more efficiently than the other systems. These kinetic facades can control excess daylight, and the recommended range can be provided for daylight penetration (Kensek & Hansanuwat, 2011).

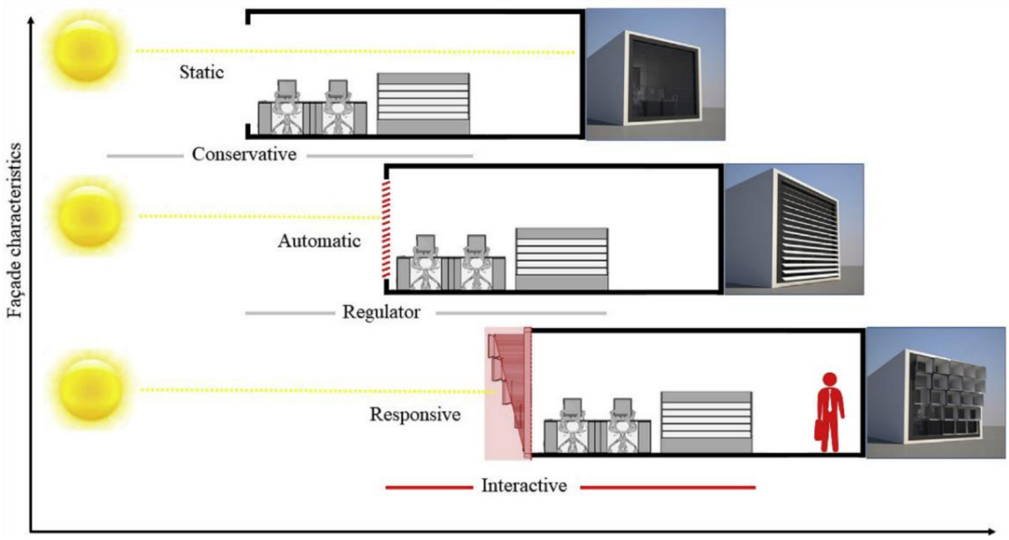

Figure 2.10. Different facade functions and the relationship with the sun and user behavior (S. M. Hosseini et al., 2019)

Mahmoud and Elghazi (2016) compare two motion typologies for an office building, rotation, and translation, to observe which is more effective for daylight performance. Results show that both typologies improved the daylight conditions; however, rotation motion performed better than translation (Mahmoud & Elghazi, 2016). Tabadkani, Roetzel, Li, & Tsangrassoulis (2021) also claims that in office buildings, hexagonal adaptive systems defined as Kaleidocycle can provide maximum visual comfort level based on the users' preferences for future smart envelopes.

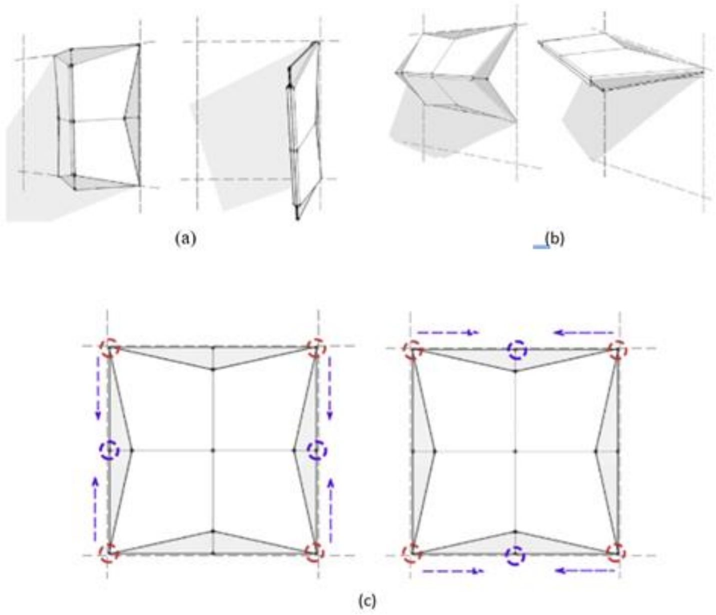

Figure 2.11. Horizontal shading (a), vertical shading (b), and kinematics (c) of Oxalis Oregana-inspired facade morphology (W. T. Sheikh & Asghar, 2019)

2.5.4 Kinetic Movement Technologies

Zuk and Clark (1970) state that the logic behind kinetic structures is very similar to the system of the human body. According to this, actuators are like muscles and tendons which provide and control the body's movement, and sensors are represented by eyes, which transmit signals from the external surroundings. The working principle and components of kinetic architecture can be arranged based on this natural system of the human body (Zuk & Clark, 1970).

Since computational technology has developed in the last years, usage of these technologies has become inevitable (Elmokadem et al., 2018; Ramzy & Fayed, 2011). Fox and Kemp (2009) state that "A kinetic environment without the computation is like a body without a brain: incapable of moving." (2009, p. 58). By using technological systems such as sensors and processors, kinetic architecture can gather information about environmental conditions. As a result, it can control and respond to these conditions (Fox & Kemp, 2009).

Kinetic facades are not simple since they have many components and movement systems. However, according to Pesenti, Masera, Fiorito, and Sauchelli (2015), nature-inspired movement designs and modules are less energy consumption as they are already a natural mechanism (Pesenti et al., 2015).

i. Sensors

Kinetic facades have moveable elements and make this movement according to the information collected from environmental conditions. So, these facades should have a device to understand these conditions and gather information, called sensors. The sensor can be used as that first step. They can collect data from exterior conditions such as temperature, light, and wind. By using that data, dynamic facades can change shapes to adapt to environmental conditions to prevent undesired situations such as extra daylight penetration, solar heating, and excess cooling (Fakourian & Asefi, 2019; Fox & Kemp, 2009)

ii. Actuators

Addington and Schodek (2004) state that input energy conversion from a signal coming from the sensors into action is actualized by an actuator. There is a variety of systems of actuators for a specific movement (Matin & Eydgahi, 2019).

According to Kolarevic and Parlac (2015) and Matin, Eydgahi, and Shyu (2017), there is a classification for actuating technologies which are mechanical, electrical, pneumatic, and hydraulic actuators (Matin & Eydgahi, 2019).

Linear actuators can be used in dynamic facades that track the position of the sun and arrange themselves according to it. Therefore, these facades, with their movement, can protect the interior of the building from extra light and glare as is designed for the facade of Al Bahar Tower. Additionally, to provide automatic movement for the windows of the facade for ventilation, an automatic actuation system is used to create movement (Alotaibi, 2015).

iii. Energy Supply of Control Systems

The control mechanism of kinetic panels requires energy. Photovoltaic (PV) panels implemented on the roof of a building can supply the power needed to move kinetic panels when the sun is in the sky. Additionally, the energy demand for the movement of components can be provided by inserting PV cells into the panels (Fakourian & Asefi, 2019).

iv. Material-Based Technologies

Automated facade technologies are often used in buildings; however, using smart materials is not very common (Böke, Knaack, & Hemmerling, 2020).

Formentini and Lenci (2018) point out that using Shape Memory Alloy (SMA) wires as an actuator and thermal sensor provides movement to a kinetic facade panel without an energy supply which has been significant in the last decades since energy consumption has been increasing. SMA can change its shape under different temperature conditions. When the temperature is low, deformation occurs. On the contrary, when it is heated, the original form returns (Fakourian & Asefi, 2019; Pesenti et al., 2015).

Formentini and Lenci (2018) state that Nitinol consisting of Nickel and Titanium is generally preferred as an SMA wire since it is a biocompatible, ductile, corrosion-resistant, and high-shape recovery metal alloy. They point out that aluminum can be chosen to design a kinetic panel for the experiment of ventilated facades due to its cost efficiency, thermal inertia, flexibility, and thickness variations. In their experiment, a rectangular aluminum panel with L-shaped aluminum profiles is used, as seen in Figure 2.12. As previously mentioned, SMA wires were connected to these panels to move the panel. An industrial hair dryer for summer conditions and a cooling spray for winter conditions is chosen in order to observe the wires' deformation and panels' movement under low and high temperatures (Formentini & Lenci, 2018).

In the research by Kensek and Hansanuwat (2011), a kinetic overhang system is proposed. The physical model consists of a structural frame and panels that can be bent. As shown in Figure 2.13, aluminum is chosen as the material (Kensek & Hansanuwat, 2011).

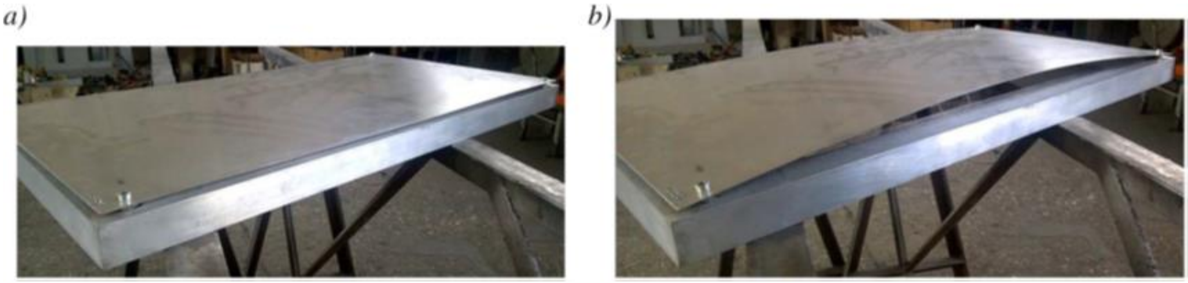

Figure 2.12. Physical model by using aluminum sheets and closed (a) and opened (b) positions (Formentini & Lenci, 2018)

2.5.5 Digital Tools to Design and Evaluate Kinetic Facades

In order to evaluate daylighting performance and create energy models for kinetic facades, software such as Rhinoceros, Grasshopper, and Diva can be utilized by using the website of EnergyPlus to obtain weather data for a specific location (S. M. Hosseini et al., 2019; Tabadkani et al., 2021). In addition to that, another simulation program, which is called eQuest and Autodesk's 3ds Max Design, can also be helpful for daylight simulations. WinAir4 is the software that provides simulations for ventilation. A model from Ecotect can be created, and this model can be imported to

WinAir. Solar Advisor Model from the National Renewable Energy Laboratory can be chosen to simulate energy production (Kensek & Hansanuwat, 2011).

Figure 2.13. Physical model of proposed panel system (Kensek & Hansanuwat, 2011)

Tabadkani, Valinejad Shoubi, Soflaei, and Banihashemi (2019) mention Grasshopper's Honeybee Plug-in for grid-based daylight simulation and Ladybug for analysis of the selected sky conditions' cloud coverage is used.

Arduino, an open-source programming language, Parallax's Basic Stamp, Sx-Key, and Propellor can be chosen to program the devices that can connect the software and the hardware of the designed system (Fox & Kemp, 2009).

2.5.6 Evaluation of Kinetic Facades

Altın and Orhon (2016) argue that adaptive facades can reduce energy consumption by responding and adapting to the exterior environmental conditions without decreasing indoor environmental quality.

There are many advantages of that dynamic facade, including controlling sunlight, providing thermal insulation, and adapting to different climatic conditions. As a result of these benefits, they are useful to reduce energy consumption and provide occupants' comfort. (Fakourian & Asefi, 2019; Nielsen et al., 2011)

Kinetic facades give an opportunity to create more efficient spaces in different orientations under different climatic circumstances and improve indoor environmental quality by means of preventing extra glaring and heating. Since these facades can regulate the environmental conditions, need of air-conditioning can be mitigated; thus, they are effective in reducing energy consumption (Kensek & Hansanuwat, 2011; Ramzy & Fayed, 2011). They are also essential to provide a high-performance design that considers energy efficiency, communication, and sustainability (Di Salvo, 2018). Nady (2017) states that with an appropriate design of kinetic facade systems, ventilation can be provided efficiently to the building.

According to Bakker et al. (2014), most occupants have positive thoughts about kinetic facades. However, they are more satisfied when they also have manual control over the facade besides its automatic movement. Their study shows when the configuration of the facade has discrete transitions with less frequency, occupants feel more comfortable.

Even though there are many advantages of dynamic facades, they are complex designs; thus, these facades can have a high cost to be constructed and maintained (Alotaibi, 2015; Fakourian & Asefi, 2019; Mahmoud & Elghazi, 2016). Since kinetic panels have a mechanism of transformation and movement, their element can create noise pollution during shape changes. However, this negative effect can be reduced depending on the design of moveable panels (Bakker et al., 2014; Fakourian & Asefi, 2019).

CHAPTER 3

MATERIALS AND METHOD

In this chapter, materials and research methodology are explained with the data collection and analysis details. Measurement method, selected case study building, facade morphologies from the existing publications, facade design, and simulation software are shown as the materials. As the methodology, simulations of the base cases and design cases are presented with the selection of facade typologies.

3.1 Materials

Kinetic facades as a solution to space use in terms of thermal and visual comfort are investigated in an existing case study building in this research. The facade morphologies from the literature, the weather data of Ankara, the Middle East Technical University (METU) Cafeteria Building, and simulation software are discussed as the materials of the study.

3.1.1 Facade Morphologies

This research claims kinetic facades are effective for thermal and visual comfort in space use, and the main purpose is to observe a moveable facades difference in terms of these two comfort conditions regardless of a specific design. Hence, existing facade morphologies from the literature were reviewed for an effective and simple facade design, which can be sustainable for the operation of the building. Google Scholar, Taylor & Francis Online, ScienceDirect, and METU Library were used to find related publications. A total of 70 publications were analyzed, and the ones including potential morphologies were selected.

3.1.2 Weather Data

The case study building is on the METU campus in Ankara, Turkey. The city is in central Anatolia, and the coordinates are 39°53' N and 32°47' E. It is 920 meters above level height (Google Earth, n.d.).

Ankara has different climatic properties locally. The steppe climate, which is distinctive for Central Anatolia, is dominant in the south, and the Black Sea climate, which is rainy and temperate, can be seen in the north. July-August is the hottest month, while January is the coldest one. Generally, it has a continental climate; therefore, its winter temperatures are low, and summer temperatures are high (T.C. Ankara Valiliği, n.d.).

Climate Consultant 6.0 software is used to illustrate various weather graphs of Ankara. These graphs are produced according to Adaptive Comfort Model in ASHRAE Standard 55-2010. EnergyPlus Weather (EPW), retrieved from OneBuilding (n.d.), was used for all simulations and climate analysis.

During the whole year, August has the highest air temperature, with a value of more than 35 °C, while January has the lowest one, with a value of lower than -20 °C, as shown in Figure 3.1. According to the graph, it can be said that the air temperature is above the comfort zone between May and October, with a temperature of 25 °C.

According to Figure 3.2, the difference between direct normal radiation and diffuse radiation is higher from June to October in the whole year. Hence, it can be concluded the city is not cloudy during this period. The graph in Figure 3.3 also shows this period has a clearer sky than the other months of the year. September has the clearest sky, with a sky cover percentage below 40 at the average high value, while December has the less clear one, with a sky cover percentage over 90 at the average high value.

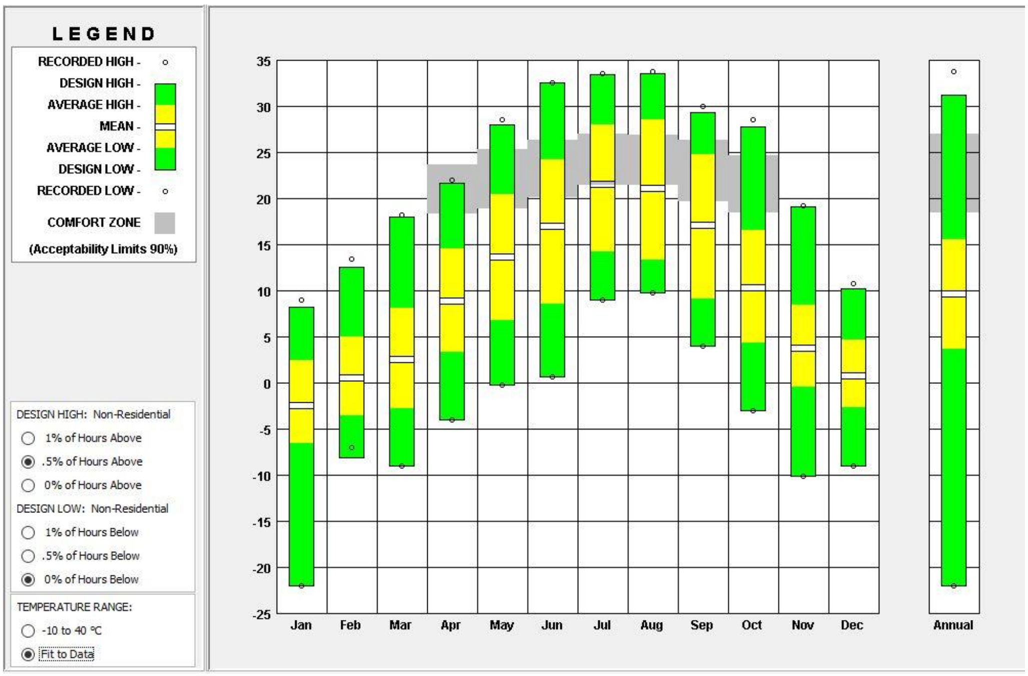

Figure 3.1 Comfort Zone and Temperature Range of Ankara during the year, produced by Climate Consultant 6.0

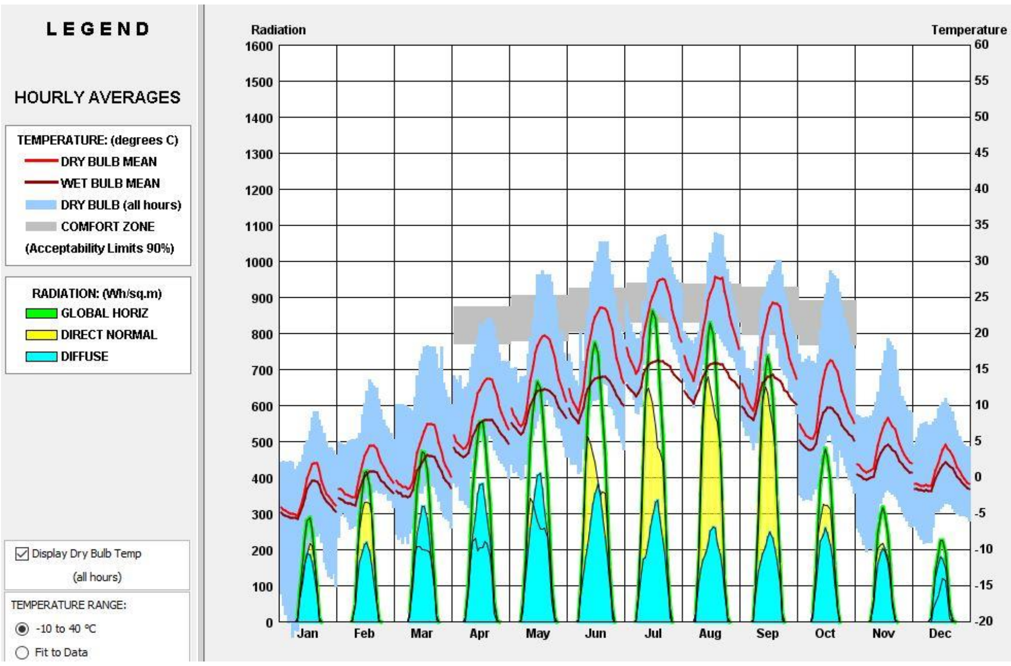

Figure 3.2 Monthly Diurnal Averages and Comfort Zone of Ankara during the year, produced by Climate Consultant 6.0

From April to October direct normal radiation range has the highest values, as shown in Figure 3.4. They are over 40000 lux for the monthly average high value. August has the highest illumination with a value of over 70000 lux, and December has the lowest one with a value of around 10000 lux.

According to these graphs, the months between May to October are the most uncomfortable months, thermally and visually.

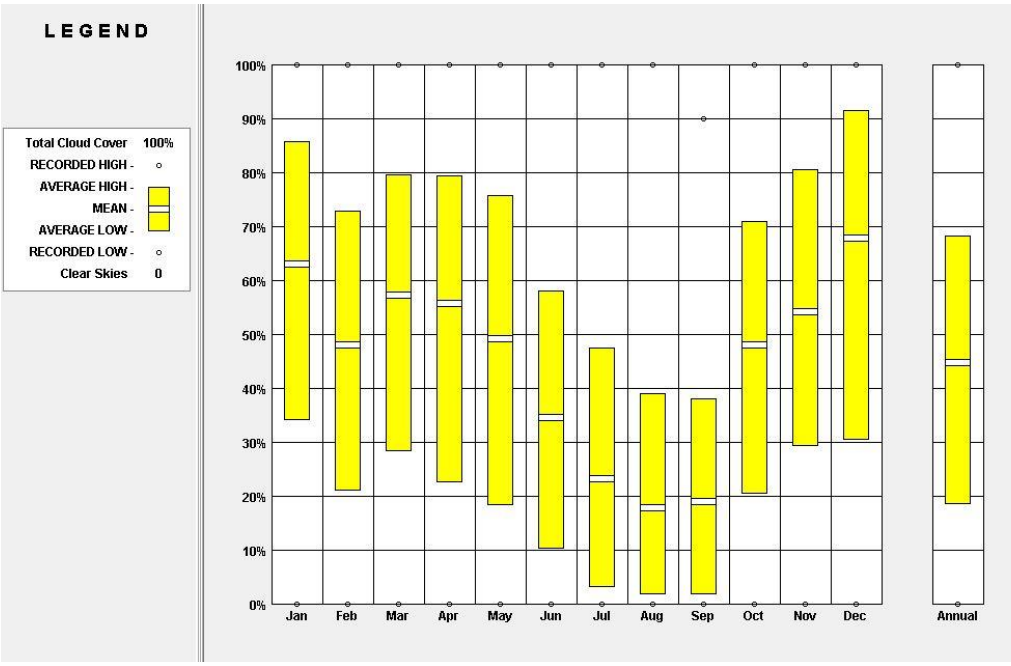

Figure 3.3 Sky Cover Range of Ankara during the year, produced by Climate Consultant 6.0

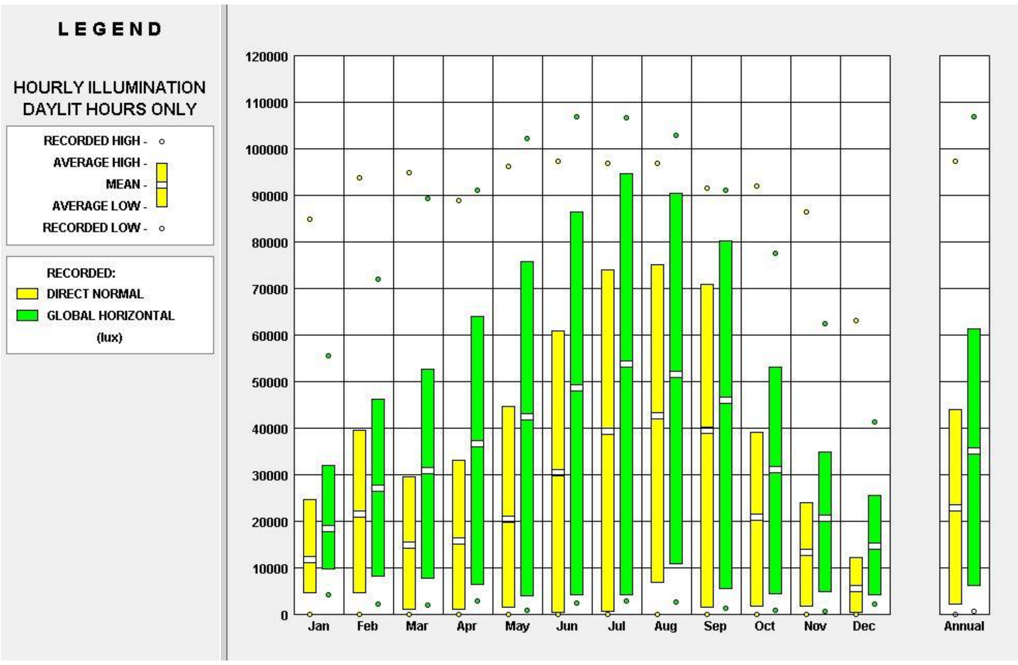

Figure 3.4 Illumination Range of Ankara during the year, produced by Climate Consultant 6.0

3.1.3 Case Study Building

This research aims to detect the thermal and visual comfort that affects space usage in a case study building with large, glazed facades and the possible enhancements of applying kinetic facades to provide solutions for the areas of discomfort. Regarding this aim, the population of the study is non-residential buildings with glazed facades, and the sample is cafeteria buildings where people can have lunch and dinner. METU Cafeteria building, seen in Figure 3.5, is selected as the case study building in this sample. It has highly glazed facades for whole dining halls.

METU Cafeteria Building, designed by architect Behruz Çinici, which was started to construct in 1962, has been in service for students since 1965 (ODTÜ Kafeterya Müdürlüğü, n.d.). It is in the center of the campus, and students can use it for lunch and dinner, meaning it is used twice a day.

It has an approximately seven-degree angle difference from the North direction to the West, as seen in the roof plan in Figure 3.6. It has two stories and three different dining halls on each floor, as shown in the plan layouts of the ground and first floors in Figure 3.7 and Figure 3.8, respectively. South and east halls are open to students. The upper north hall is used for the academic staff, and the bottom north is used as the a la carte section. All photographs can be seen in Appendix A.

(a) (b)

Figure 3.5 Exterior (a) and interior (b) views of the South dining hall of METU Cafeteria, pictured by the author

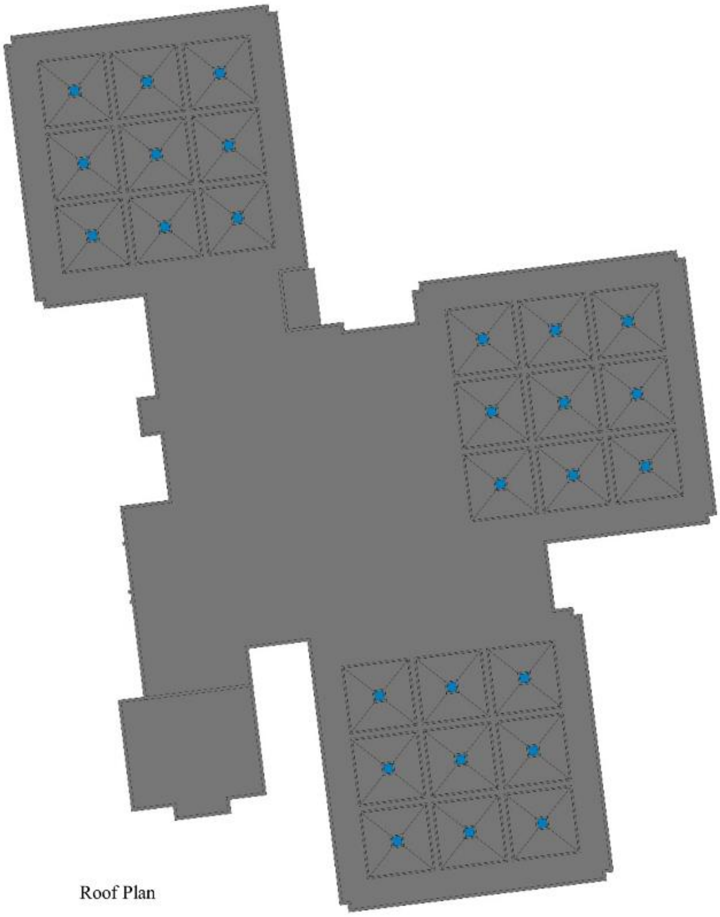

Figure 3.6 Roof Plan of METU Cafeteria Building

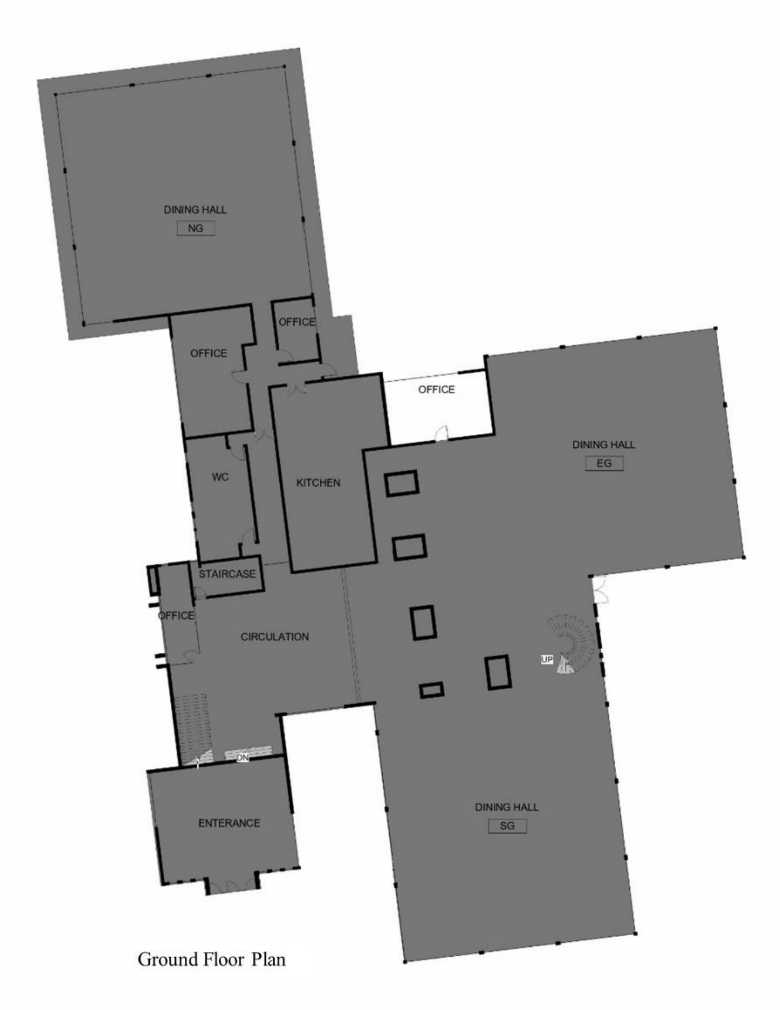

Figure 3.7 Ground Floor Plan of METU Cafeteria Building

Figure 3.8 First Floor Plan of METU Cafeteria Building

The geometrical properties and the glazing ratios of the southern dining halls, selected for the design case interventions as the focus section, can be seen in Table 3.1 and Table 3.2. The criteria for the selection are explained in Section 3.2 and Chapter 4. Detailed plans and sections with the measurements can be seen in Appendix B.

Table 3.1 Geometrical properties of south dining halls

Floor	Room (m) (length x width x height)	Glazing (m) (length x height)			
		East	South	West	North
Ground	19.58 x 21.89 x 4.3	2.05 x 4.3	1.85 x 4.3	2.05 x 4.3	
First	22.86 x 23.61 x 4	2.26 x 4	2.26 x 4	2.26 x 4	1.38 x 4

Table 3.2 Wall areas and window-to-wall ratios of the south dining halls

Floor	Total Wall Area (m^2)				Window to Wall Ratio (%)			
	East	South	West	North	East	South	West	North
Ground	94.2	83.9	94.2		94	95	94	
First	94.4	91.45	94.4	6.52	96	99	96	85

3.1.4 Measuring Tools and Software

The TESTO 405-V1 tool, shown in Figure 3.9, was used to measure existing thermal conditions in six dining halls, and the data was recorded accordingly on a specific day and hour.

An existing Revit model of the case study building was used as the primary model. Based on this model, 3D Rhinoceros models were prepared for the selected dining halls, not as a whole model with two floors but each floor separately for the simulations. Grasshopper interface was used for parametric scripting of simulations and kinetic facade design. Ladybug and Honeybee plugins were used to detect the base and design cases' thermal comfort and visual comfort conditions. EPW weather data, retrieved from OneBuilding (n.d.), was used for all simulations and climate analysis. The optimal facade openings were detected with Galapagos Evolutionary Solver for each focus dining hall.

(a) (b)

Figure 3.9 Thermal data collections from the dining tables with TESTO 405-V1 measuring device (a) and a closer look at the data recorded on the screen (b)

A Lux meter RO1335 by Rotronic Figure 3.10 was used to measure the existing lux conditions of the first floor of the south dining hall to calibrate the simulation results, which are mentioned in the following chapters in detail. Velux Daylight Visualizer was also used as a part of the calibration.

Figure 3.10 Lux meter RO1335 by Rotronic to measure illuminance in the METU cafeteria dining halls

3.2 Method

The methodology of this research first establishes the existing conditions in the case study building. Afterward, it focuses on the improvements of thermal and visual comfort conditions affecting space use and the results of applying these. The existing data was obtained by both measurements for all dining halls and simulations for the selected ones, while the design case data was collected by simulation. In this scope, the methodology of this research has seven steps as follows:

i. Measuring the existing temperature values of the existing building and taking photos from the interior,
ii. Selecting the uncomfortable section of the building according to field measurements and modeling these dining halls in Rhinoceros, and simulating them as a base case scenario using Grasshopper interface with Ladybug and Honeybee plugins,
iii. Analyzing existing publications and selecting two optimal kinetic facade typologies considering weather data of Ankara, simplicity, improvement results, and applicability of the modules,
iv. Modeling one of the selected morphologies by using Rhinoceros and Grasshopper and detecting the optimized opening conditions of facade modules Galapagos Evolutionary Solver, then testing it for one of the dining halls by using two different materials, i.e., ETFE and metal,
v. Selecting the more efficient material, the result of the previous step, and applying it to two facade morphologies for detecting the optimized openings with Galapagos, and integrating it for the facade of two selected dining halls,
vi. Designing fixed shadings and integrating them into the case study building facade with the same material as the kinetic facades,
vii. Getting simulation results of all design scenarios using Ladybug and Honeybee plugins and comparing them with the base case scenario. All scenarios can be seen in Table 3.3.

Table 3.3 Simulation Scenarios

Scenario	Definition
Base Case	Existing facade of the case study dining halls
Design Case 1	Fixed shadings
Design Case 2	Kinetic facade morphology adapted from the design of W. T. Sheikh & Asghar (2019)
Design Case 3	Kinetic facade morphology adapted from the Al Bahar Towers

3.2.1 Measurements of Existing Conditions of METU Cafeteria Building and the Selection of the Case Section

Existing temperature data for each table was collected on the 30th of July 2021, between 1 and 1.30 pm, before the simulations, using TESTO 405-V1. The outdoor temperature was 34 °C.

In the plan view, every dining table is named according to which floor and dining hall they are located. They are numbered from left to right and from top to bottom. Abbreviations are shown in Table 3.4. For instance, SG-A1 (South Ground Floor, Row A Column 1) corresponds to the leftmost dining table in the dining hall on the ground floor of the south section. The first floor of the north section was measured for three points instead of tables due to the differences since it is the academic part.

Figure 3.11, Figure 3.12, Figure 3.13, Figure 3.14, Figure 3.15, and Figure 3.16 shows the naming of the dining tables on the ground floor and first floor of the south, east, and north sections, respectively. The corresponding temperature data to the tables are explained in the results and discussion chapter

.

Table 3.4 Abbreviations used in plan views for tables to name the different locations for temperature data

Location	Abbreviation in Plan View
South Ground Floor	SG
South First Floor	SF
East Ground Floor	EG
East First Floor	EF
North Ground Floor	NG
North First Floor	NF
Rows	from A to I
Columns	from 1 to 8

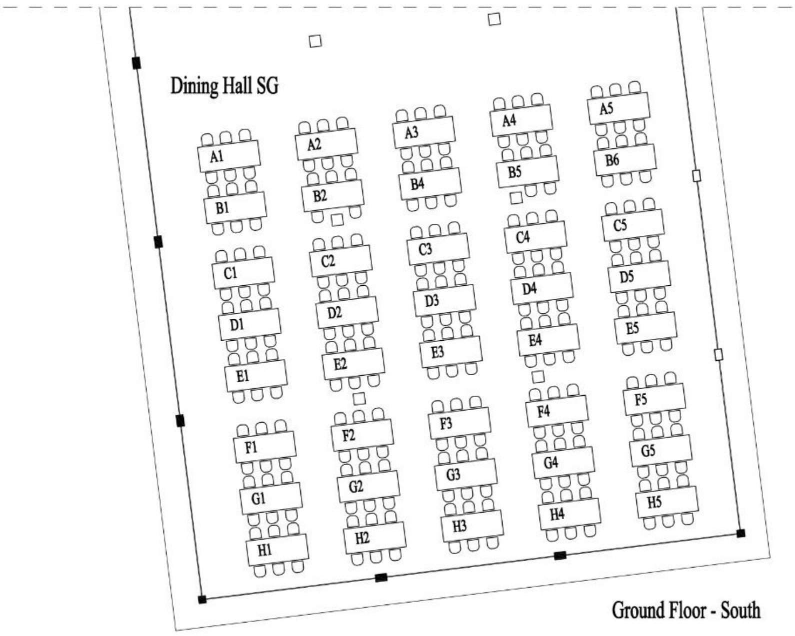

Figure 3.11 Ground Floor Plan and Temperature Data Notation of South Dining Hall

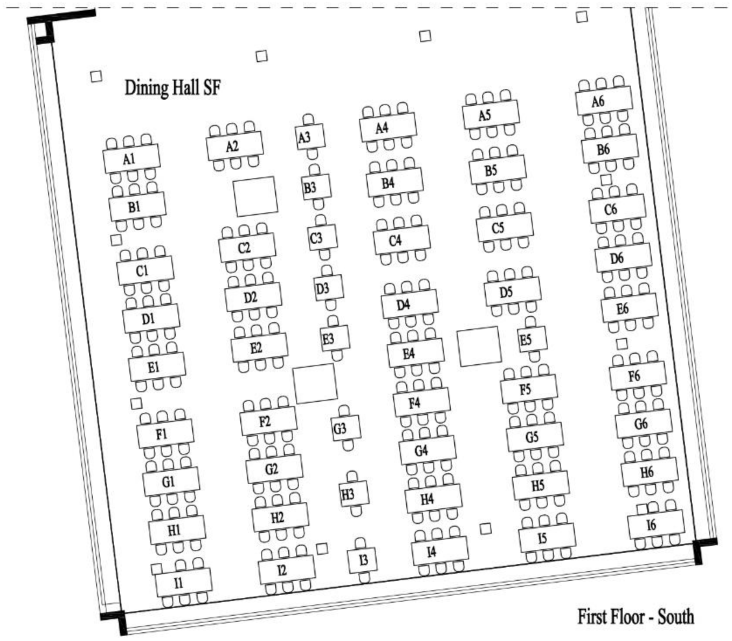

Figure 3.12 First Floor Plan and Temperature Data Notation of South Dining Hall

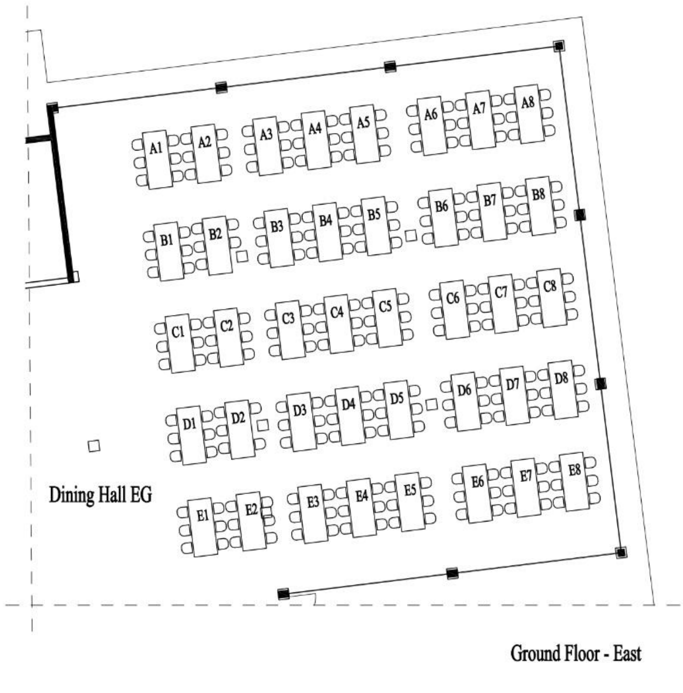

Figure 3.13 Ground Floor Plan and Temperature Data Notation of East Dining Hall

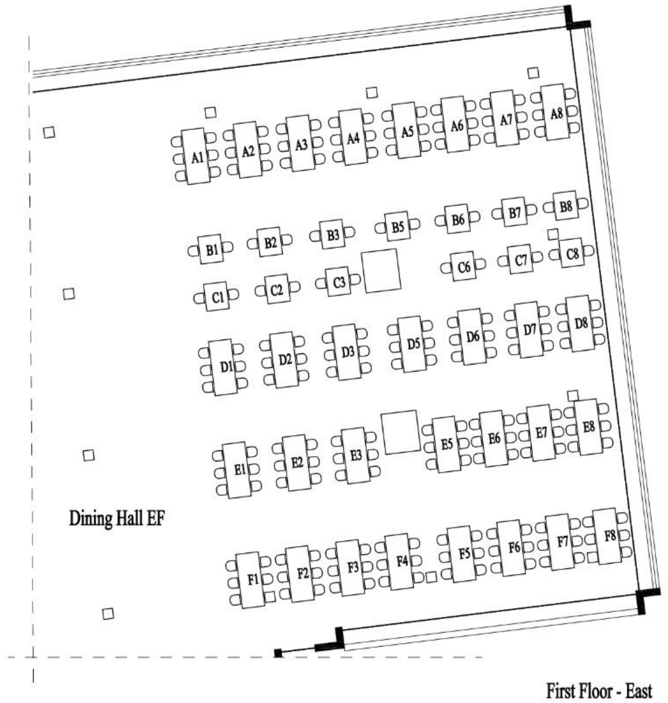

Figure 3.14 First Floor Plan and Temperature Data Notation of East Dining Hall

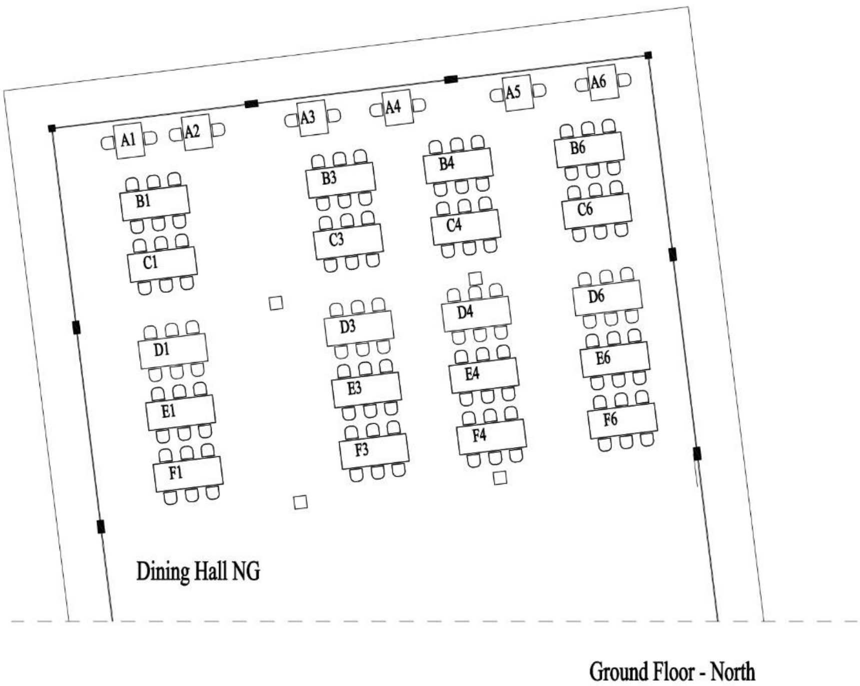

Figure 3.15 Ground Floor Plan and Temperature Data Notation of North Dining Hall

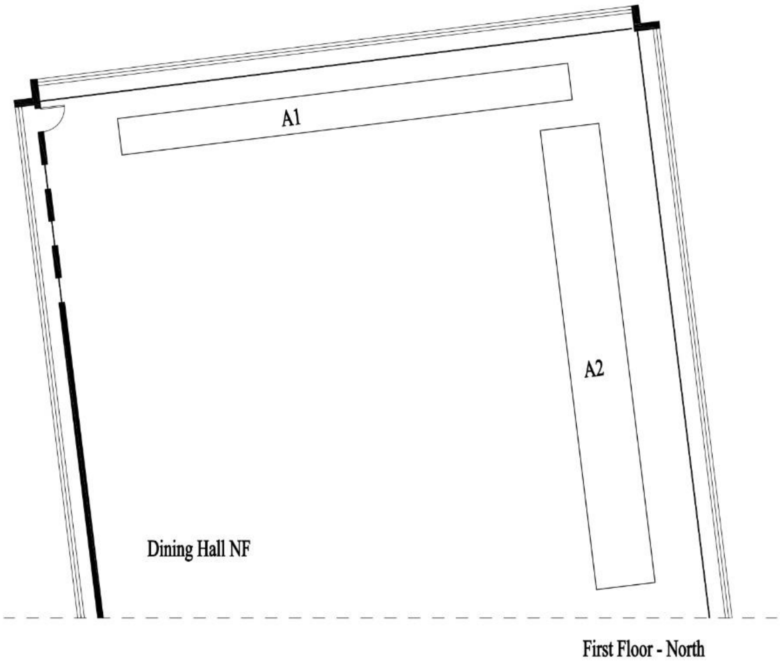

Figure 3.16 First Floor Plan and Temperature Data Notation of North Dining Hall

According to these field measurement results, the section with higher temperature values, causing discomfort, for both the ground and first floor was detected, and the most uncomfortable one was selected for the simulations.

As previously mentioned, for the calibration of the simulation results of HoneyBee, the field illuminance values were measured with the RO 1335 for the first floor of the south section. The data was collected on the 24th of November 2022, between 12.30 and 1.15 pm, with 10380 lux of exterior illumination. The data were organized according to the notation given in Figure 3.12.

3.2.2 Facade Morphology Selection and Design

A literature survey was completed for the facade morphology using Google Scholar, Taylor & Francis Online, ScienceDirect, and METU Library databases. The related articles published between 2015 to 2022 were reviewed with a total of 70 publications. The most related 23 facades from these publications were classified and indicated according to the morphology, inspiration, and material technology of the facade, applied case study building, and the climate, response input and output, movement type, base case parameters, design considerations, and results.

Böke et al. (2020) investigate eleven adaptive facades of the actual building applications. These real facade examples are classified according to applied building type, facade material technology, facade function, location, and user control, as can be seen in Table 4.9 in the section 4.2.

As stated in Chapter 2, kinetic facades can have disadvantages, while the operation phase of the building due to maintenance difficulties of the system is very complex. Therefore, they can also create discomfort if they are not working properly. Hence, the criteria for selecting the morphology amongst these 23 different facades was considered the simplest and more sustainable since the main objective was to detect moveable facade impact. Two different facade morphologies were selected, one from the proper theoretical results and one from the actual case application results.

The results of these classifications and selections are mentioned in the results and discussion chapter.

Selected facade morphology was modeled with Grasshopper, and Galapagos Evolutionary Solver was used to detect the optimized movement for the specific month and hour, i.e., 8^{th} of June at 1 pm. The reason for the specific time and the optimization details are explained in Section 3.2.3 in detail. These morphologies are defined as shading in the design case simulations.

One of the selected facade morphologies was tested for translucent and reflective materials, i.e., ETFE and white metal. The one having better results was selected for all design case scenarios.

3.2.3 Simulation

The ground and first floors of the focus study section were modeled and simulated separately. Overhang due to the top floor is defined as a shading surface to reflect the shading effect of the top floor in the scenarios for the bottom hall. The top floor was modeled 430 m above ground. Surfaces and masses are modeled for the ground and first floors using Rhinoceros, as can be seen in Figure 3.17 and Figure 3.18, respectively. The “Create Honeybee” step is used to define these surfaces and masses in the Grasshopper interface, and the building program is defined as a “Full-Service Restaurant,” as seen in Figure 3.19.

In the current plans, table layouts correspond to approximately 2 to 4 meters grids. Therefore, the grid size of sensors was defined as 2 meters, and the distance from the floors was considered 0.75 meters, which is the table height.

According to the graphs explained in Section 3.1.2, thermal and visual comfort is lower from May to October. Amongst these months, since the last weeks of the spring semester are more busy due to the final exams, the period was considered from the 15th of May to the 15th of June; these dates were selected for the scope of this research.

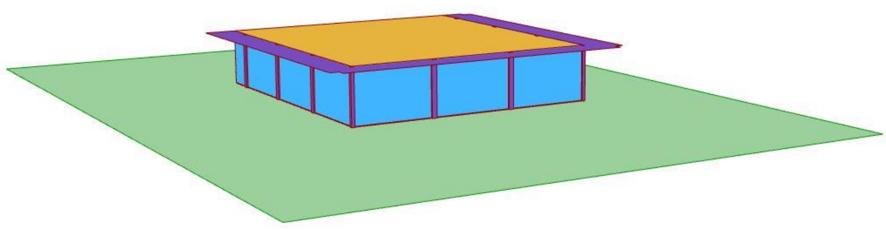

Figure 3.17 Honeybee Model of Ground Floor of the South Section

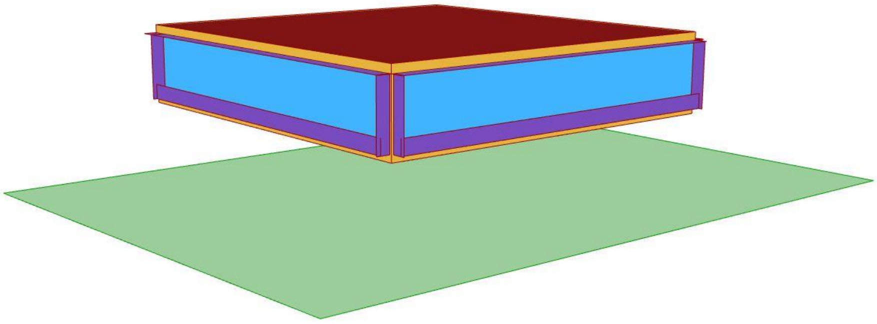

Figure 3.18 Honeybee Model of First Floor of the South Section

Four different parameters were analyzed by using Ladybug and Honeybee: illuminance, daylight factor, annual daylight for UDI, and adaptive comfort for operative temperatures. In UDI and Daylight Factor simulations (scripts can be seen in Figure 3.20 and Figure 3.21), since they do not require a specific period, the average annual results were obtained. For the adaptive comfort simulations, the period was defined between the 15th of May and the 15th of June, as in Figure 3.22.

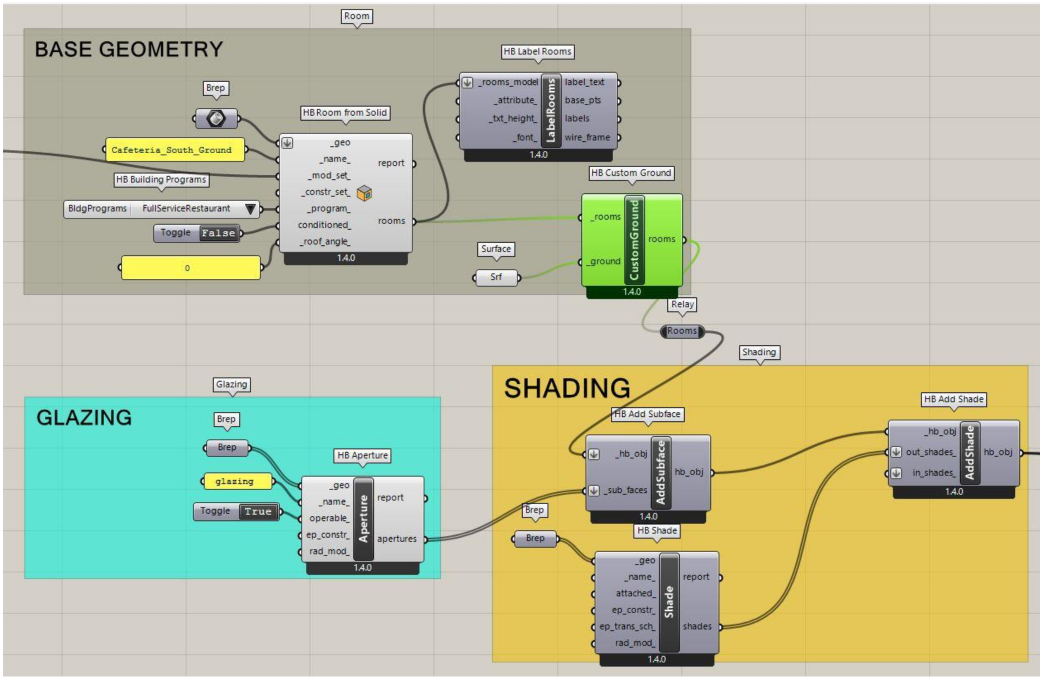

Figure 3.19 Script of the Definition of the Honeybee Model with the rooms, glazing, and shading

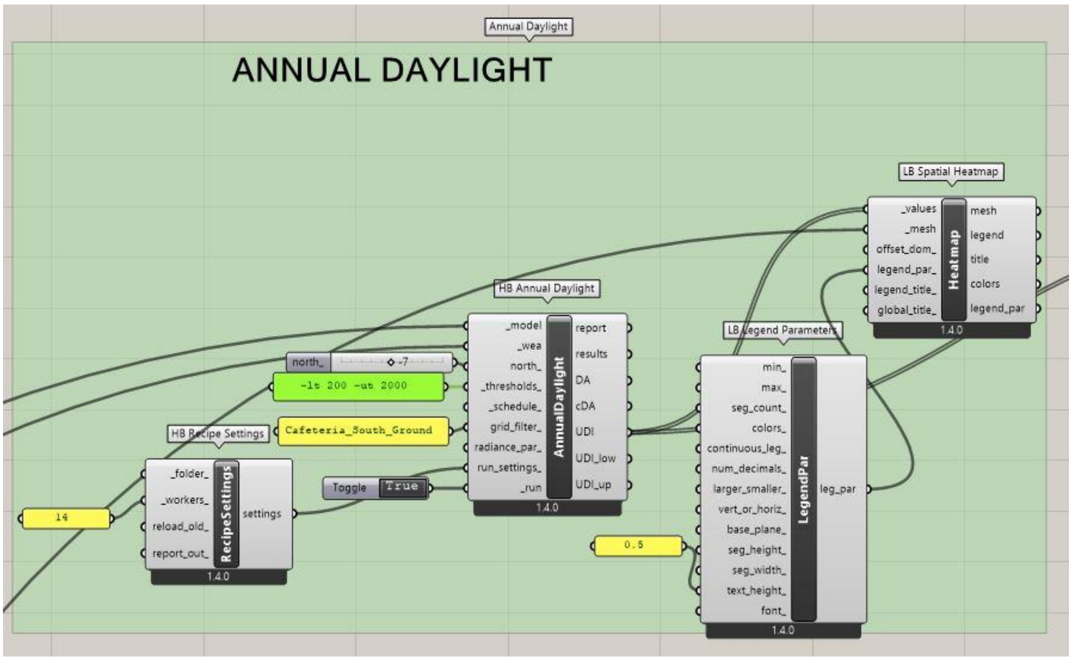

Figure 3.20 Script of the Definition of Annual Daylight for UDI

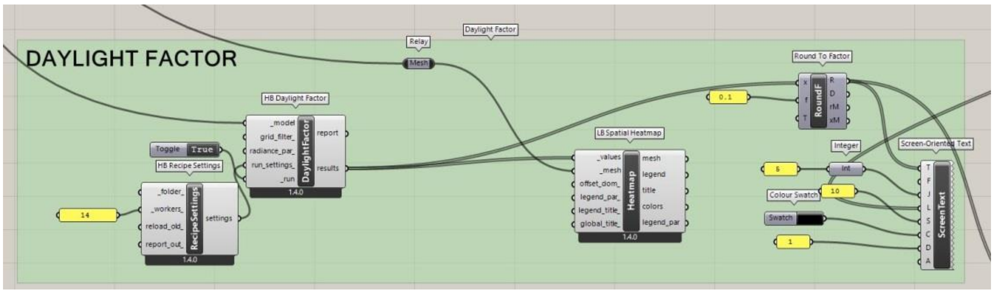

Figure 3.21 Script of the Definition of Daylight Factor

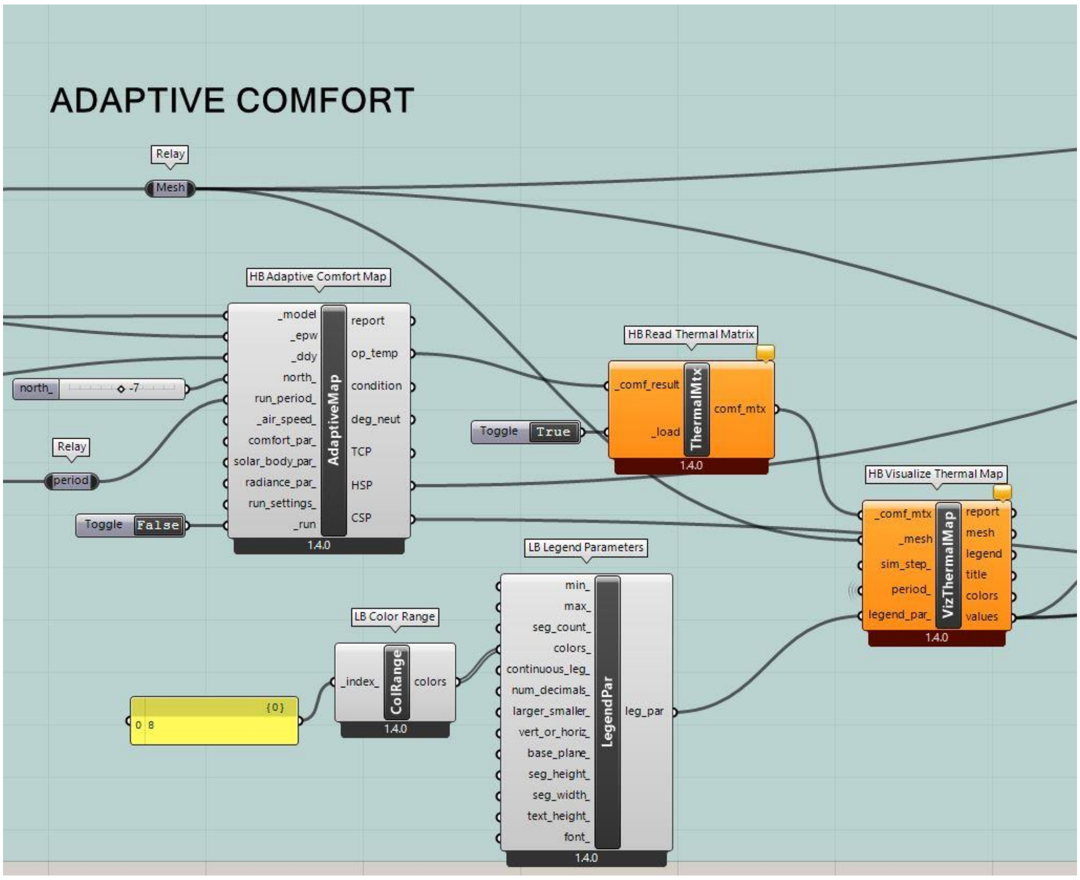

Figure 3.22 Script of the Definition of Adaptive Comfort for Operative Temperatures

Since the illuminance results from a point-in-time grid-based component, it requires a specific day and month. Therefore, dry bulb temperature analysis was completed for the selected time range, i.e., between the 15th of May and the 15th of June, and the 8th of June was determined as the specific day and month for the illuminance simulations, as can be seen in Figure 3.24.

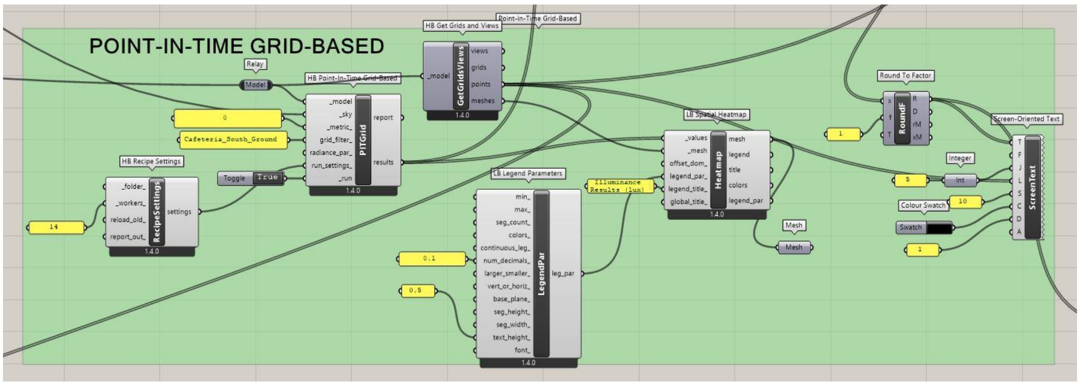

Figure 3.23 Script of the Definition of Point-in-Time Grid-Based for Illuminance

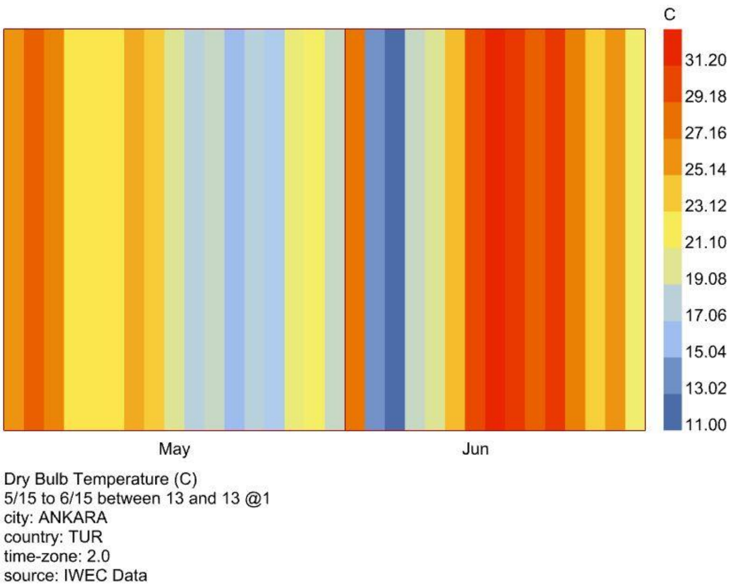

Figure 3.24 Dry Bulb Temperature Analysis with Ladybug from 15th of May to 15th of June

The material properties of the existing building were defined as given in Table 3.5 for the simulations as the modifiers. Grey concrete reflectance ratio was also used for terrazzo tiles in the simulations.

Table 3.5 Optical properties of surface materials of METU Cafeteria Building (Guan, 2011; Kalzip, 2009; Marceau & VanGeem, 2008)

Surface	Material	Dining Hall	Optical Properties (%)
Exterior Wall	Concrete	All	35
Interior Wall	Concrete	All	35
Interior Ceiling	Concrete	First	35
Interior Ceiling	Metal, white	Ground	77
Interior Floor	Terrazzo Tiles	All	35
Glazing	Clear, double glass	All	81

Two different materials, i.e., painted metal and ETFE, were simulated to see the effect of a reflective material and a translucent one. The metal properties were defined as stated in Table 3.5. The result of Flor, X. Liu, Sun, Beccarelli, Chilton, and Wu's (2022) research shows that fritted ETFE with switch ability can provide more contributions for efficient daylight conditions to the building than clear or fritted ones. Therefore, it was used as one of the material options for the facade modules. The optical properties of ETFE for simulation are shown in Table 3.6.

The illuminance simulations were obtained for one of the kinetic facades, and the results were compared. The one with more sensors in the desired range was selected and applied as material to all design cases.

For all design cases of the first floor, the concrete railway was assumed to be removed to integrate the facades into the whole glazing.

Table 3.6 Optical properties of ETFE used for simulations taken from (Flor et al., 2022)

Surface	Diffuse Reflectance	Specular Transmittance	Diffuse Transmittance
ETFE (Dense Fritted)	41.3 %	0.4 %	3.6 %

i. Calibration Results of the Field Measurements and Simulations

As mentioned in the previous sections, the illuminance values of the first floor of the south section for all tables were measured by a RO 1335 lux-meter on the 24th of November between 12.30 to 1.15 pm. These results were compared with the ones obtained from Velux Daylight Visualizer. The Revit model of the dining hall was imported into the software. Since Velux Daylight Visualizer can only simulate the 21st of months, the 21st of November at 1 pm was selected. Afterward, the 21st of June at 1 pm was chosen as a day in June, and the results were compared to the Honeybee ones for the same date.

Similar to the illuminance results, the simulation temperature data was also calibrated with the field measurements. The field data was obtained on the 30th of June at 1 pm; therefore, the first floor of the south section was simulated for the same day and hour. The results were compared to each other, and calibration was completed.

ii. Base Case

The base case consisted of the ground and first floor of the south part of the METU Cafeteria Building. All materials and scripts were defined as it is presented in Section 3.2.3.

According to EN 12464-1 (2002), the self-service restaurant should be at least 200 lux, and a range is mentioned in the same standard. 300 lux was considered the highest limit for illuminance according to this range.

As a result of a literature survey, UDI was defined as a minimum of 100 lux and a maximum of 2000 lux, and the metric has accepted a minimum of 50% UDI received by the sensors in this range during the whole year for the occupied hours while 2% to 5% was considered as the acceptable range for daylight factor.

According to ISO 7730 (2005), the operative temperature should be 24.5 °C with a tolerance ± 1.5 °C. After calibrating the results for illuminance and operative temperature, the results were evaluated according to these ranges.

After modeling the base case, design cases are integrated into these as the interventions into the facade. In the following sections, these interventions are explained.

iii. Fixed Shadings

The intervention of fixed shadings is defined as design case 1. The same properties as the base case were used for the building.

Sun angles were taken from the Climate Consultant 6.0 sun shading chart, shown in Figure 3.25, for the west and south facades, as 20° and 68°, respectively. As can be seen in Figure 3.26., vertical sunshades were integrated at 2 meters intervals at a depth of 75 cm for the west facade, in accordance with the angles. However, the existing cantilever caused by the first floor creates an overhang for the ground floor, which provides enough shading to the south facade, according to the calculated angle. Therefore, no additional louvers were designed for this facade.

As can be seen in Figure 3.27, vertical louvers with 75 cm depth were designed at 2 meters intervals for the west facade of the first floor, while for the south facade, horizontal louvers with 80 cm depth, one for the top and one for the middle of the window, were integrated since they can maintain/ provided shading.

ETFE was used as the material for louvers. The shadings were modeled in Rhinoceros and defined to Grasshopper interface with “Brep” component as shading object.

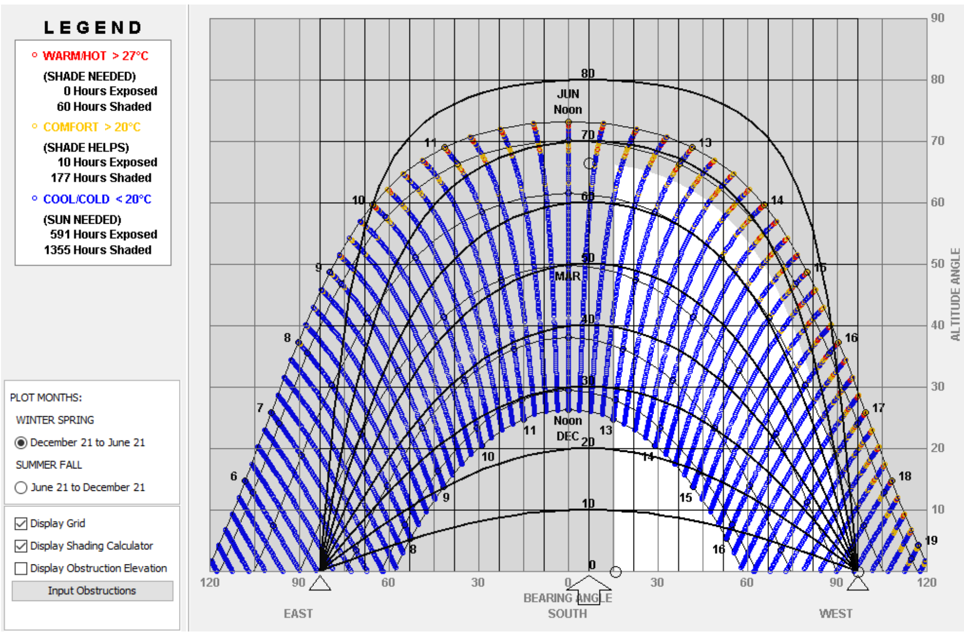

Figure 3.25 Sun shading chart of Ankara, produced by Climate Consultant 6.0

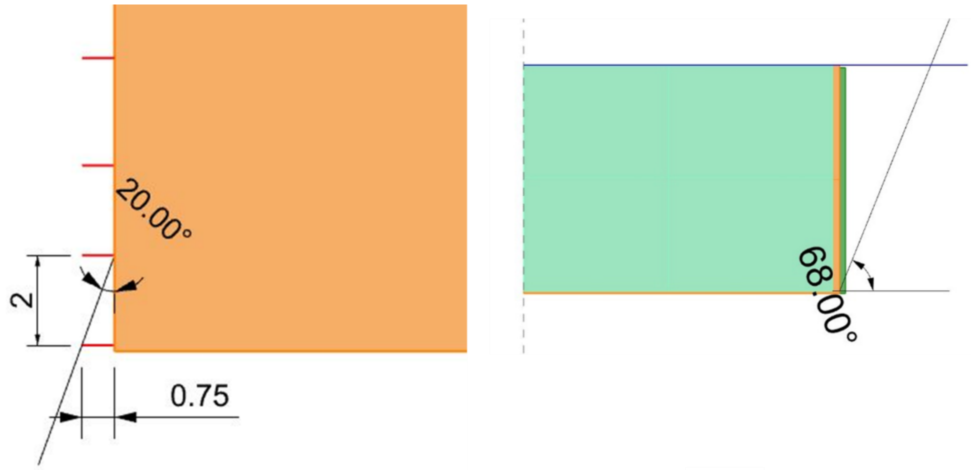

(a) (b)

Figure 3.26 Shading calculations of the ground floor for the west facade from the plan view (a) and south facade from the section view (b)

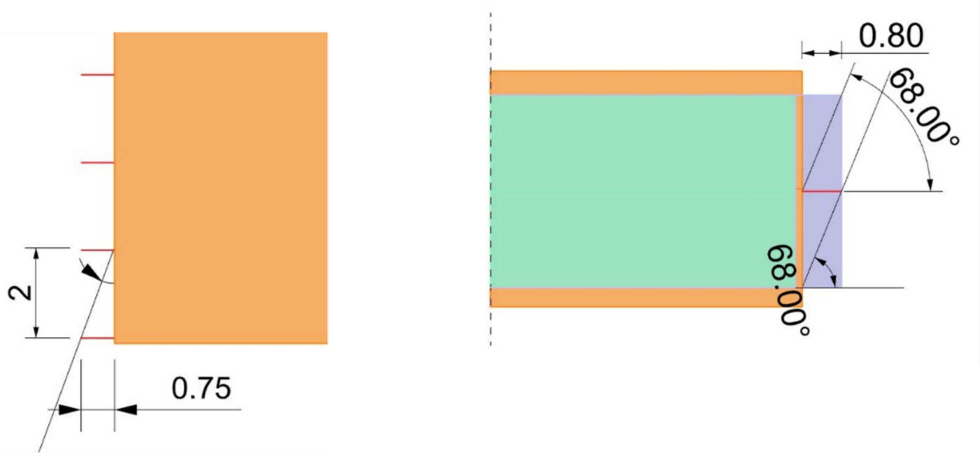

(a) (b)

Figure 3.27 Shading calculations of the first floor for the west facade from the plan view (a) and south facade from the section view (b)

iv. Kinetic Facade with Square Modules

As design case 2 scenario, kinetic facade modules were adapted from the design of W. T. Sheikh and Asghar (2019). Square modules with 2x2 meter dimensions were integrated, which can move horizontally and vertically for the south and west facades, respectively, as seen in Figure 3.28.

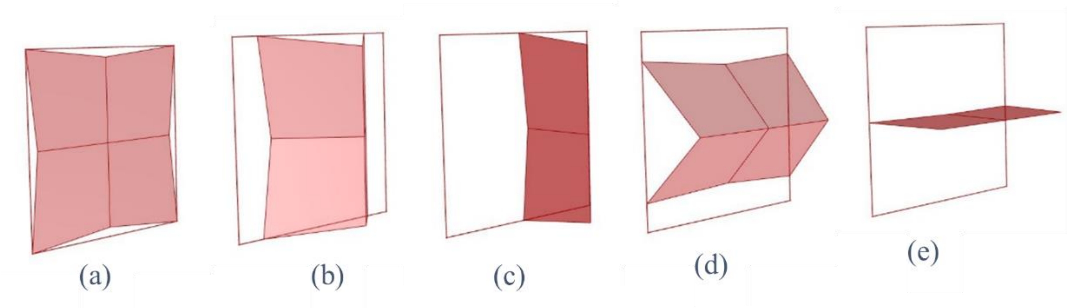

Figure 3.28 Kinetic facade modules adapted from the study of W. T. Sheikh and Asghar (2019) with the options of fully close (a), half-open vertically (b), fully open vertically (c), half-open horizontally (d) and fully open horizontally (e)

The geometry and the movement of the modules were created in the Grasshopper interface. Since each module should move separately, these scripts were repeated for each one of them. There are 36 modules, 18 for the west and 18 for the south facade, integrated into the ground floor, while 44 modules, 22 for the west and 22 for the south facade, were integrated into the first floor.

As a translucent material, the optical properties of ETFE were used for the modifier component. The facade geometry was defined as shading to the building.

v. Kinetic Facade with Al Bahar Towers Modules

The kinetic facade consisted of the adaptation of Al Bahar Towers modules that were applied as design case scenario 2. Triangles with the dimension of 2x2x2 meters were created as one module. Different openings can be seen in Figure 3.29.

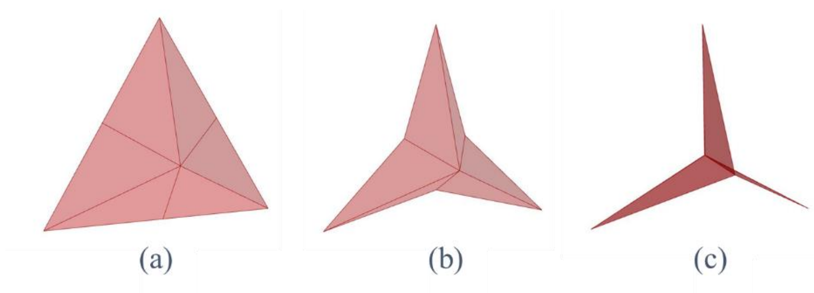

Figure 3.29 Kinetic facade modules adapted from Al Bahar Towers with the options of fully close (a), half-open (b), and fully open (c)

As in the previous kinetic facade morphology, each module script was created separately using the Grasshopper interface. Sixty modules, 30 to the west and 30 to the south facade, were placed to the ground floor, and 84 modules, 42 to the west and 42 to the south facade, were integrated into the first floor.

Similarly, with all design interventions, ETFE was defined as the material. Facade modules were interpreted as shading to the existing model.

vi. Optimization of the Kinetic Facade Modules

Galapagos Evolutionary Solver was used for the optimization of the module openings under the desired conditions for the 8th of July at 1 pm. The algorithm was inspired and adapted from the methodology published by M. M. El Sheikh (2011)

The illumination range of 200 lux and 300 lux was defined as the optimization parameter, as shown in Figure 3.30. The total number of sensors in this range was converted to “True” and “1” from this point. Afterward, these numbers were summed up and connected to Galapagos as the “Fitness” parameter. Since the aim is to increase the sensors in the defined range, Galapagos was adjusted to maximize this value. The facade openings were based on these maximized number of sensors according to illuminance range.

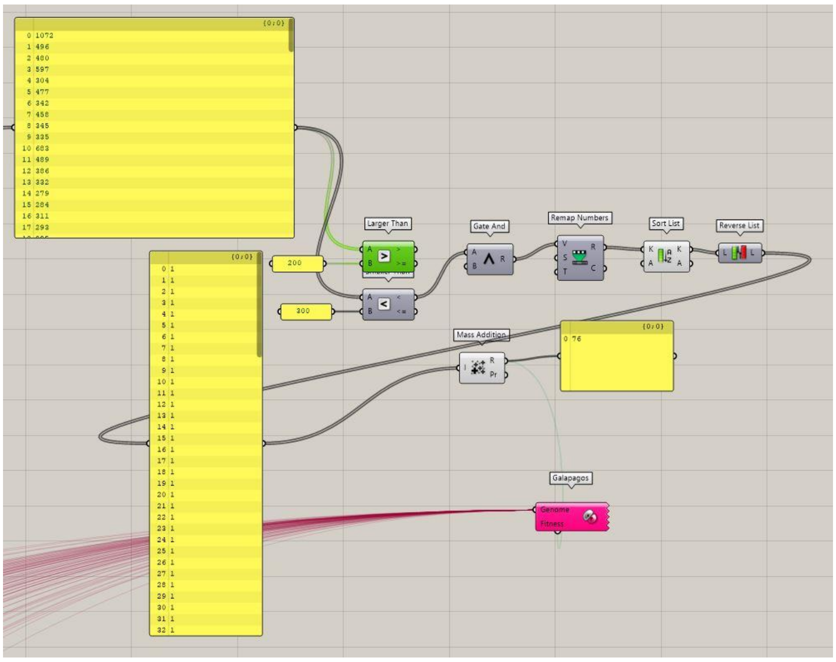

Figure 3.30 Optimization script with Galapagos adapted from the methodology by M. M. El Sheikh (2011)

CHAPTER 4

RESULTS AND DISCUSSION

The existing conditions with both measurements (TESTO 405-V1 and RO 1335) and simulation and design case conditions as a result of simulations are presented in this chapter. Selected kinetic facade morphologies are also discussed. Consequently, thermal comfort with the operative temperature and visual comfort with illuminance, daylight factor, and UDI results are compared between the base case and design case scenarios, i.e., fixed shadings and two different kinetic morphologies, for the south section of the METU Cafeteria Building under related sections.

4.1 Data Collected with the TESTO 405-V1 and the Result of the Case Section Selection

This section presents the results of the temperature measurement device, i.e., TESTO 405-V1, for thermal comfort conditions of the existing building as an initial step. As mentioned, data for each table was collected for all dining halls on the 30th of July 2021, between 1 and 1.30 pm. The results were organized and presented according to table locations, and the notations were explained in section 3.2.1.

Table 4.1 and Table 4.2 shows the temperature data results of the south-ground and first floors, respectively. According to these results, it is observed that tables near glazing have higher temperature values than the other ones. When the floors are compared, it is seen that the tables on the first floor have higher temperature values than the ones on the ground floor.

Overall, it is concluded the temperature results are not comfortable for both floors of the south section.

Table 4.1 Data Collected in degrees Celsius (°C) with TESTO 405-V1 for the Ground Floor of the South Dining Hall on 30th of July 2021, between 1 and 1.30 pm

Location	1	2	3	4	5
A	28.6	28.7	29.0	29.0	29.2
B	29.0	29.0	29.1	29.1	29.2
C	29.1	29.1	29.1	29.1	29.2
D	29.1	29.1	29.1	29.1	29.2
E	29.1	29.1	29.1	29.1	29.2
F	29.1	29.1	29.1	29.1	29.2
G	29.1	29.1	29.1	29.1	29.2
H	29.2	29.2	29.2	29.2	29.3

Table 4.2 Data Collected in degrees Celsius (°C) with TESTO 405-V1 for the First Floor of the South Dining Hall, on the 30th of July 2021, between 1 and 1.30 pm

Location	1	2	3	4	5	6
A	32.0	32.1	32.1	32.1	32.3	32.6
B	32.0	No Table (NT)	32.1	32.1	32.4	32.8
C	32.0	32.1	32.1	32.3	32.5	33.5
D	32.0	32.1	32.5	32.5	32.8	33.7
E	32.0	32.5	32.5	32.8	33.4	33.9
F	32.0	32.5	NT	33.5	33.8	33.9
G	32.0	32.7	32.7	33.8	33.9	34.0
H	32.0	32.7	32.7	33.9	34.0	34.2
I	32.1	34.2	34.2	34.2	34.2	34.4

As opposed to the south dining halls, tables near glazing have lower temperature data, as seen in Table 4.3 and Table 4.4 for the ground and first floors of the east section, respectively. The tables on the first floor have higher temperature values than the ones on the ground floor, similar to the south section.

It is determined that the temperature results are within the discomfort range for both floors of the south section.

Table 4.3 Data Collected in degrees Celsius (°C) with TESTO 405-V1 for the Ground Floor of the East Dining Hall, on 30th of July 2021, between 1 and 1.30 pm

Location	1	2	3	4	5	6	7	8
A	28.4	28.4	28.4	28.4	28.4	28.4	28.4	28.3
B	28.4	28.4	28.4	28.4	28.4	28.4	28.4	28.3
C	28.6	28.4	28.4	28.4	28.4	28.4	28.4	28.3
D	28.6	28.4	28.4	28.4	28.4	28.4	28.4	28.3
E	28.6	28.6	28.6	28.5	28.6	28.4	28.6	28.3

Table 4.4 Data Collected in degrees Celsius (°C) with TESTO 405-V1 for the First Floor of the East Dining Hall, on the 30th of July 2021, between 1 and 1.30 pm

Location	1	2	3	4	5	6	7	8
A	32.3	32.0	31.3	30.9	30.5	30.4	30.1	32.3
B	32.3	31.9	31.7	NT	31.3	31.0	30.6	30.3
C	32.7	32.7	32.4	NT	NT	32.0	31.5	31.0
D	32.5	32.3	32.3	NT	32.0	31.6	31.3	31.0
E	33.0	32.8	32.7	NT	32.7	32.5	32.0	31.5
F	33.8	33.6	33.0	32.5	32.4	32.4	32.4	32.0

In the north dining halls, tables near glazing similarly have lower temperature values than the east section. The results of the ground and first floors of the north section can be seen in Table 4.3 and Table 4.4, respectively. The tables on the first floor have higher temperature values than the ones on the ground floor, as for the other two sections.

In conclusion, it is seen that temperature ranges are not comfortable for both floors of the north section.

Table 4.5 Data Collected in degrees Celsius (°C) with TESTO 405-V1 for the Ground Floor of the North Dining Hall, on the 30th of July 2021, between 1 and 1.30 pm

Location	1	2	3	4	5	6
A	29.4	29.6	29.6	29.6	29.6	29.6
B	29.4	NT	29.4	29.4	NT	29.4
C	29.4	NT	29.4	29.4	NT	29.4
D	29.4	NT	29.4	29.4	NT	29.4
E	29.4	NT	29.4	29.4	NT	29.3
F	29.4	NT	NT	29.4	NT	29.3

Table 4.6 Data Collected in degrees Celsius (°C) with TESTO 405-V1 for the First Floor of the North Dining Hall, on the 30th of July 2021, between 1 and 1.30 pm

Location	1	2
A	30.1	31.5

Since the south section has the highest values for both ground and first floors, with 29.2 °C and 34.4 °C, respectively, it was selected as the focus study section of the METU Cafeteria Building.

Field measurement results of illuminance values, recorded on the 24th of November 2022 between 12.30 and 1.15 pm, are presented in Table 4.7. According to these results, it was observed the first floor of the south dining halls has the illuminance values 1498 lux as the highest and 103 lux as the lowest. The illuminance outside was recorded to be 10,380 lux as the sky was overcast. These data were used to calibrate the simulations, explained in Section 4.3.

Table 4.7 Data Collected in lux with the RO 1335 lux-meter for the First Floor of the South Dining Hall on 24th November 2022 between 12:30 pm and 1.15 pm

Location	1	2	3	4	5	6
A	550	103	220	180	230	435
B	582	No Table (NT)	180	282	232	586
C	480	232	290	240	232	445
D	366	232	280	120	287	380
E	366	170	280	120	287	494
F	565	400	NT	303	453	494
G	600	400	365	303	500	518
H	600	400	365	303	600	600
I	1006	830	830	830	1473	1498

4.2 Design of Kinetic Facade

Amongst the 23 facades shown in Table 4.8, it can be concluded that kinetic facades have a positive impact on the comfort conditions for different climates and morphologies. However, as stated in the literature review, when the system is too complicated, unexpected results may occur. As a result of this, the comfort conditions may be affected negatively. Because even if these facades have a significant result in calculations in the design phase, they may not be working properly during the operation phase, as expected. The selected morphologies were taken into consideration these circumstances; hence, two morphologies were chosen as follows:

i. Based on biomimicry with Oxalis Oregana leaf, the facade design by W. T. Sheikh and Asghar (2019) was adapted as the design case 2 to the case study section. According to the research done by W. T. Sheikh and Asghar (2019), it is a facade design inspired by nature with a less complicated mechanism, and the results show that it is effective for highly glazed buildings. It is also movable in both vertical and horizontal directions. The research also states concrete results of the effectiveness of this facade morphology (W. T. Sheikh & Asghar, 2019). In the scope of this research, it is tested with modules of 2 x 2 meters. These measures were calculated according to the azimuth and altitude angles of Ankara. So, it was tested for a different climate and building type to observe if it is also effective for these different parameters.
ii. As design case 3, the morphology of Al Bahar Towers was adapted to the case study building. As stated in the research by Shahin (2019), it can reduce solar heat gain by 50%. It is a facade with triangle modules applied to a highly glazed tower building. Moreover, since it is a real case application, it is seen that during the operative phase, it is also effective. Therefore, it can be concluded that it is one of the most successful real case facade morphologies. As it is in design case 2, it is also tested for a different climate and building type with the 2x2x2 meters of triangular shape.

Table 4.8 Facade Morphologies from the Literature

#	Reference	Morphology/Inspiration/ Material Technology	Case Study Building/Climate	Response Input and Output / Movement	Design Consideration/Result	Advantages / Disadvantages
1	(W. T. Sheikh & Asghar, 2019)	Biomimicry Oxalis Oregana leaf 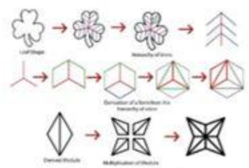	-20-story office (highly glazed facade) Tricon Corporate Center in Lahore, Pakistan -Hot & Humid in hot, dry summer	-Horizontal -Vertical	Energy consumption (32% reduction) 50% of interior space between 500-750 lux	-solution for highly glazed buildings -effective for both high and low sun angles
2	(Shahin, 2019)	Smart Materials (polymer ETFE) – ETFE Diaphragm	The Barcelona Media – ICT Building	-solar heat gain - Indoor Air Quality (IAQ)	-20% less energy consumption (no occupants' interaction)	-smart material usage -less cost (ETFE) -less weight (ETFE)
3	(Shahin, 2019)	Shading screen as a curtain wall – micro-perforated glass & PTFE panels	Al-Bahar Towers	-Motion of the sun -solar heat gain -glare - IAQ	-50% less solar heat gain	-real building application
4	(Formentini & Lenci, 2018)	 SMA as energy-free thermal sensors and actuators	NA (mock-up)	-temperature -ventilation	-ventilated facade based on temperature changes	-designed for ventilation, opaque modules - material properties for actuation; not a mechanical device

Table 4.8 (continued)

5	(Di Salvo, 2018)	Arab mashrabiya pattern 240 Square Steel Diaphragms, photoelectric cells – the central computer Smart materials & Technology	Monde Arab be in Paris	-light	-providing thermal, visual comfort and well-being based on occupant's need -increasing sustainability by decreasing energy consumption and environmental impacts	-real building application -complex
6	(Tabadkani et al., 2019)	Origami/paper folding Timing-based hexagonal Kaleidocycle pattern 	Single office space in Tehran, Iran	Four extreme & mediate time hours -solstice and equinox days (12 pm)	-UDI Threshold: 300 lux -Acceptable Daylight Glare Probability: Lower than 0.35 -Comfortable Daylight Glare Index: Lower than 24 -Acceptable Glare Comfort: Imperceptible Glare -achieved the standards	-complex design

Table 4.8 (continued)

7	(Dawit Melaku, 2016)	 Aluminum sheet Diagonal pattern	Tropical Climate – Addis Ababa The large glazed 15-story building	-2.30-4.00 pm selected as critical hours	-providing thermal, visual comfort and well-being -east, west is effective with vertical shading -north, south is effective with horizontal shading -protecting 80% of direct solar radiation	-diagonal pattern for a clearer view -aluminum sheet (ease of fabrication, transportation, and workability)
8	(Pesenti et al., 2015)	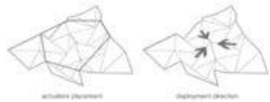 Origami with SMA wires and actuators (smart materials), Ron Resch pattern	NA	NA	-comparing different folding configurations for deformation percentage	-lightweight and flexible geometry -material properties for actuation; not a mechanical device -sustainable solution
9	(Nagy, Svetozarevic, Jayathissa, Begle, Hofer, Lydon, Willmann, & Schlueter, 2016)	 Facade with PV module, HoNr Building of ETH campus (full-scale)	-moderate climate Geneva, Switzerland	-shading, temperature, light levels	-providing thermal and visual comfort -25% energy saving	-modular; simple -control system for complexity -lightweight, simple structure for support -feasible for large-scale buildings -PV panels for energy

Table 4.8 (continued)

10	(S. M. Hosseini & Heidari, 2022)	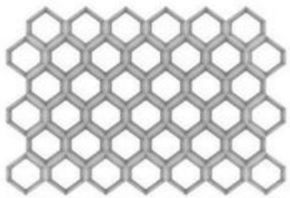 -hexagonal pattern -Orosi elements -3 layers (static-dynamic-static)	-hot desert climate, clear sky Yazd, Iran	-solstice and equinox days as critical days	-UDI: 5.61 times increase - Exceeded Useful Daylight Illuminance (EUDI): 91.8% decrease -preventing visual discomfort	-identify customized results -detect the designer's ambition -simple
11	(Khezri & Rasmussen, 2022)	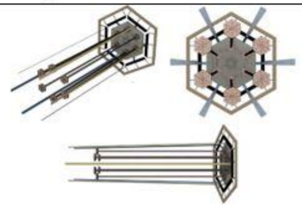 -SMA wires -buckling property	NA	NA	-shading -ventilation	- material properties for actuation -complex
12	(Ardabili, 2020)	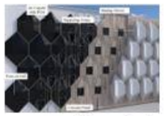 Smart bio-skin -PCM, SMA	-hot, humid region Kish Island, Iran	-control heat gain and infiltrated air	-energy consumption -comfort provision -43% thermal load reduction	- material properties for actuation -sustainable solution -not designed for the glazing facade

Table 4.8 (continued)

13	(S. M. Hosseini, Mohammadi, Schröder, & Guerra-Santin, 2021)	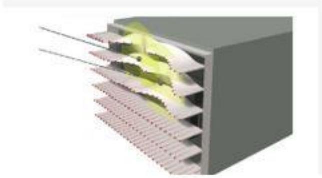	-hot desert climate, clear sky Yazd, Iran	-daylight -visual comfort -solstice and equinox days (9 am - 12 pm – 3 pm)	For south: -proper SDA 60.5% -UDI 90.47% -EUDI 2.94% For east and west -proper SDA 49.56% -UDI 83.28% -EUDI 13.1%	-multiple occupants' visual comfort improvement -facade with complex geometry
14	(Le-Thanh, Le-Duc, Ngo-Minh, Nguyen, & Nguyen-Xuan, 2021)	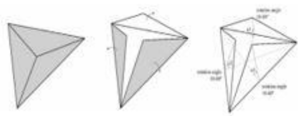 -origami paper	-hot and humid, tropical monsoon climate Ho Chi Minh City, Vietnam	-shape -daylight -buildings orientation	-reduction of annual sunlight exposure by 9% to 42%	-achievement of credits for LEED v4 -simple
15	(Cimmino, Miranda, Sicignano, Ferreira, Skelton, & Fraternali, 2017)	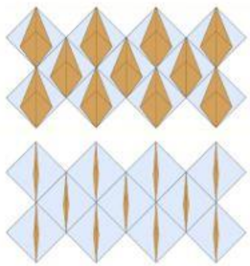 -tensegrity	-a building on the campus of the University of Salerno	-wind -solar energy	-wind harvest -solar energy production	-reduction of carbon-dioxide emissions -reduction of energy consumption -not designed for the glazing facade

Table 4.8 (continued)

16	(Rizi & Eltaweel, 2021)	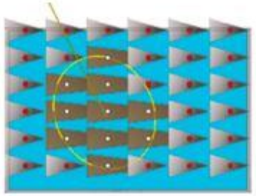	- Tehran, Iran	-heat gain -daylight -solstice and equinox days	- improved visual comfort by 76% -improved heat gain by 60%	-partial view of outside
17	(S. M. Hosseini, Mohammadi, Schröder, & Guerra-Santin, 2020)	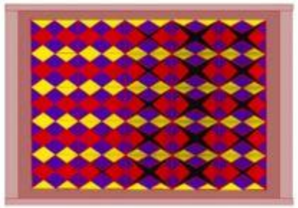 -Orosi elements	-hot desert climate, clear sky Yazd, Iran	-daylight -visual comfort -solstice and equinox days (9 am - 12 pm – 3 pm)	-UDI -DA -EUDI -colored glass facade with a 0-45 pivot angle is the most effective	-provide aesthetic and psychological effects, daylight controller, privacy, view to the outside, religious belief, repelling insect
18	(S. M. Hosseini et al., 2019)	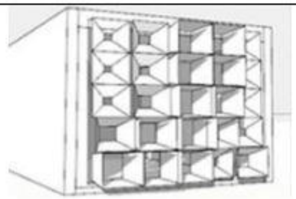 -2d and 3d scale facades	-hot desert climate, clear sky Yazd, Iran	-visual comfort -heat gain -solstice and equinox days (9 am - 12 pm – 3 pm)	-3d scale configuration is more effective	-less complex

Table 4.8 (continued)

19	(Tabadkani, Banihashemi, & M. R. Hosseini, 2018)	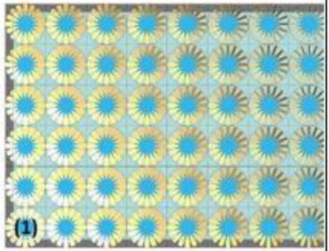 -Rosetta modules	-Tehran, Iran	-visual comfort	- 10% decrease in visual discomfort -glare-free indoor	-achievement of credits for LEED v4
20	(Yi, Sharston, & Barakat, 2019)	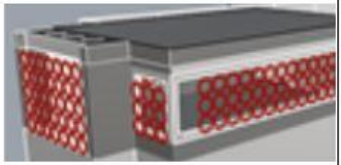 -auxetic shading structure	-Miami; Champaign; Sitka, US	-illuminance levels -glare probability - December 21st -for Miami; Champaign;(8 a.m.-12 p.m.-4 p.m.) for Sitka; Champaign;(9 a.m.-12 p.m.-3 p.m.)	-effective in preventing excessive sunlight	-complex

Table 4.8 (continued)

21	(Michael, Gregoriou, & Kalogirou, 2018)	 -ETFE as material	-Nicosia, Cyprus	-daylight factor -uniformity daylight factor -different angles for modules -solstice and equinox days	-allowing natural daylight -decreasing glare	-simple -possible to provide a holistic approach to the environment
22	(Mahmoud & Elghazi, 2016)	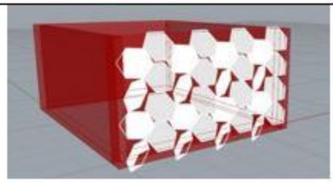 -Hexagonal	-hot, humid climate Malaysia	-rotational movement -translation movement -solstice and equinox days (9 a.m.-12 p.m.-3 p.m.)	Rotational motion -50% daylight improvement in summer & spring -30% in daylight improvement in autumn and winter	-basic geometry properties
23	(Ahmed, Abdel-Rahman, Bady, & Mahrous, 2016)	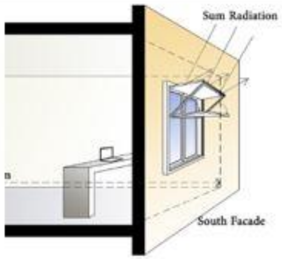	-New Borg Al-Arab city, Alexandria, Egypt	-20th of July to 20th August 2015	-2-3°C decrease in summer -20% energy saving 15% relative humidity decrease	-less complex -movement with motors

Table 4.9 Buildings with kinetic shading and their properties, adapted from (Böke et al., 2020)

#	Building & Type	Facade Material Technology	Functions	Location	User Control
1	Tringle Cologne /Office	Lamella in double facade	-Solar Shading -Glare Protection -Daylight Radiation Control -Visual Contact Control	Internal louvers	Yes
2	Q1 Thyssen Krupp Headquarter /Office	Metal-glass layer, vertically oriented metal louvers (vertical lamella)	-Solar Shading -Glare Protection -Visual Contact Control	Exterior Envelope	Yes
3	Oval Offices /Office	Shutters	-Solar Shading -Glare Protection -Visual Contact Control	Exterior Envelope	Yes – for each room
4	Z_Zwo /Office	External aluminum blinds (jalousie)	-Solar Shading -Light Deflection -Glare Protection -Daylight Radiation Control -Visual Contact Control -Sound Insulation	External blinds	Yes
5	KFW Westerkade /Office	Flared elements & colored motor-driven ventilation flaps / Lamellas	-Solar Shading -Glare Protection -Daylight Radiation Control -Ventilation -Visual Contact Control	Exterior Envelope	Yes
6	Post Tower	Lamellas	-Solar Shading -Glare Protection -Visual Contact Control	Exterior Envelope	NA

Table 4.9 (continued)

7	Kap am Südkai	Lamella	-Solar Shading -Light Deflection -Daylight Radiation Control -Visual Contact Control	Exterior Envelope	Yes – for each room
8	HDI Gerling Headquarters	External Sun Blinds	-Solar Shading -Light Deflection -Daylight Radiation Control	External blinds	NA
9	Horizon L'Oréal Headquarters	-Internal sun shading lamellas -Double facade (Sun shading lamellas)	-Solar Shading (E) -Light Deflection (E) -Glare Protection (I) -Visual Contact Control (I)	Internal lamellas & external facade	Yes
10	Vodafone Campus / Office	-internal blinds with automation system/sun shading lamellas	-Solar Shading -Glare Protection -Daylight Radiation Control -Visual Contact Control	Internal blinds	NA
11	Case Capricorn House	-sun shading lamellas	-Cooling, heating & ventilation -Solar Shading -Light Deflection -Glare Protection -Daylight Radiation Control -Visual Contact Control -Artificial light	Exterior Envelope	

4.3 Simulation Results

This chapter covers the simulation results of the ground and first floors of the focused section, i.e., the South dining halls. They were completed separately for each floor. Illuminance, daylight factor, annual daylight for UDI, and adaptive comfort for operative temperatures were completed for the base case and all design case scenarios. There are 90 sensors of measurements for the ground floor and 121 for the first floor.

After the base case results, the comparison between the translucent and reflective material, i.e., ETFE and painted metal, is discussed. Design cases are presented according to the selected material. Finally, all scenarios are compared.

4.3.1 Calibration Results of the Field Measurements and Simulations

i. Illuminance Results

The comparison between field measurements and the Velux Daylight Visualizer was completed as the initial step for the calibration. As seen in Table 4.7 and Figure 4.1, the illuminance results are very similar, changing from approximately 100 lux to 1500 lux. Therefore, it is concluded that Velux's simulation results can be considered a comparison for Honeybee for June.

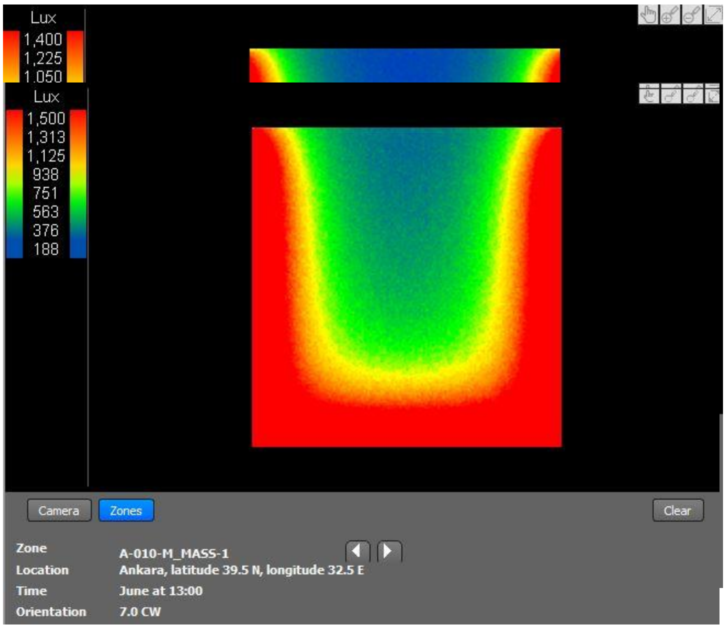

Figure 4.1 Illuminance Results of the First Floor of the Base Case on the 21st of November at 1 pm, in Velux Daylight Visualizer

Figure 4.2 Illuminance Results of the First Floor of the Base Case on the 21st of June at 1 pm, in Velux Daylight Visualizer

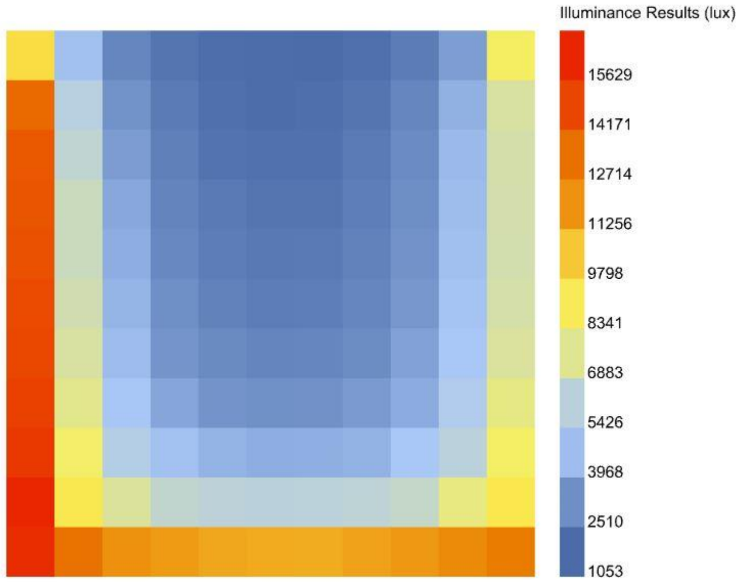

Figure 4.3 Illuminance Results of the First Floor of the Base Case on the 21st of June at 1 pm, in Honeybee

ii. Temperature Results

Table 4.2 shows the field measurements of the first floor. These results were compared to the operative temperature data of the same date obtained from Honeybee, which can be seen in Figure 4.4. Approximately 1.5 times higher results occurred, so the results are calibrated accordingly.

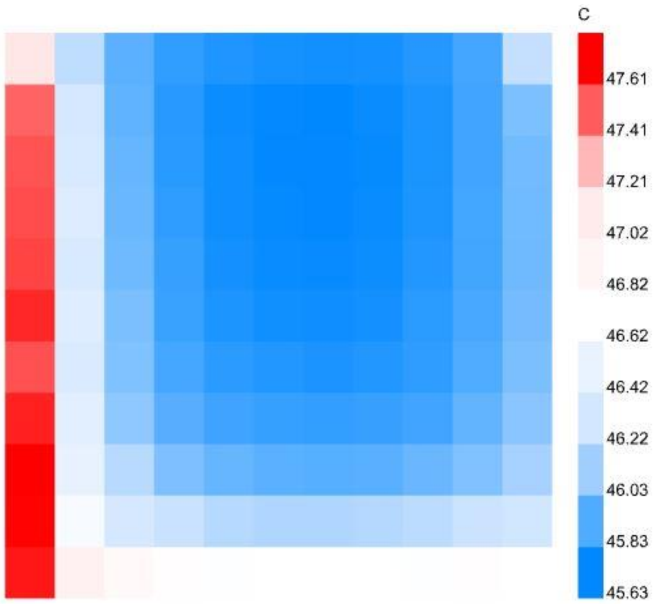

Figure 4.4 Operative Temperature Results of the First Floor of the Base Case on the 30th of July at between 11 am to 14 pm, in Honeybee

4.3.2 Base Case Results

As the focus study, the existing building was modeled in Rhinoceros for the ground and first floors of the South section. It was defined as Grasshopper interface with the material properties presented in the previous chapter.

i. Ground Floor

The illuminance results vary between 105 and 930 lux for the existing ground floor, as seen in Figure 4.5. Near glazing, the sensors have higher values, while the middle and inner parts have lower ones. Nineteen sensors are in the range of the desired illuminance values. Twenty-eight sensors are below 200 lux, while 43 are above 300 lux, as seen in Table 4.10. It means that the dining hall has excess daylight for most of the sensors locations, with approximately 48% more light than defined.

Figure 4.6 shows the ground floor's operative temperatures, with 26.4 °C as the highest and 25.7 °C as the lowest for sensors. Similar to the illuminance results, the results are higher for the sensors close to the windows. The lowest values are obtained in the middle of the hall. There are 71 sensors in the comfortable range. According to Table 4.11, none of the sensors are below the threshold. On the other hand, 19 sensors are above the upper limit. Hence, approximately 79% of the sensors are in the comfort range, which can be interpreted as the dining hall is comfortable in terms of operative temperature.

Daylight factor results can be seen in Figure 4.7 Daylight factor results of the ground floor of the base case These results show 36 sensors are between 2% and 5%. While 4 are below the threshold and 50 are above the threshold, as in Table 4.12. The light is higher than the desired range in most areas, with a ratio of approximately 56%.

According to Figure 4.8, UDI results of the dining hall vary between 7% and 97%. The inner parts of the dining hall have more useful daylight during the year, while the ones near the glazing have less. In other words, 93% of daylight at the periphery is not necessary, and only 7% is. This is because of the excessive daylight amount, as the illuminance and daylight factor results show. According to Table 4.13, 35 sensors are greater than or equal to 50% UDI, corresponding to almost 39% of the total area.

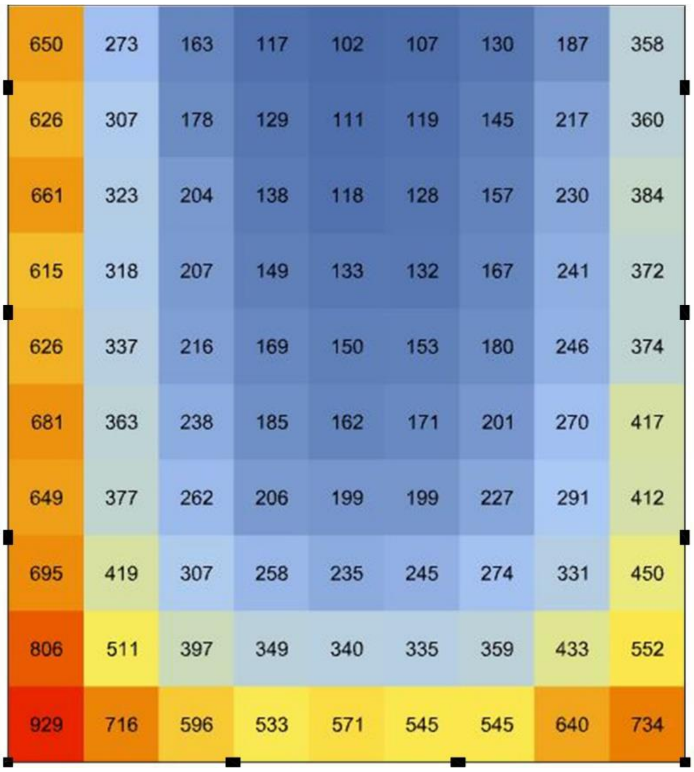

Figure 4.5 Illuminance results in lux of the ground floor of the base case on the 8th of June at 1 pm

Table 4.10 Number of sensors corresponding to the illuminances range of the ground floor of the base case

Number of sensors	Illuminance values (lux)
28	<200
19	≥200, ≤300
43	>300

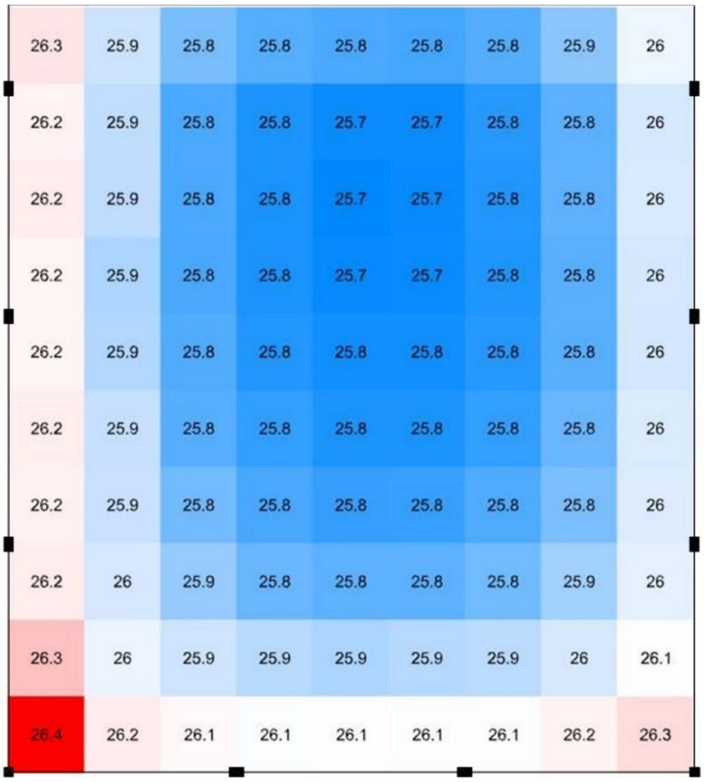

Figure 4.6 Operative temperature results in °C of the ground floor of the base case between 15/5 to 15/6 at 1 pm

Table 4.11 Number of sensors corresponding to the operative temperature range of the ground floor of the base case

Number of sensors	Operative temperature values (°C)
0	<23
71	≥23, ≤26
19	>26

ii. First Floor

Figure 4.9 shows the illuminance results, varying between 105 lux and 1399 lux. Similar to the ground floor, the middle part has lower results, while the sensors near the windows have higher ones, especially the west of the hall. As can be seen in Table 4.14, there are 22 sensors in the defined range, while 27 of them are below the threshold. Almost 60% of the sensors, corresponding to 72, are above the threshold. Therefore, it is observed top floor has a very high daylight amount for most of the areas.

The operative temperatures simulated for the first ground are presented in, Figure 4.10. The highest value is 26.7 °C while the lowest one is 25.6 °C. The pattern is identical to the illuminance results, meaning the areas near the windows have higher values, and the inner parts have lower. There is no sensor below 23 °C, as shown in Table 4.15. However, 24 of them are above the comfort range. Ninety-seven sensors are in the desired range, which is proximately 80% of the sensors.

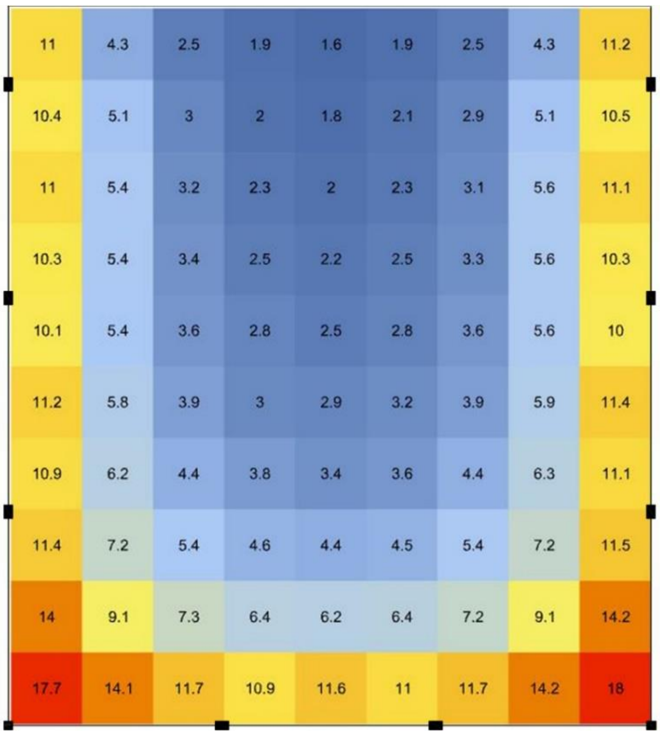

Figure 4.7 Daylight factor results of the ground floor of the base case

Table 4.12 Number of sensors corresponding to the daylight factor range of the ground floor of the base case

Number of sensors	Daylight factor values
4	<2%
36	≥2%, ≤5%
50	>5%

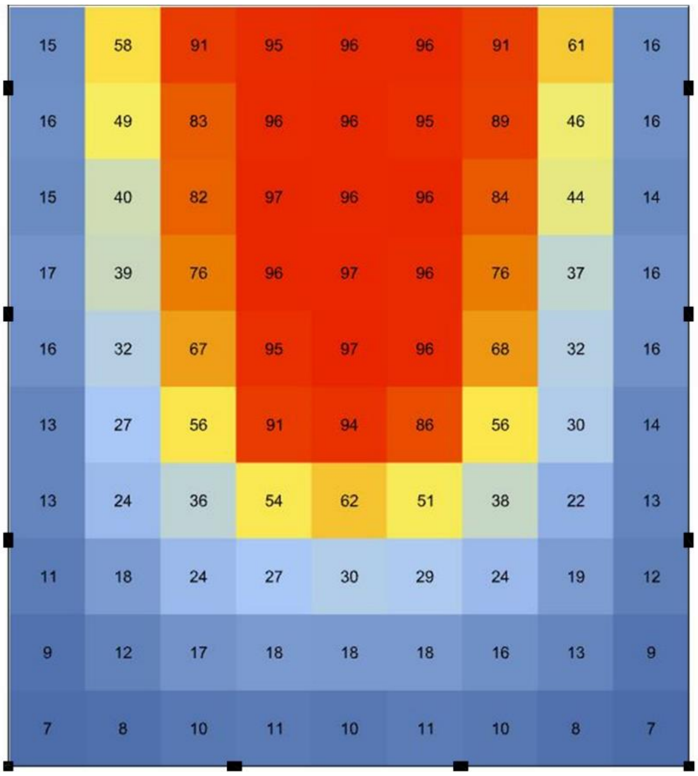

Figure 4.8 UDI Results of the ground floor of the base case

Table 4.13 Number of sensors corresponding to the UDI values of the ground floor of the base case

Number of sensors	UDI values
55	<50%
35	≥50%

Figure 4.11 presents the daylight factor results. Forty of the sensors are between 2% and 5%. There are 4 sensors below 2% and 77 sensors above %5, as it is shown in Table 4.16. According to these results, approximately 64% of the sensors receive high daylight.

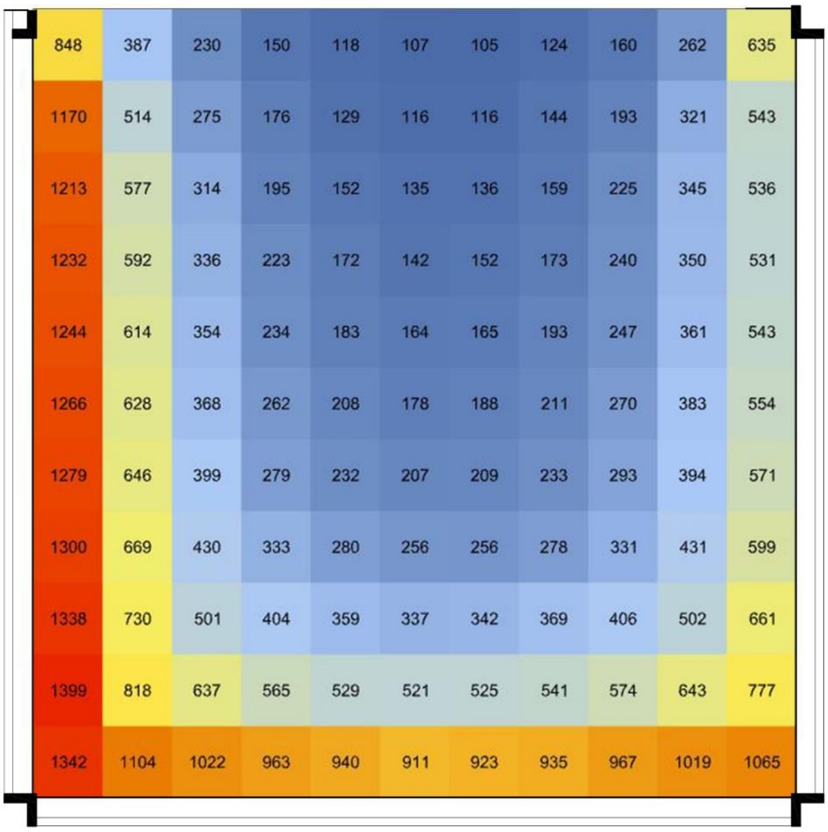

Figure 4.9 Illuminance results in lux of the first floor of the base case on the 8th of June at 1 pm

Figure 4.12 shows that UDI results change between 6% and 96%. A similar pattern can be seen as the ground floor results. The sensors near the glazing have less UDI value because of having more daylight, and the inner parts have a higher UDI percentage during the year. Table 4.17 shows there are 58 sensors equal or greater than 50% of UDI. This means approximately 48% of the total sensors are in the desired range.

Table 4.14 Number of sensors corresponding to the illuminances range of the first floor of the base case

Number of sensors	Illuminance values (lux)
27	<200
22	≥200, ≤300
72	>300

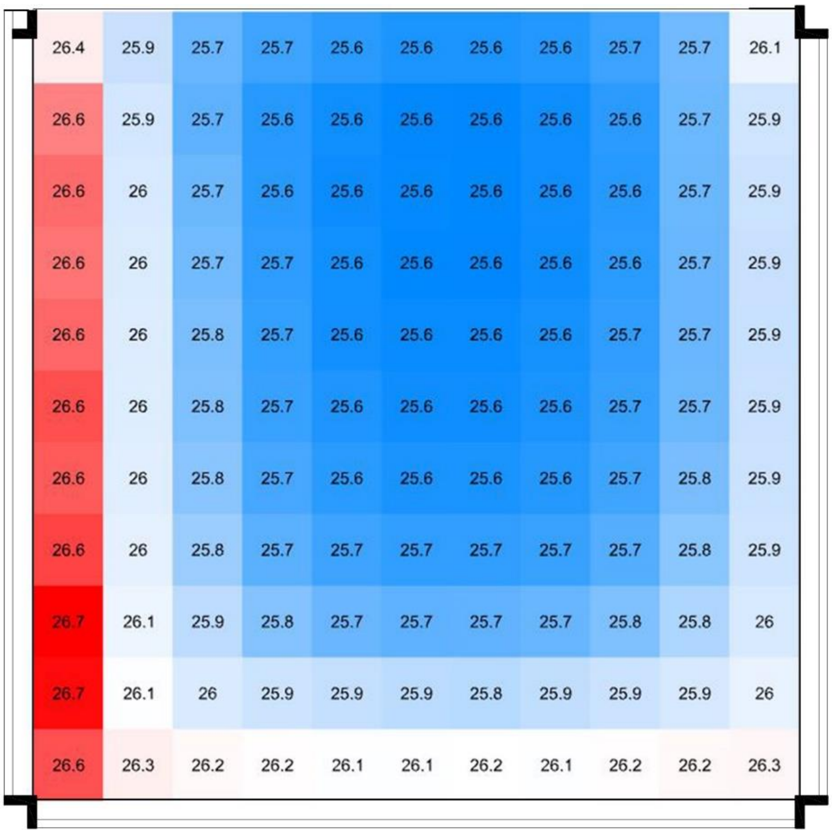

Figure 4.10 Operative temperature in °C results of the first floor of the base case between 15/5 to 15/6 at 1 pm

Table 4.15 Number of sensors corresponding to the operative temperature range of the first floor of the base case

Number of sensors	Operative temperature values (°C)
0	<23
97	≥23, ≤26
24	>26

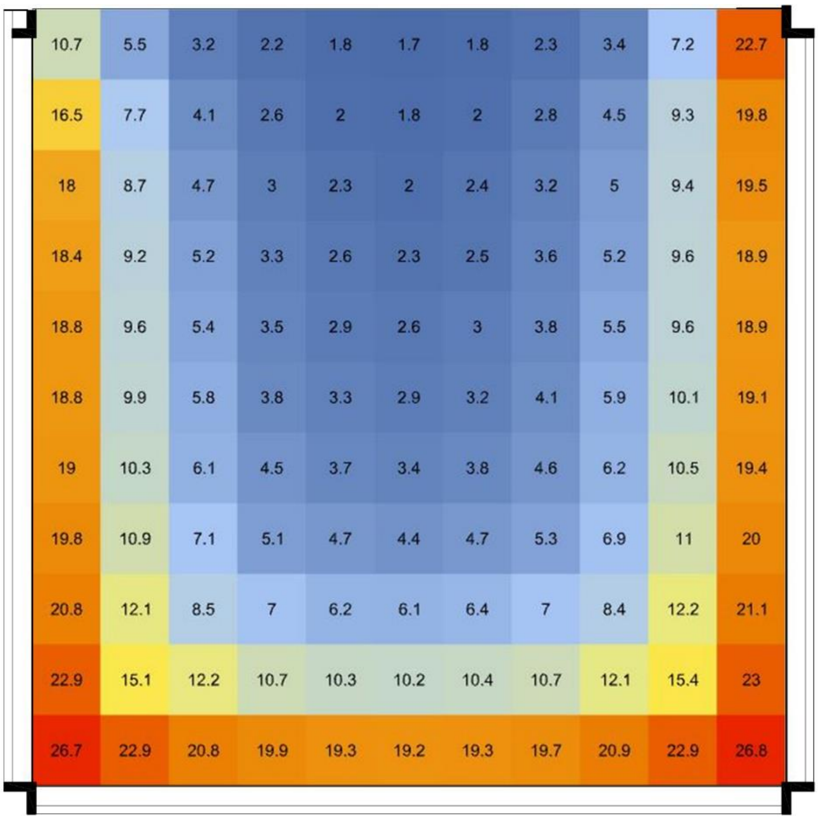

Figure 4.11 Daylight factor results of the first floor of the base case

Table 4.16 Number of sensors corresponding to the daylight factor range of the first floor of the base case

Number of sensors	Daylight factor values
4	<2%
40	≥2%, ≤5%
77	>5%

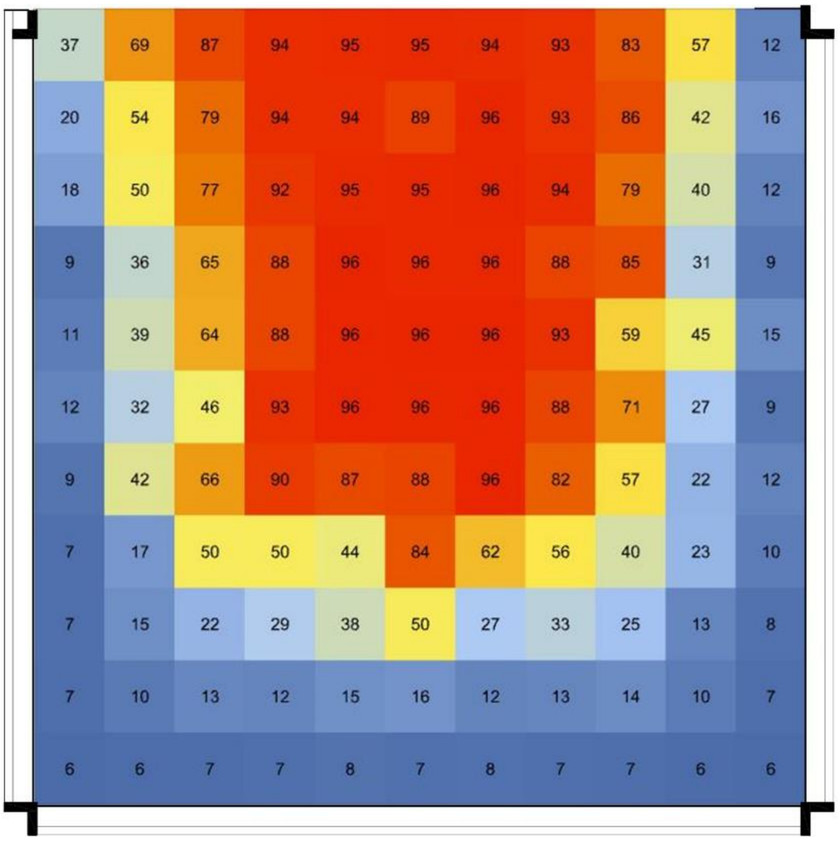

Figure 4.12 UDI Results of the first floor of the base case

Table 4.17 Number of sensors corresponding to the UDI values of the first floor of the base case

Number of sensors	UDI values
63	<50%
58	≥50%

4.3.3 Comparison of ETFE and Metal Modules

Two different materials, ETFE as the translucent material and painted metal as the reflective one, were applied to one of the selected kinetic morphologies', i.e., design case 2, and the one that is more efficient results was chosen as the material for all design scenarios. However, as can be seen in Figure 4.13 and Figure 4.14, both results have 25 sensors between 200 lux and 300 lux. Therefore, ETFE was chosen for the rest simulations since it is a translucent material and does not block the outside view completely.

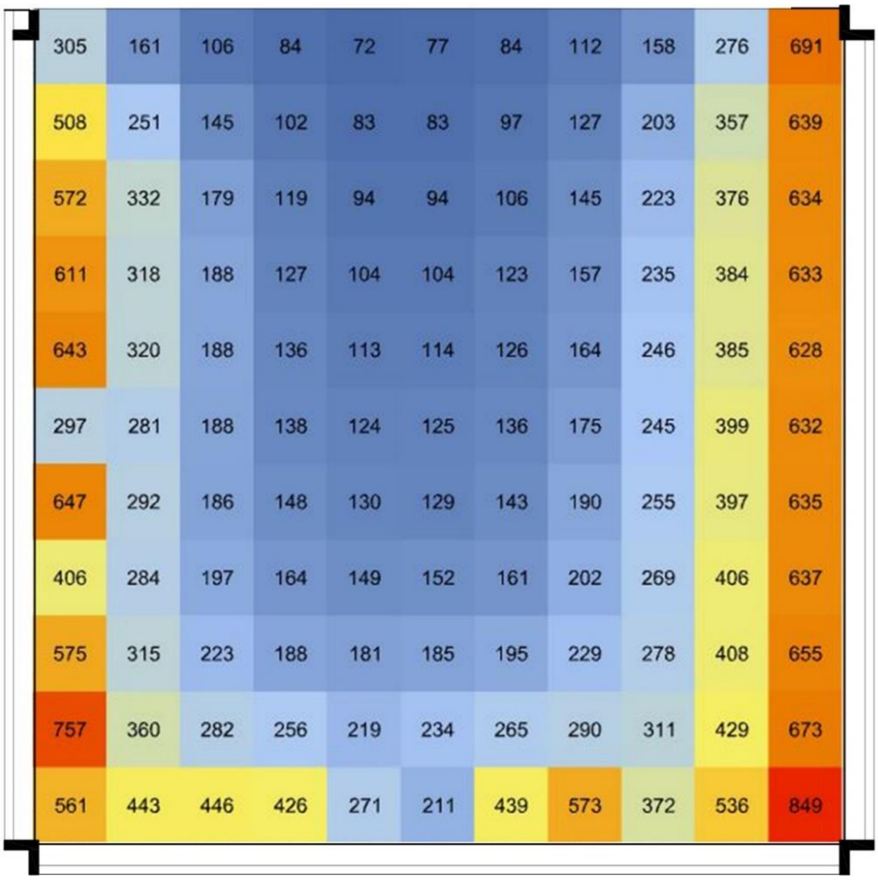

Figure 4.13 Illuminance results in lux of the first floor of the 2x2 modules with metal on the 8th of June at 1 pm

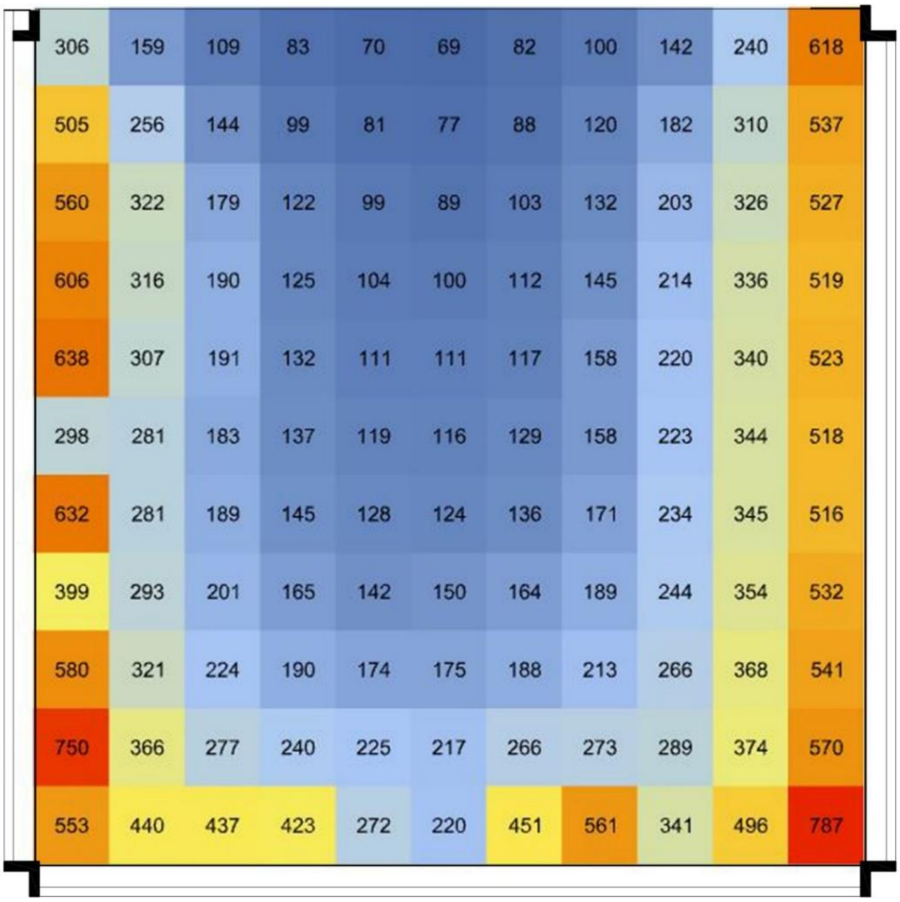

Figure 4.14 Illuminance results in lux of the first floor of the 2x2 modules with ETFE on the 8th of June at 1 pm

4.3.4 Fixed shadings

Fixed shadings with ETFE as the material were applied to both floors of the south section. These were modeled in Rhinoceros and defined to Grasshopper interface as shadings. All existing building materials were defined as the same as the base case. The results are presented in the following sections.

i. Ground Floor

Fixed vertical fin shadings were integrated into the west facade as stated in the methodology. The model of the ground floor of design case 1, created with Grasshopper interface, can be seen in Figure 4.15.

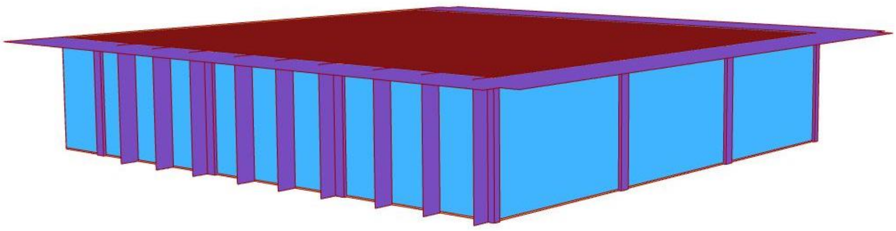

Figure 4.15 Model of the ground floor of design case 1

The illuminance results of the ground floor of design case 1 are presented Figure 4.16. According to these results, 130 lux and 982 lux are the lowest and the highest values, respectively. Twenty-one sensors are in the desired range, as stated Table 4.18. The sensors above the threshold are 55, while the ones below it are 14. In this case, it can be concluded that almost 62% of the sensors receive an excessive amount of daylight. In addition, sensors near glazing have more daylight in comparison to the inner parts.

Figure 4.17 shows the operative temperature results of the ground floor of design case 1. The highest value is 25.9 °C while the lowest one is 25.2 °C. According to Table 4.19, all the sensors are in the desired range.

According to the daylight factor results presented in Figure 4.18, 35 sensors are in the desired range. On the other hand, none of the sensors are below 2%, meaning there are no very dark areas, while 55 sensors have more daylight than the threshold, according to Table 4.20. The daylight amount is higher for the areas near the windows.

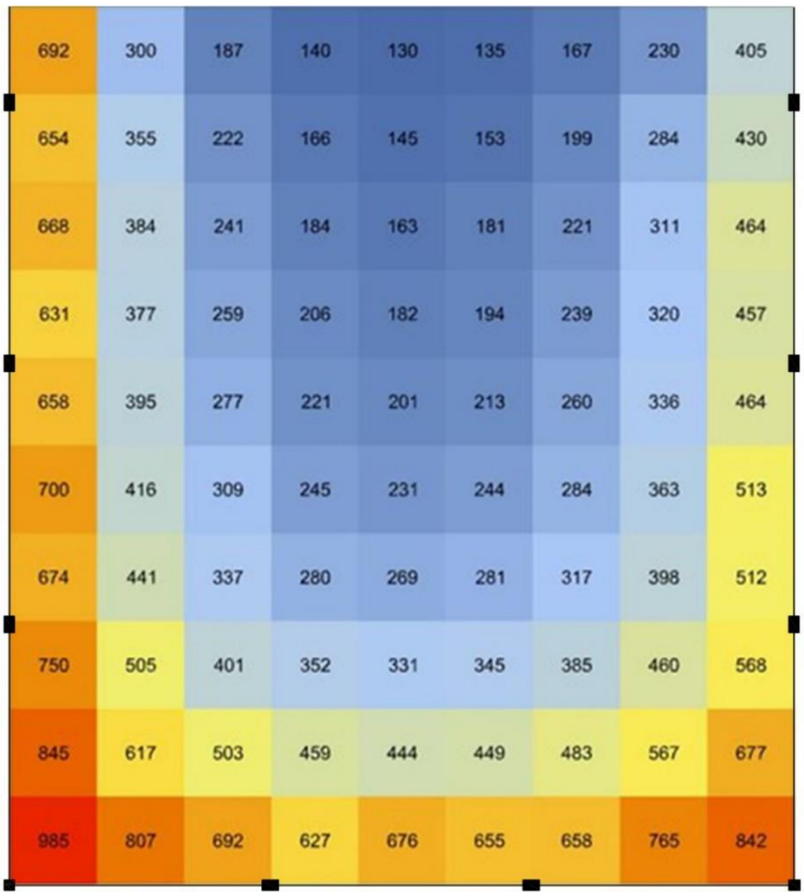

Figure 4.16 Illuminance results in lux of the ground floor of the design case 1 on the 8th of June at 1 pm

Table 4.18 Number of sensors corresponding to the illuminances range of the ground floor of the design case 1

Number of sensors	Illuminance values (lux)
14	<200
21	≥200, ≤300
55	>300

UDI results of design case 1 change between 6% and 97%. The sensors near glazing have less UDI during the year, probably due to the extreme lighting conditions, as given in Figure 4.19. According to Table 4.21, 23% of the sensors provide the desired UDI value, which is 21 sensors.

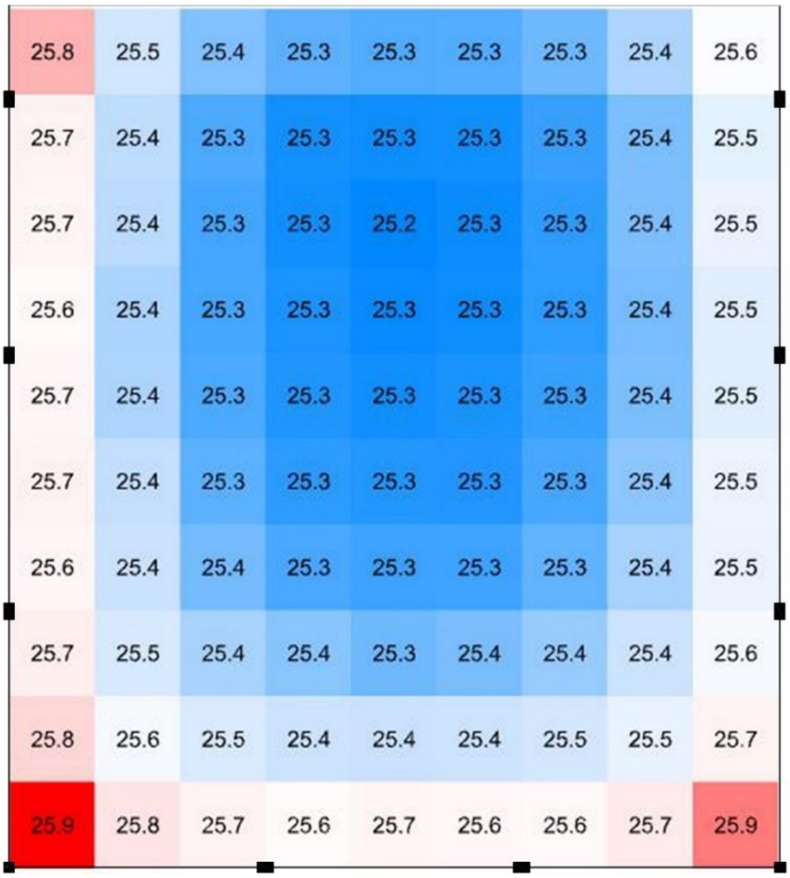

Figure 4.17 Operative temperature results in °C of the ground floor of the design case 1 between 15/5 to 15/6 at 1 pm

Table 4.19 Number of sensors corresponding to the operative temperature range of the ground floor of the design case 1

Number of sensors	Operative temperature values (°C)
0	<23
90	≥23, ≤26
0	>26

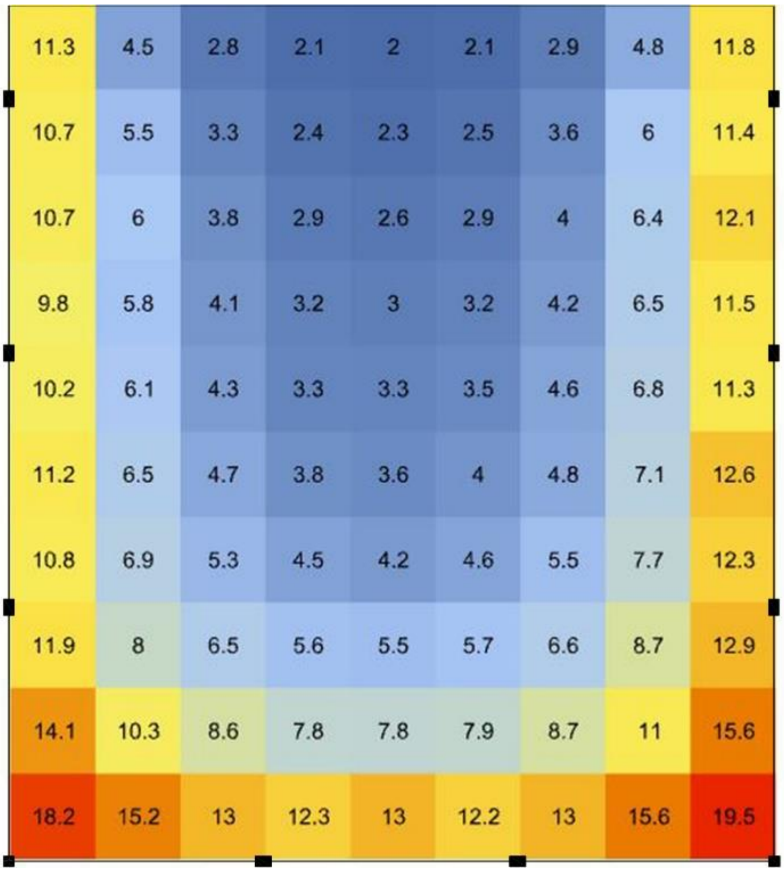

Figure 4.18 Daylight factor results of the ground floor of the design case 1

Table 4.20 Number of sensors corresponding to the daylight factor range of the ground floor of the design case 1

Number of sensors	Daylight factor values
0	<2%
35	≥2%, ≤5%
55	>5%

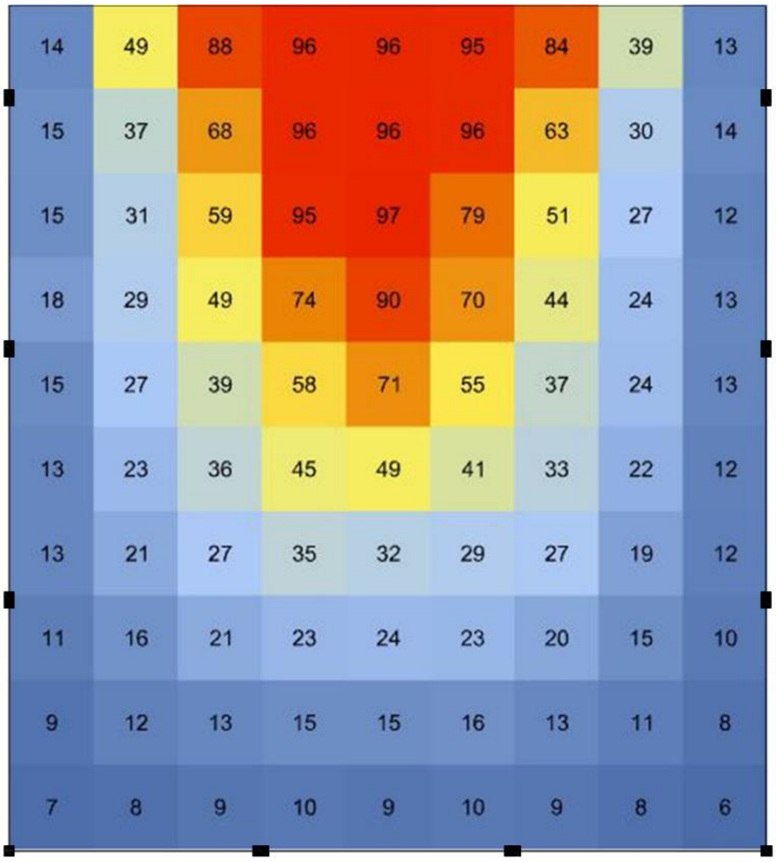

Figure 4.19 UDI results of the ground floor of the design case 1

Table 4.21 Number of sensors corresponding to the UDI values of the ground floor of the design case 1

Number of sensors	UDI values
69	<50%
21	≥50%

ii. First Floor

Figure 4.20 shows the model of design case 1, which has fixed shadings for the south and west facade.

Figure 4.21 presented 108 lux is the lowest value while 1358 lux is the highest for the first floor of design case 1, as the illuminance results. Sensors near windows are higher than the other ones. Table 4.22 shows there are 24 sensors between the desired range. On the other hand, 73 sensors are above the desired value, approximately 60% of the total. It is deduced that most of the areas have excessive daylight.

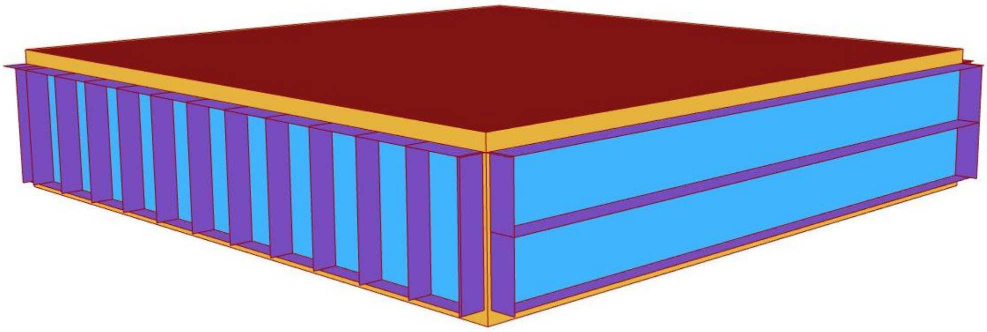

Figure 4.20 Model of the first floor of design case 1

The operative temperature is presented in Figure 4.22. According to these results, the maximum temperature is 26.6 °C, and the minimum one is 25.5°C. The west part of the hall has higher values than the other parts. Table 4.23 shows that there is no sensor below 23 °C. Majority of the sensors, i.e., 106, are in the desired range with a ratio of almost 88%. Fifteen sensors are above 26 °C. It can be concluded that most of the dining hall is comfortable.

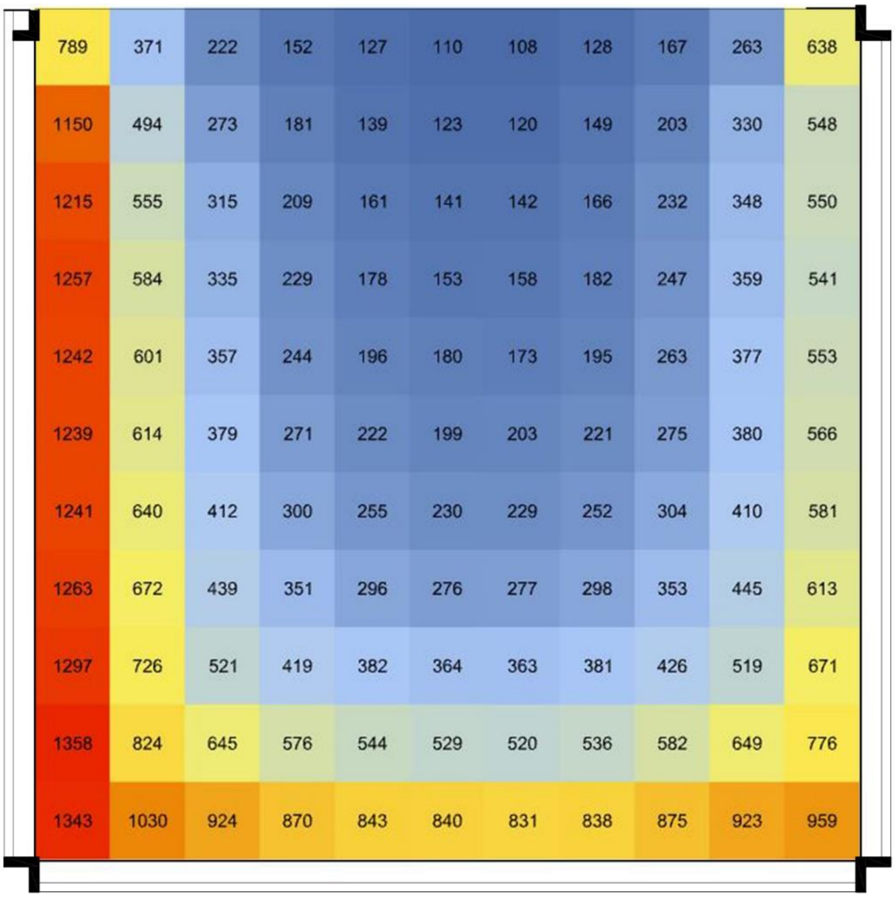

Figure 4.21 Illuminance results in lux of the first floor of the design case 1 on the 8th of June at 1 pm

Table 4.22 Number of sensors corresponding to the illuminances range of the first floor of the design case 1

Number of sensors	Illuminance values (lux)
24	<200
24	≥200, ≤300
73	>300

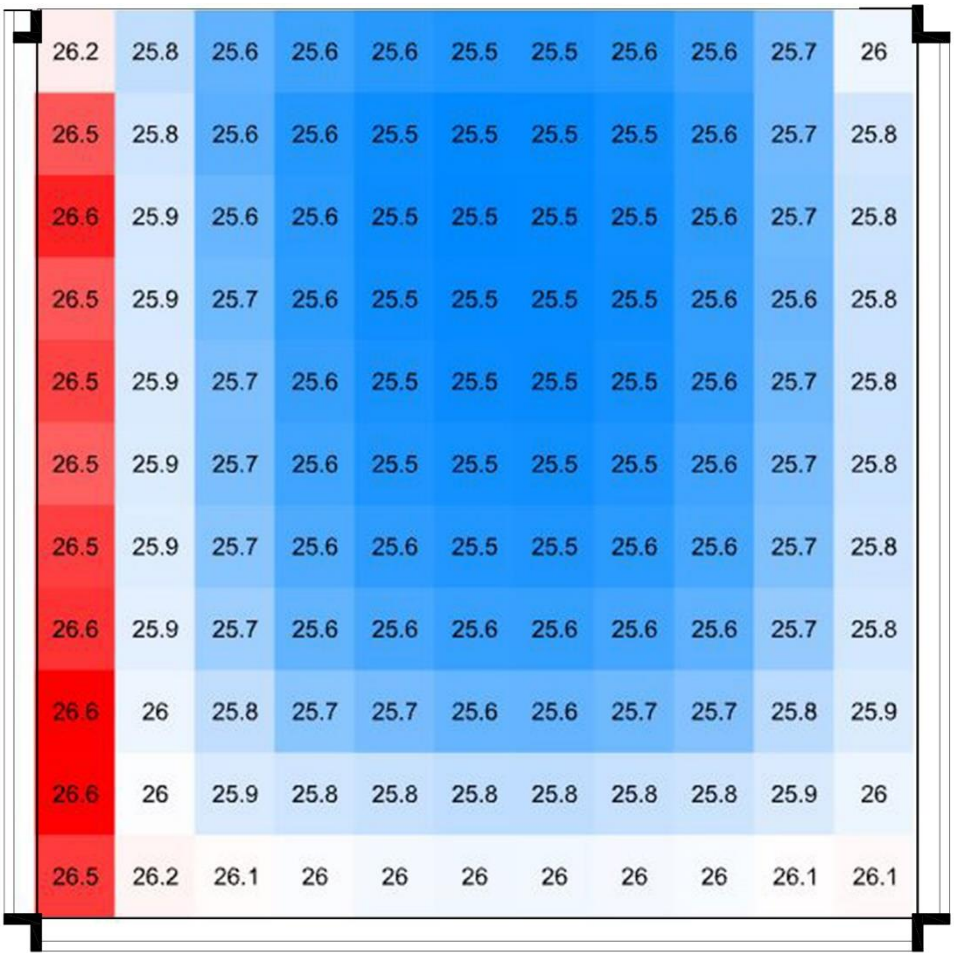

Figure 4.22 Operative temperature results in °C of the first floor of the design case 1 between 15/5 to 15/6 at 1 pm

Table 4.23 Number of sensors corresponding to the operative temperature range of the first floor of the design case 1

Number of sensors	Operative temperature values (°C)
0	<23
106	≥23, ≤26
15	>26

According to daylight factor results presented in Figure 4.23 and Table 4.24, 40 sensors are between 2% and 5%. Seventy-seven sensors are above the threshold while 4 of them are below. The daylight is higher approximately 64% of all sensors.

The results of Figure 4.24 show UDI vary between 6% and 97%. The sensors near the windows have less UDI value since the daylight amount is higher these parts. On the other hand, the inner parts have more useful daylight. Fifty-eight sensors are in the desired value, corresponding 48% of the total sensors, as shown in Table 4.25.

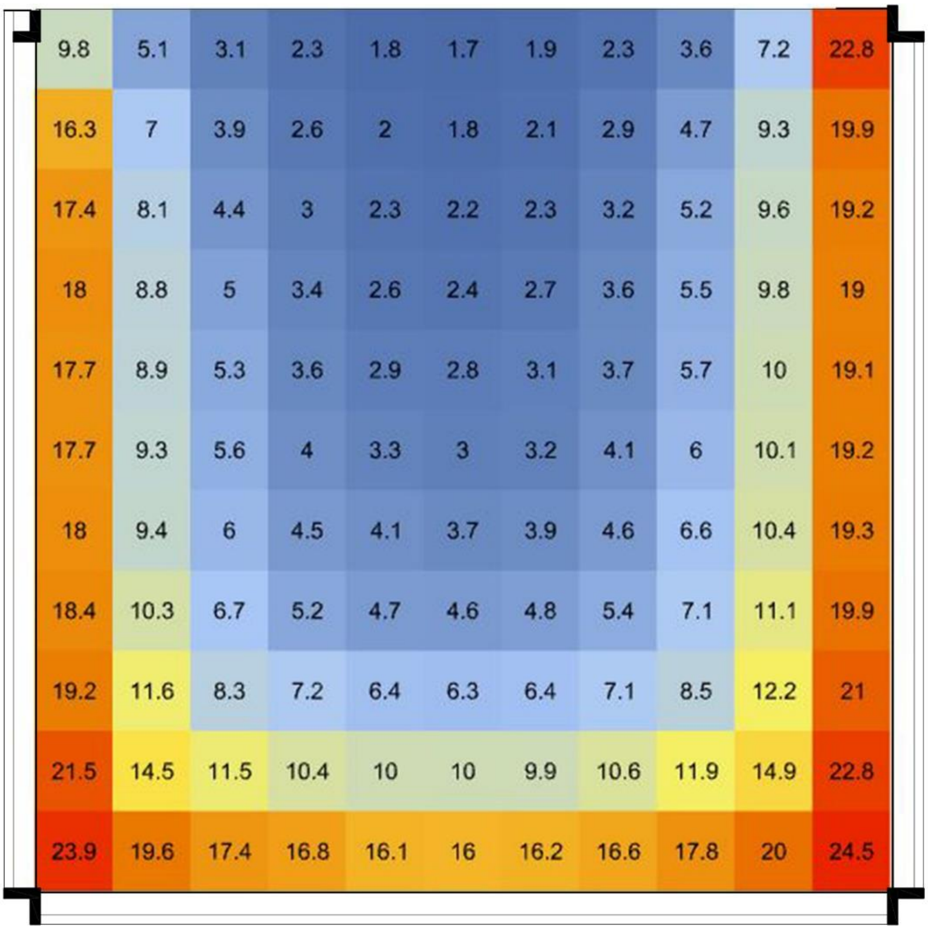

Figure 4.23 Daylight factor results of the first floor of the design case 1

Table 4.24 Number of sensors corresponding to the daylight factor range of the first floor of the design case 1

Number of sensors	Daylight factor values
4	<2%
40	≥2%, ≤5%
77	>5%

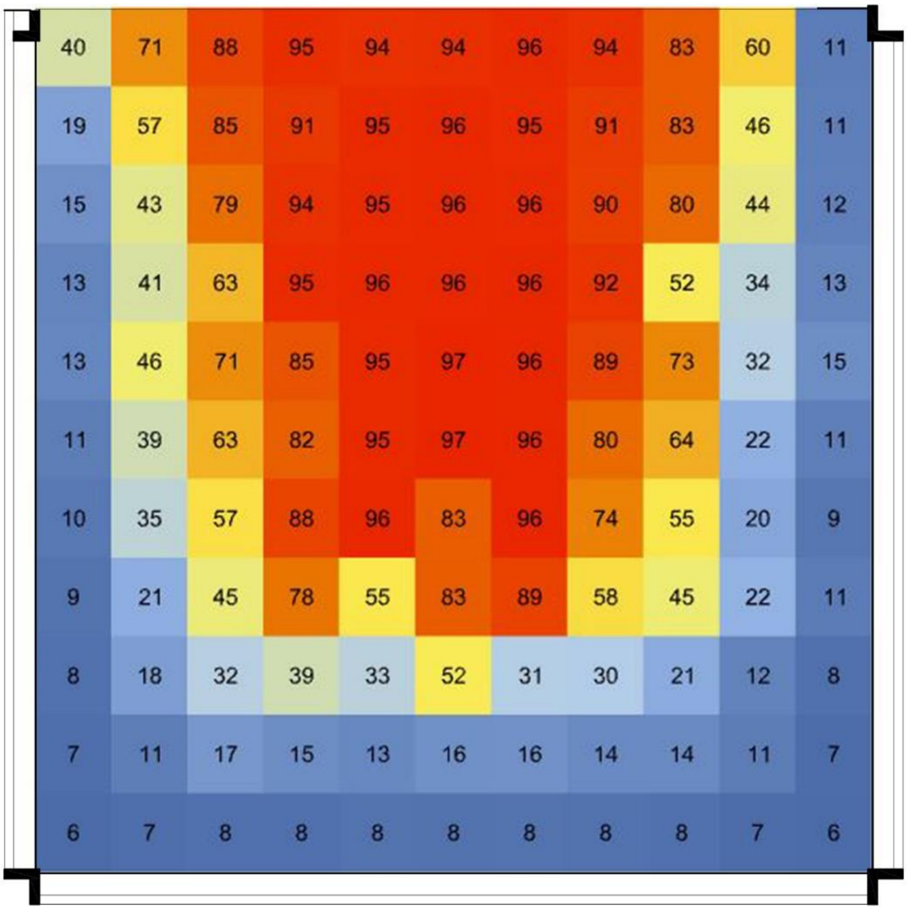

Figure 4.24 UDI results of the first floor of the design case 1

Table 4.25 Number of sensors corresponding to the UDI values of the first floor of the design case 1

Number of sensors	UDI values
63	<50%
58	≥50%

4.3.5 Kinetic Facade with Square Modules

Design case 2 is consisted of kinetic facade square modules with 2x2 meters, moving horizontally for the south and vertically for the west facades. It is a design adapted from the proposal of W. T. Sheikh & Asghar (2019). ETFE was used as the material for the modules. Other materials were defined as they are in the base case scenario. The concrete railing in front of the windows has been removed to apply the modules. All results of design case 2 are explained in the following sections.

i. Ground Floor

The optimized kinetic modules of the building's south and west facade can be seen in Figure 4.25.

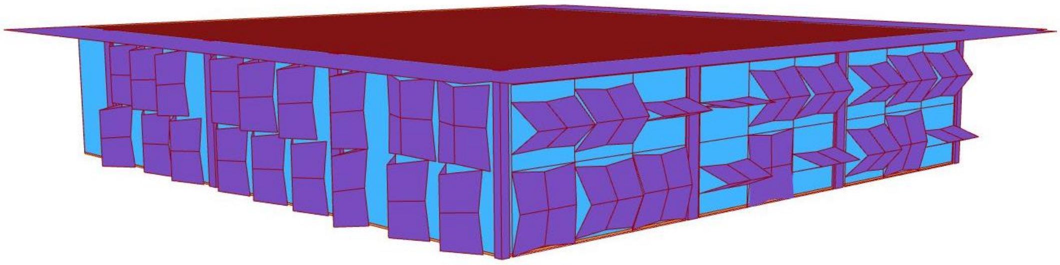

Figure 4.25 Model of the ground floor of design case 2

The illuminance results are introduced in Figure 4.26. According to these, there are two points that have the highest values with 652 lux. There are no applied modules on these windows; hence, they have more daylight than the defined range. The inner parts are darker since the sensors near the grid have less light, which means the inner parts may not have useful daylight. However, these facade openings are the best scenario for the interior since it is optimized. Table 4.26 shows that 31 sensors are in the desired range, while 34 are below and 25 are above. Most areas are darker, with a ratio of approximately 38%.

According to the operative temperature results in Figure 4.27, after implementing the kinetic facade with square modules, the maximum temperature is 24.7 °C while the minimum is 24.1 °C. All the sensors are in the range between 23 °C and 26 °C, as can be seen in Table 4.27. Therefore, it can be concluded that the room is comfortable in terms of temperature.

The daylight factor has the lowest values in the center of the room while the higher ones near the glazing, as seen in Figure 4.28. There are 55 sensors in the desired range in terms of daylight factor, as can be seen Table 4.28. Seven of the sensors are below the threshold, and 28 are above. Consequently, it can be said that most of the room is in the acceptable daylight factor range, with a ratio of 61%.

UDI results change between 9% and 97%, as seen in Figure 4.29. The middle part has more useful daylight during the year. On the other hand, the sensors near the glazing have less useful daylight. There are 53 sensors equal or greater than 50% of UDI, as seen in Table 4.29. So, it can be concluded 59% of the total area is in the desired range during the year.

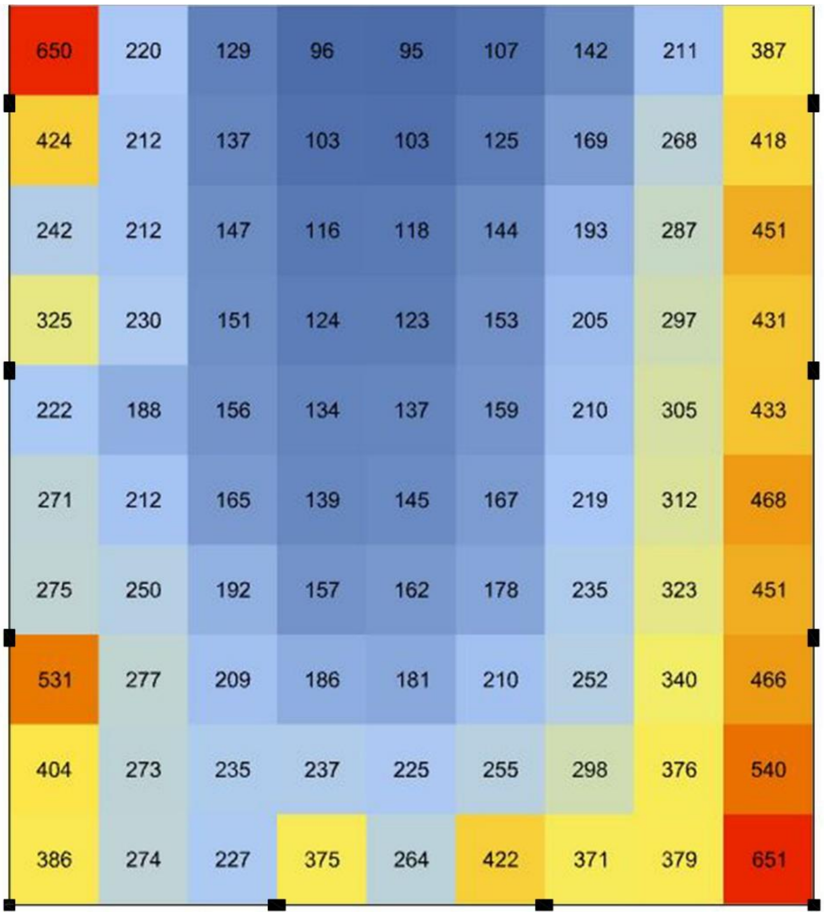

Figure 4.26 Illuminance results in lux of the ground floor of the design case 2 on the 8th of June at 1 pm

Table 4.26 Number of sensors corresponding to the illuminances range of the ground floor of the design case 2

Number of sensors	Illuminance values (lux)
34	<200
31	≥200, ≤300
25	>300

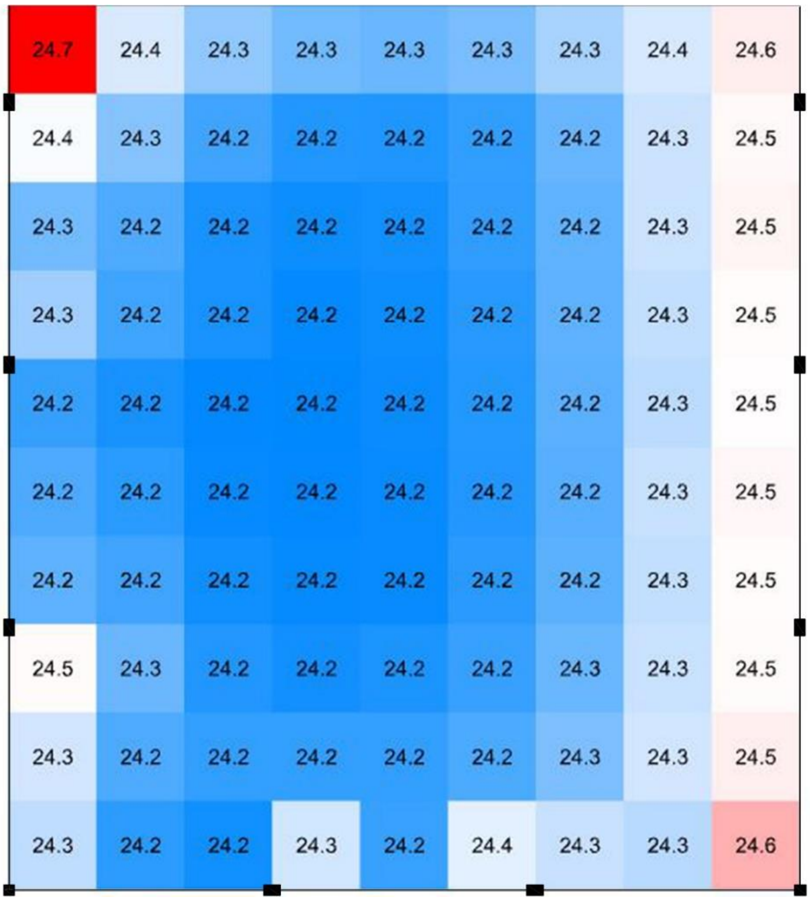

Figure 4.27 Operative temperature results in °C of the ground floor of the design case 2 between 15/5 to 15/6 at 1 pm

Table 4.27 Number of sensors corresponding to the operative temperature range of the ground floor of the design case 2

Number of sensors	Operative temperature values (°C)
0	<23
90	≥23, ≤26
0	>26

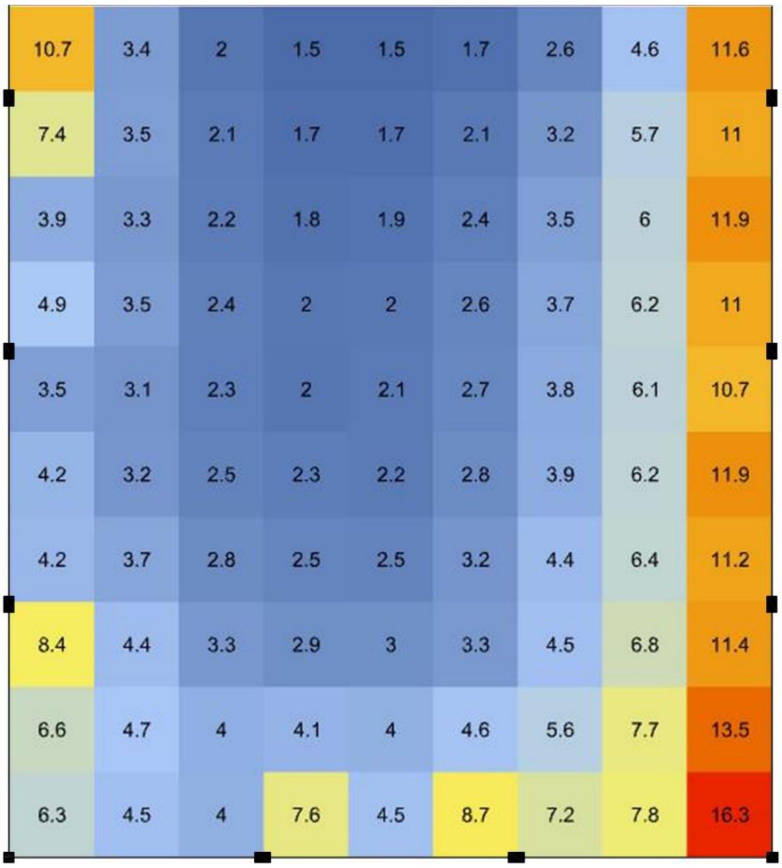

Figure 4.28 Daylight factor results of the ground floor of the design case 2

Table 4.28 Number of sensors corresponding to the daylight factor range of the ground floor of the design case 2

Number of sensors	Daylight factor values
7	<2%
55	≥2%, ≤5%
28	>5%

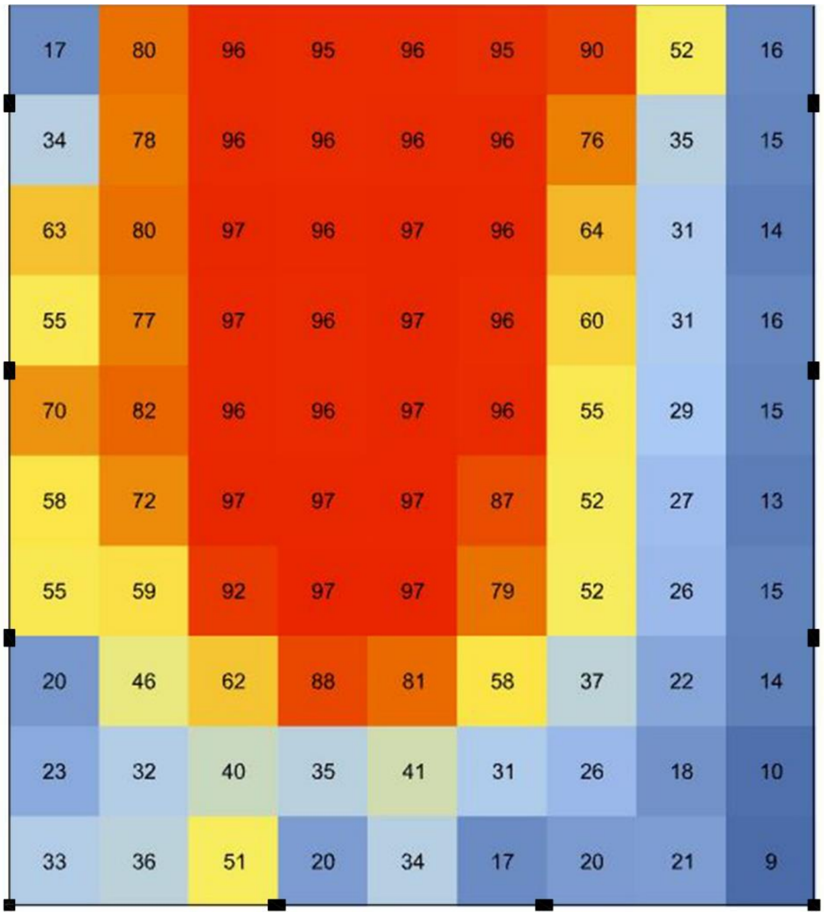

Figure 4.29 UDI results of the ground floor of the design case 2

Table 4.29 Number of sensors corresponding to the UDI values of the ground floor of the design case 2

Number of sensors	UDI values
37	<50%
53	≥50%

i. First Floor

The optimized facade openings for the first floor, which are integrated into the west and the south facades, can be seen in Figure 4.30.

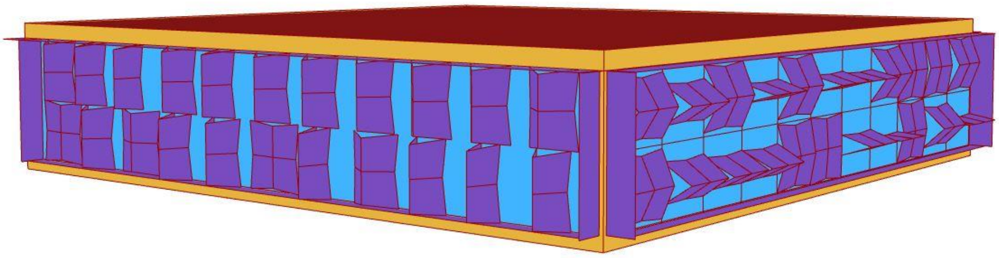

Figure 4.30 Model of the first floor of design case 2

The highest illuminance value is 787 lux, while the lowest is 59 lux, according to the results shown in Figure 4.14. The inner parts are darker; however, sensors close to windows have more daylight. According to Table 4.30, 54 sensors are below the threshold, and 42 are above. Twenty-five sensors are in the comfortable zone. It can be detected that almost 45% have insufficient lighting. This may be because interior parts receive less daylight while improving the area near glazing.

Figure 4.31 shows the operative temperature results. 24.1 °C is the lowest value, and 24.7 °C is the highest in the dining hall. All sensors are in the desired range, i.e., between 23 °C and 26 °C, as shown in Table 4.31. According to these results, it can be concluded that the room has a comfortable indoor environment in terms of operative temperature.

Daylight factor results show, as can be seen in Figure 4.32, the sensors located near the glazing of the east facade have higher values since there is no designed moveable facade. Fifty-six sensors are in the desired range, around 46% of all sensors, as seen in Table 4.32.

As shown in Figure 4.33, 10% to 94% of the area is in the range of UDI results. The eastern sensors have less useful daylight during the year. This may be because of not applying any shading to the east facade. As can be seen in Table 4.33, 89 sensors receive useful daylight in the desired range, which is 74% of the total area.

Table 4.30 Number of sensors corresponding to the illuminances range of the first floor of the design case 2

Number of sensors	Illuminance values (lux)
54	<200
25	≥200, ≤300
42	>300

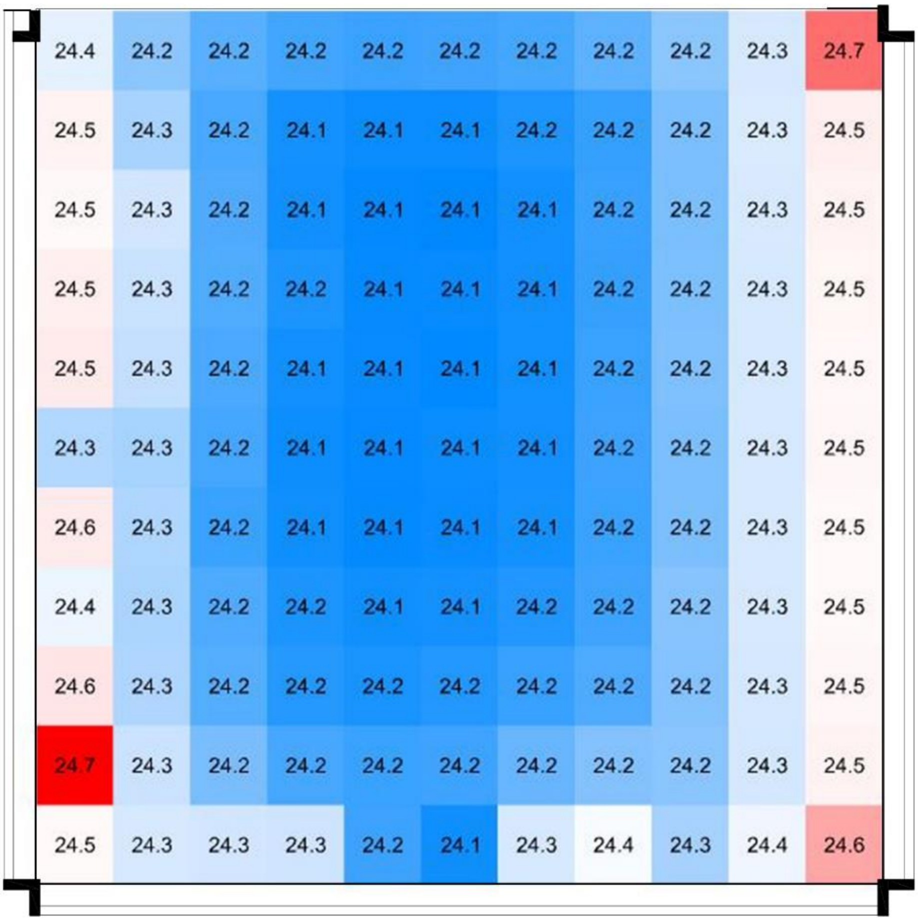

Figure 4.31 Operative temperature results in °C of the first floor of the design case 2 between 15/5 to 15/6 at 1 pm

Table 4.31 Number of sensors corresponding to the operative temperature range of the first floor of the design case 2

Number of sensors	Operative temperature values (°C)
0	<23
121	≥23, ≤26
0	>26

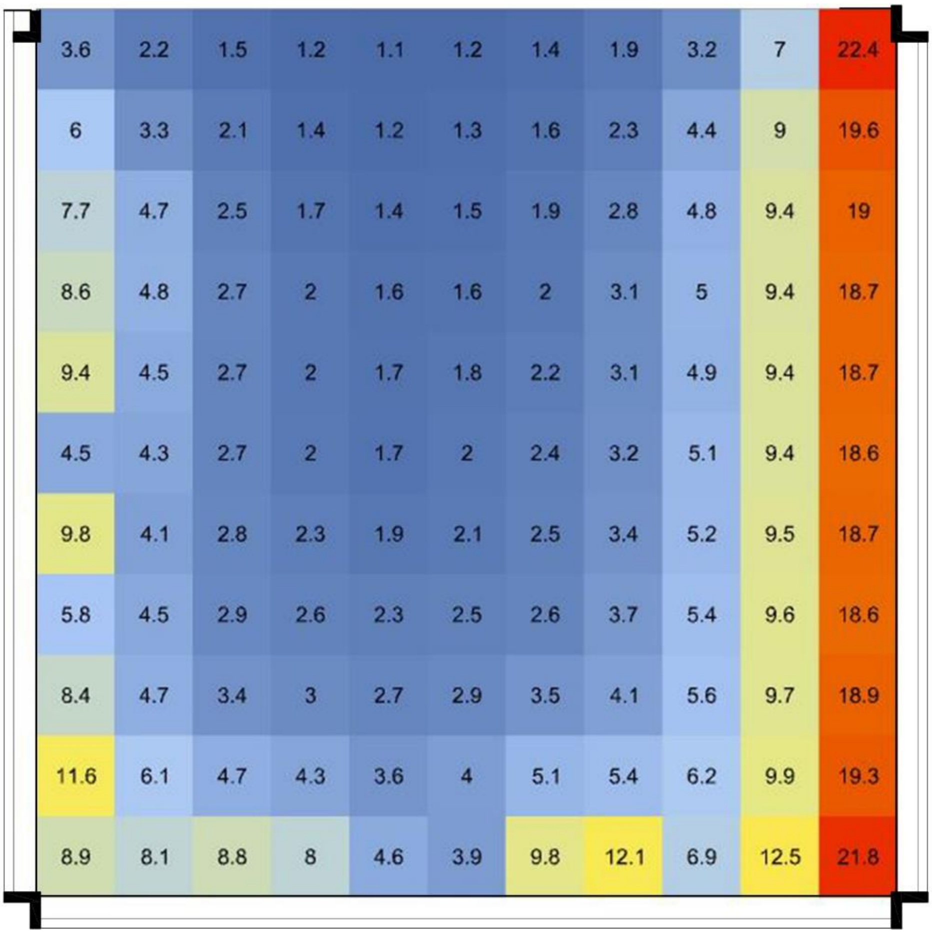

Figure 4.32 Daylight factor results of the first floor of the design case 2

Table 4.32 Number of sensors corresponding to the daylight factor range of the first floor of design case 2

Number of sensors	Daylight factor values
45	<2%
56	≥2%, ≤5%
20	>5%

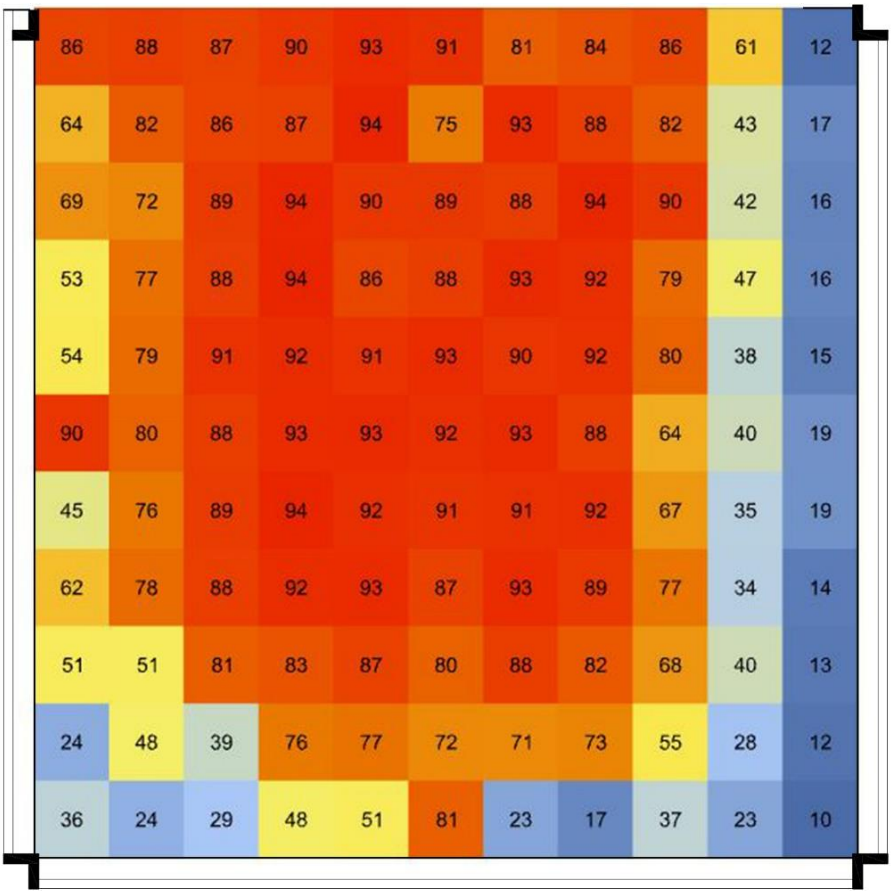

Figure 4.33 UDI results of the first floor of the design case 2

Table 4.33 Number of sensors corresponding to the UDI values of the first floor of the design case 2

Number of sensors	UDI values
32	<50%
89	≥50%

4.3.6 Kinetic Facade adapted from Al Bahar Tower Modules

The second kinetic facade morphology was adapted from the modules of Al Bahar Towers. It consists of 2x2x2 meters of triangular shape and is considered design case 2 in the scope of this research. As it was the same for the other design scenarios, ETFE was used as the facade material. The same materials of the base case were applied to the rest of the buildings' materials. The results obtained from the simulations are explained in the subsequent sections.

i. Ground Floor

Figure 4.34 shows the facade modules as a result of the optimization process. It is applied to west and south facades.

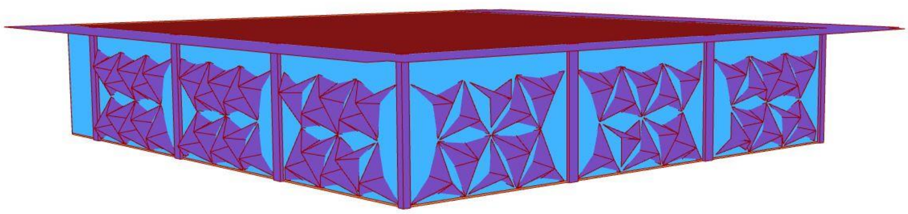

Figure 4.34 Model of the ground floor of design case 3

The illuminance results are shown in Figure 4.35. The results change between 111 lux and 827 lux. Locations near the windows have excessive daylight, while the center of the hall has less. There are 23 sensors in the range between 200 lux and 300 lux, as can be seen in Table 4.34. Twenty-three sensors are above the threshold, which means they do not have sufficient light. On the other hand, 44 sensors receive more daylight than desired. Most of the sensors are above the range, with a ratio of approximately 26%.

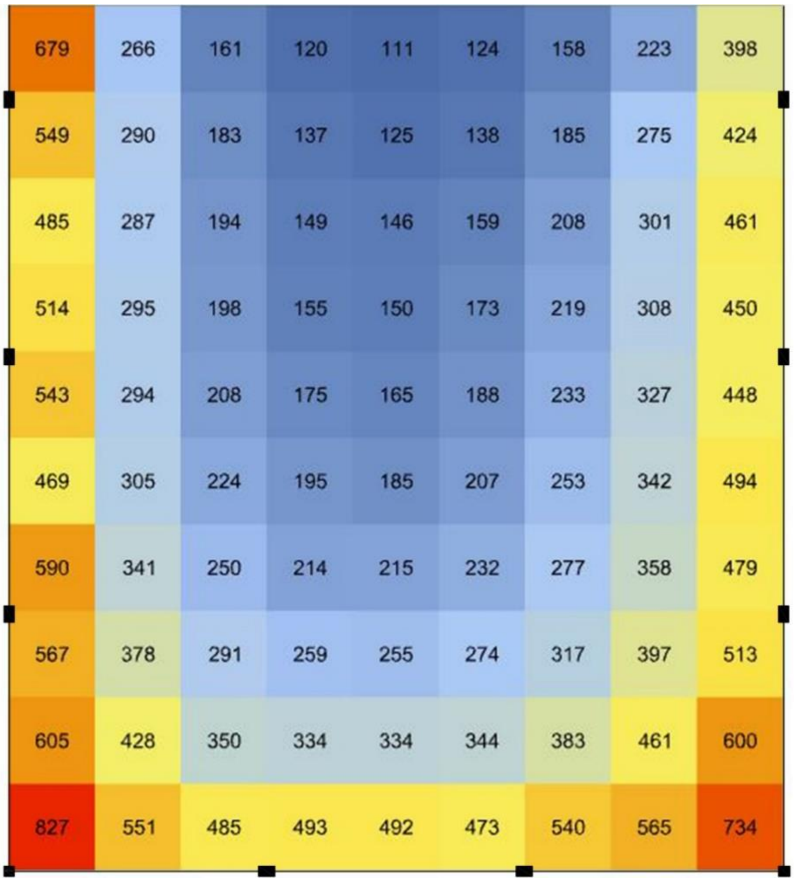

Figure 4.35 Illuminance results in lux of the ground floor of the design case 3 on the 8th of June at 1 pm

According to the results shown in Figure 4.36, the highest temperature is 25 °C, and the lowest is 24.4 °C. The three corners of the room have higher results. The one in the north-west is because there is no shading designed for that glazing. The center and the inner parts have slightly lower temperatures. Table 4.35 shows all sensors are in the comfort range.

Table 4.34 Number of sensors corresponding to the illuminances range of the ground floor of the design case 3

Number of sensors	Illuminance values (lux)
23	<200
23	≥200, ≤300
44	>300

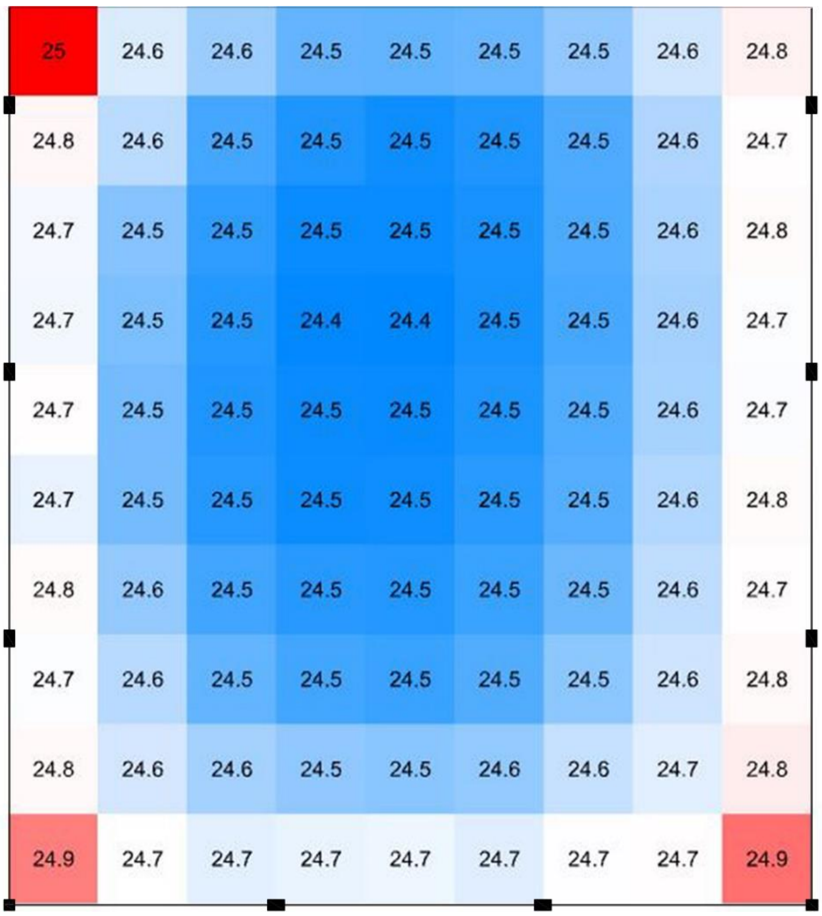

Figure 4.36 Operative temperature results in °C of the ground floor of the design case 2 between 15/5 to 15/6 at 1 pm

Table 4.35 Number of sensors corresponding to the operative temperature range of the ground floor of the design case

Number of sensors	Operative temperature values (°C)
0	<23
90	≥23, ≤26
0	>26

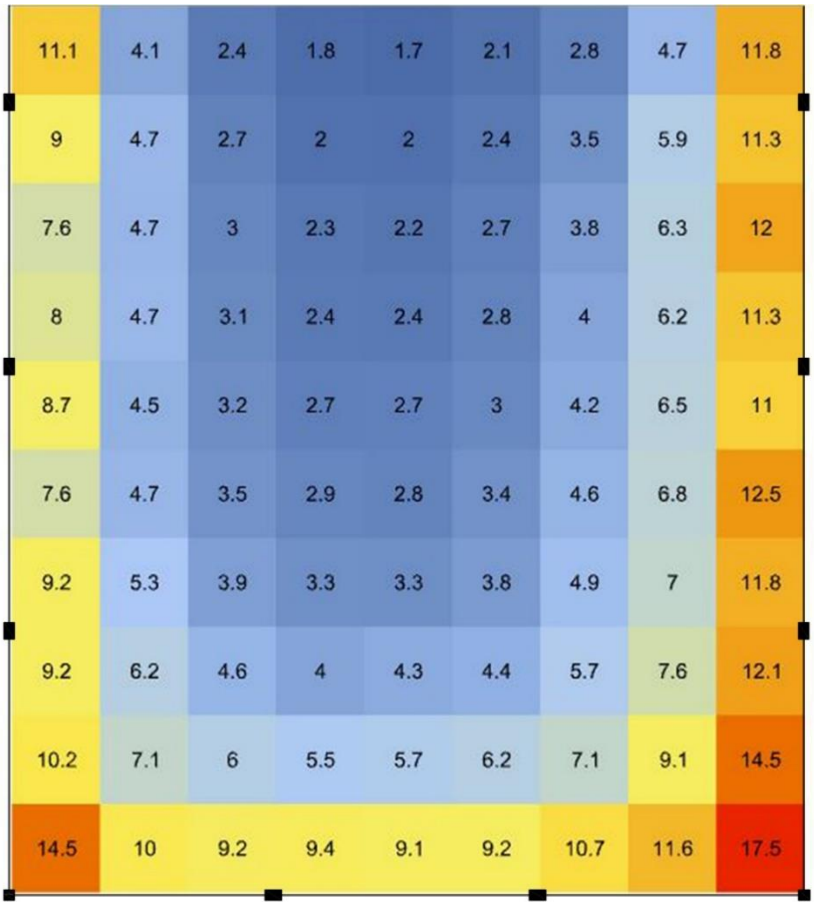

Figure 4.37 Daylight factor results of the ground floor of the design case 3

Table 4.36 Number of sensors corresponding to the daylight factor range of the ground floor of the design case 3

Number of sensors	Daylight factor values
2	<2%
44	≥2%, ≤5%
44	>5%

Figure 4.37 shows daylight factor results. The center of the dining hall is in the desired range, while the areas near the windows have higher values. As seen in Table 4.36, the number of sensors is the same for the desired range and above, with a ratio of almost 49%.

According to Figure 4.38, UDI results change between 7% and 97%. The areas near glazing are below 50%, meaning there is insufficient lighting during the year. Furthermore, as can be seen in Table 4.33 Number of sensors corresponding to the UDI values of the first floor of the design case 2, 30 sensors, corresponding to approximately 33% of all sensors, are in the desired range.

ii. First Floor

The facade modules with optimized openings can be seen in Figure 4.39. These modules were integrated into the south and west facade for the simulations.

According to the illuminance results, as seen in Figure 4.40, 94 lux is the lowest value, while 877 is the highest. South-east and south-west corners have the highest values. It could be concluded that the center of the dining hall is mostly lower than 200 lux, which is the darkest area in the hall. Thirty-two sensors are in the desired range, corresponding to approximately 26%, while 45 are below 200 lux and 44 are above 300 lux, as seen in Table 4.38.

According to Figure 4.41, temperature results show that the highest temperature is 25.2 °C, corresponding to the south-west sensor. On the other hand, the lowest temperature is 24.5 °C. All sensors have very similar results, and as can be seen in

Table 4.39, all of the sensors are between 23 °C and 26 °C, which is the desired range.

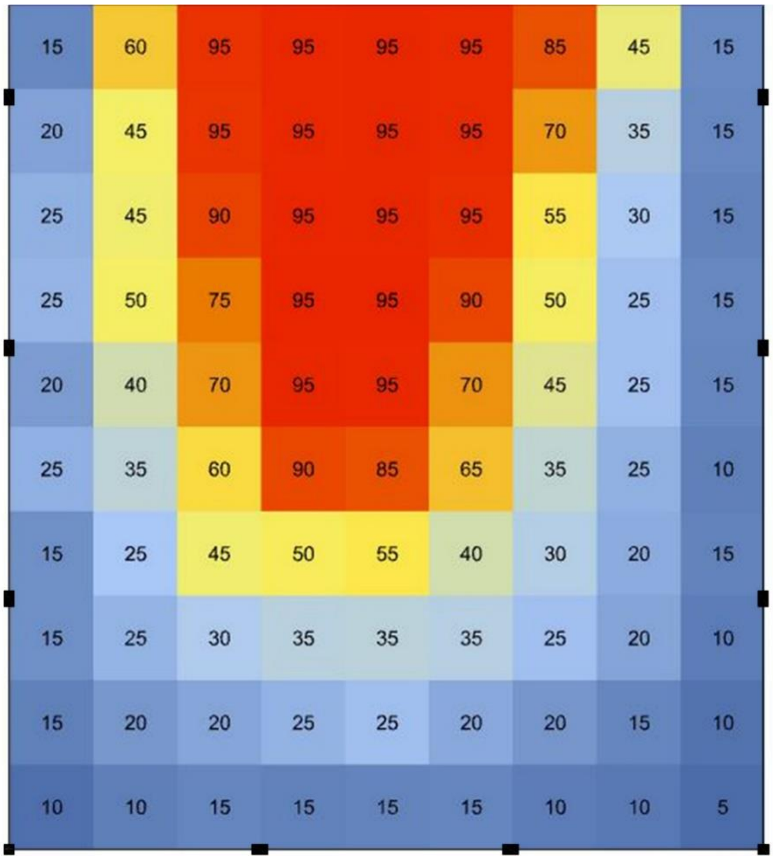

Figure 4.38 UDI results of the ground floor of the design case 3

Table 4.37 Number of sensors corresponding to the UDI values of the ground floor of the design case 3

Number of sensors	UDI values
60	<50%
30	≥50%

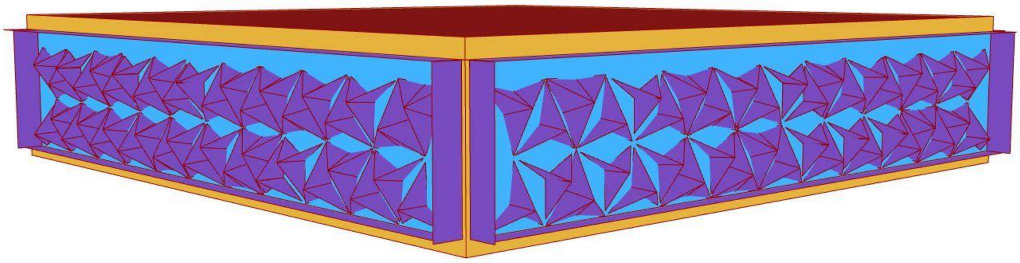

Figure 4.39 Model of the first floor of design case 3

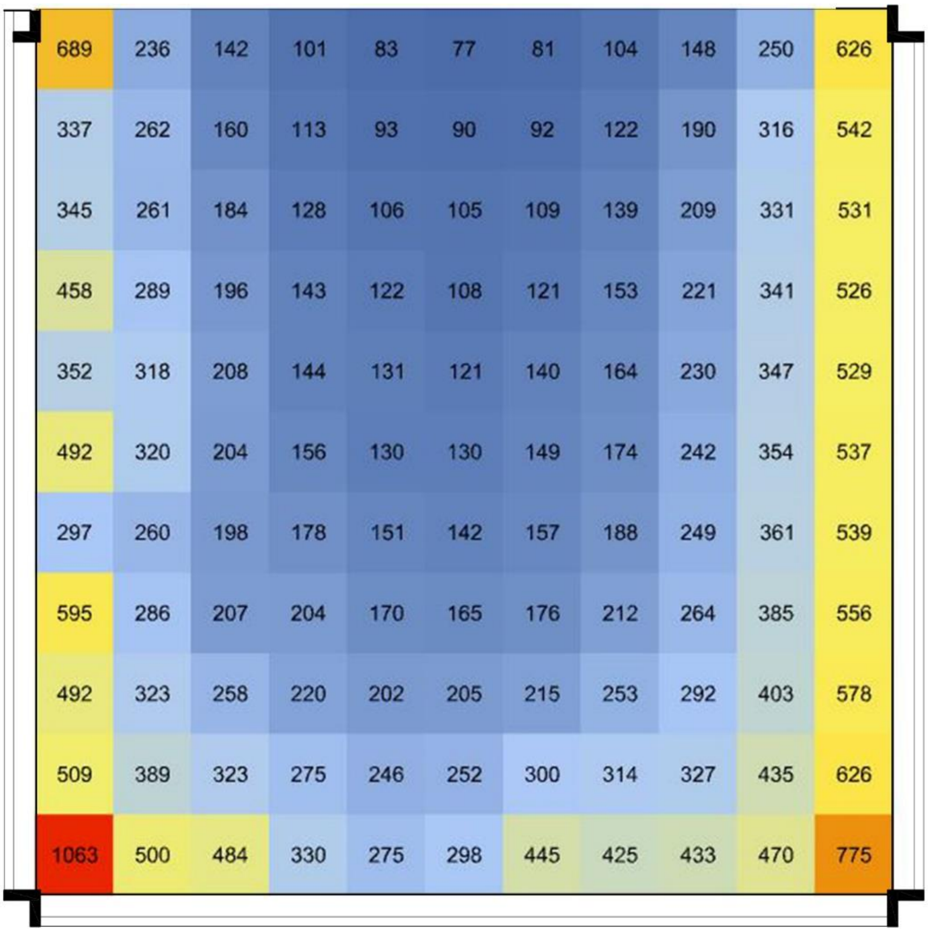

Figure 4.40 Illuminance results in lux of the first floor of the design case 3 on the 8th of June at 1 pm

Table 4.38 Number of sensors corresponding to the illuminances range of the first floor of the design case 3

Number of sensors	Illuminance values (lux)
45	<200
32	≥200, ≤300
44	>300

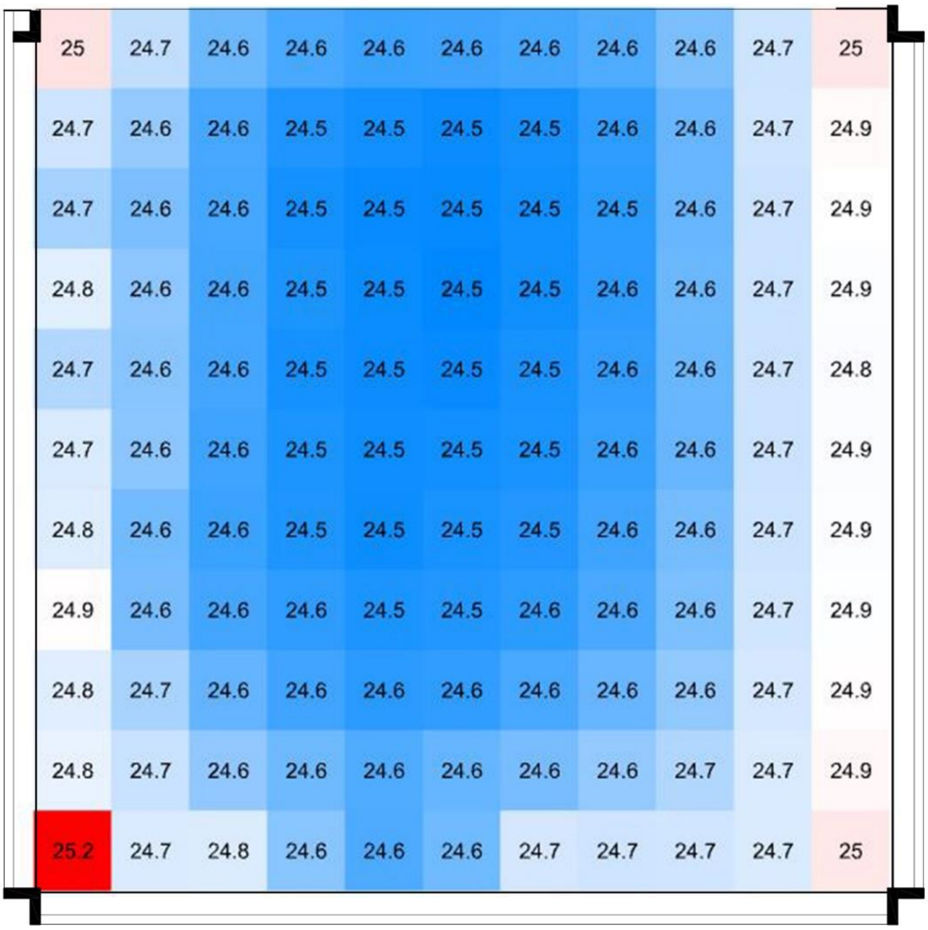

Figure 4.41 Operative temperature results in °C of the first floor of the design case 3 between 15/5 to 15/6 at 1 pm

Table 4.39 Number of sensors corresponding to the operative temperature range of the first floor of the design case 3

Number of sensors	Operative temperature values (°C)
0	<23
121	≥23, ≤26
0	>26

According to Figure 4.42, the daylight factor is higher in the eastern part of the dining hall. This is because the east facade does not have an integrated kinetic facade. Table 4.40 shows that 58 sensors, meaning almost 48% of the total area, are in the range defined as comfortable.

Figure 4.43 shows the sensors that receive the most useful daylight during the year are in the center of the hall. On the other hand, the sensors near the east glazing have less due to excessive daylight. The results in Table 4.41 show that 91 sensors are above 50% of UDI. Thus, it can be concluded almost 75% of the total area receives useful daylight at the desired range during the year.

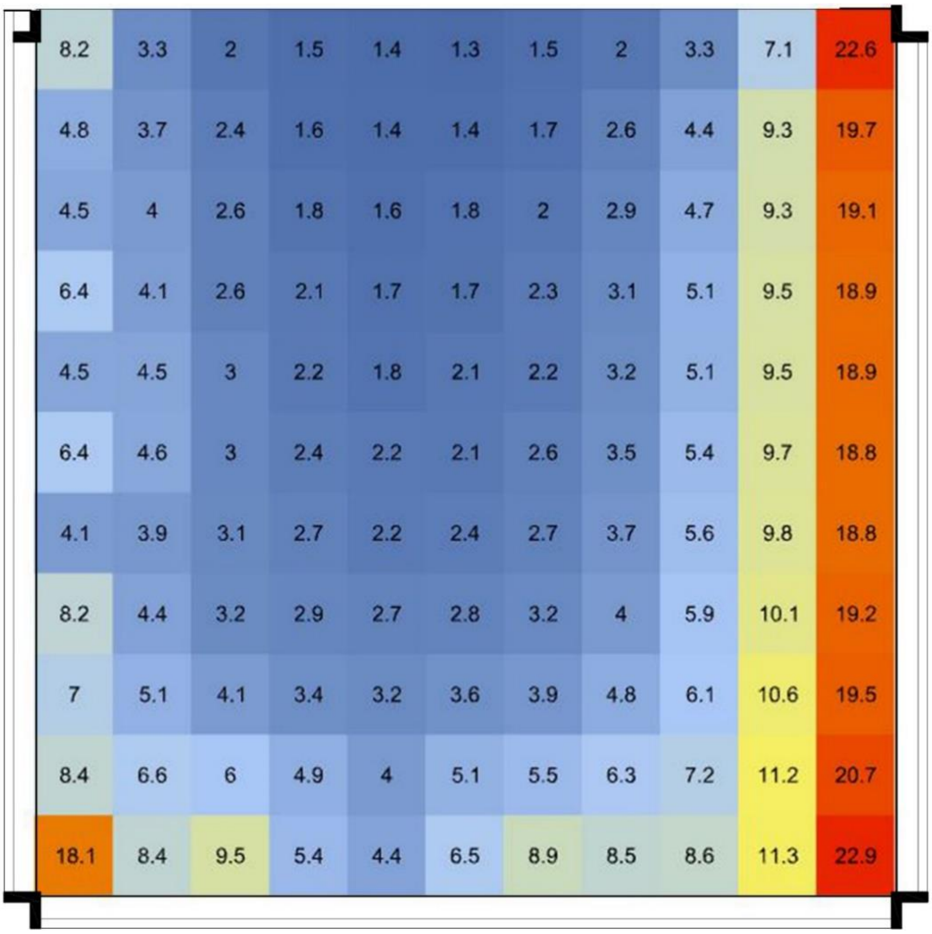

Figure 4.42 Daylight factor results of the first floor of the design case 3

Table 4.40 Number of sensors corresponding to the daylight factor range of the first floor of the design case 3

Number of sensors	Daylight factor values
14	<2%
58	≥2%, ≤5%
49	>5%

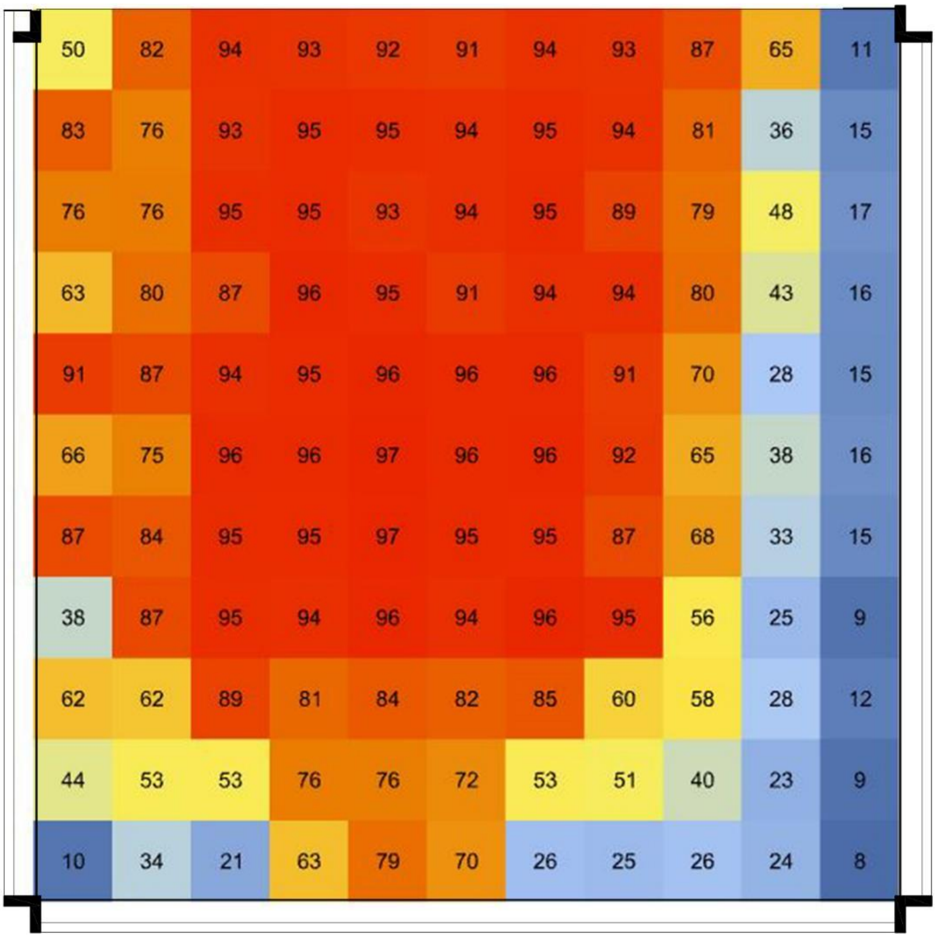

Figure 4.43 UDI results of the first floor of the design case 3

Table 4.41 Number of sensors corresponding to the UDI values of the first floor of the design case 3

Number of sensors	UDI values
30	<50%
91	≥50%

4.4 Evaluation of All Scenarios

This section presents the comparison of all scenarios according to simulation metric results, i.e., illuminance, operative temperature, daylight factor, and UDI. At first, each metric explains the different results of scenarios with all ranges for each floor separately. Then, the floors are compared for each scenario according to the results based on desired ranges.

4.4.1 Illuminance

According to Figure 4.44, it can be said that all design scenarios improved the base case conditions. However, design case 2, i.e., kinetic facade with square modules, is the most efficient scenario in terms of illuminance value between 200 lux and 300 lux. It improves daylight conditions by approximately 63% compared to the base case. Since it has moveable modules and arranges itself according to daylight, it is an expected result compared to the fixed shading and base case. On the other hand, it is concluded that this facade is more effective than design case 3 for the ground floor.

Although base case conditions of the first floor are improved by all design scenarios, the most effective one is design case 3, i.e., kinetic facade adapted by Al Bahar Towers modules, as seen in Figure 4.45. It improves the conditions by approximately 46% compared to the base case since the openings can be arranged accordingly. As a result, it is observed that these modules create more comfortable illuminance conditions for the first floor.

It is also observed that according to Figure 4.46, the scenarios have different results for the diverse floors. Design case 2 provides improved conditions for the ground floor, while design case 3 is the most efficient scenario for the first floor. However, the approximate percentages of 26% seem very similar for the ground and first floors. In this case, since the ground floor has almost 34% of sensors in the desired range for design case 2, it can be said that the kinetic facade becomes more effective for the ground floor in terms of illuminance results. This may be related to the total area since the first floor is larger than the ground floor; it may have problems maintaining optimum illuminance levels for the inner parts while arranging to reduce excessive daylight near the glazed area.

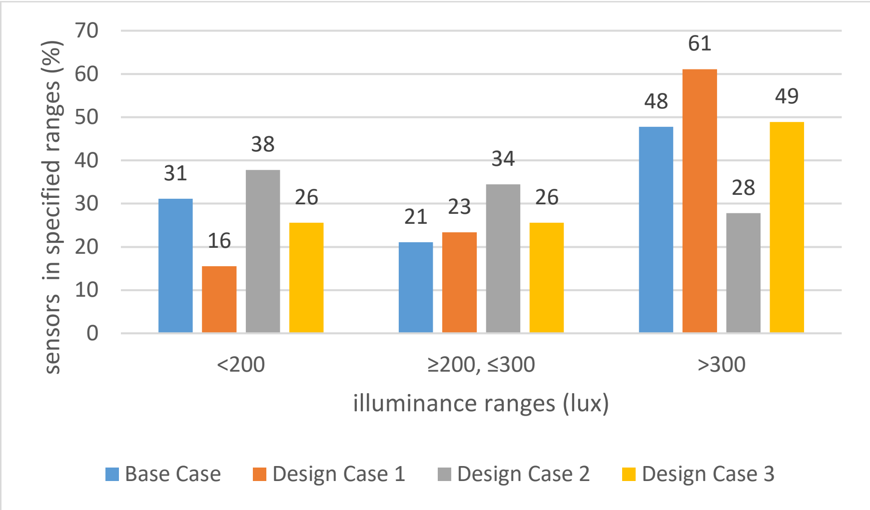

Figure 4.44 The comparison between all cases of the ground floor for all illuminance ranges

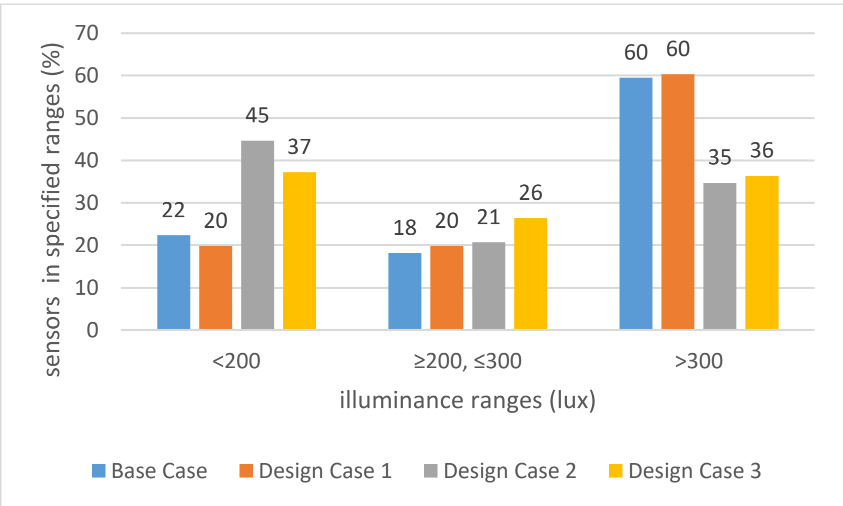

Figure 4.45 The comparison between all cases of the first floor for all illuminance ranges

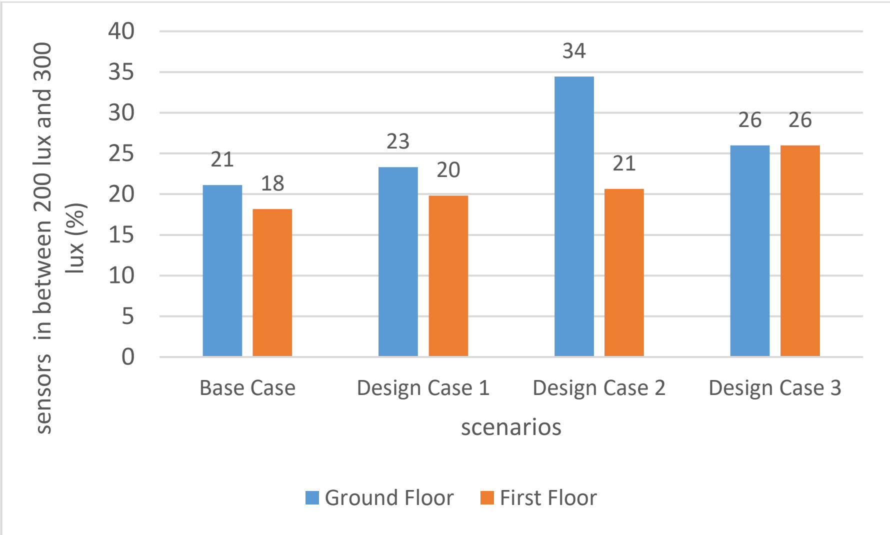

Figure 4.46 The comparison between all scenarios of two floors for the desired illuminance range

4.4.2 Operative Temperature

Figure 4.47 presents the operative temperature results for all scenarios of the ground floor. None of the sensors are below 23 ºC for all scenarios. All design interventions manage to provide a comfortable temperature for all the sensors.

Similar to the ground floor, there are no sensors below 23 ºC for any scenarios, as shown in Figure 4.48. Both kinetic facade morphologies improve the temperature conditions by providing the proper range to all sensors. They are more effective than the fixed shadings for the first floor.

According to Figure 4.49, it can be said that all scenarios can reduce excessive temperature conditions for both floors. To sum up, any shading can provide optimum temperature conditions for the ground floor, while kinetic ones are most effective due to their moveability for the first floor.

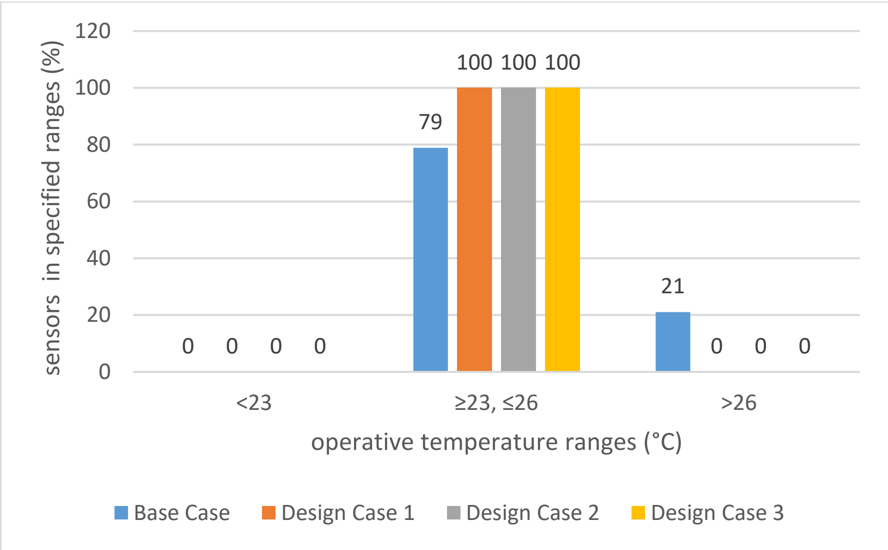

Figure 4.47 The comparison between all cases of the ground floor for all operative temperature ranges

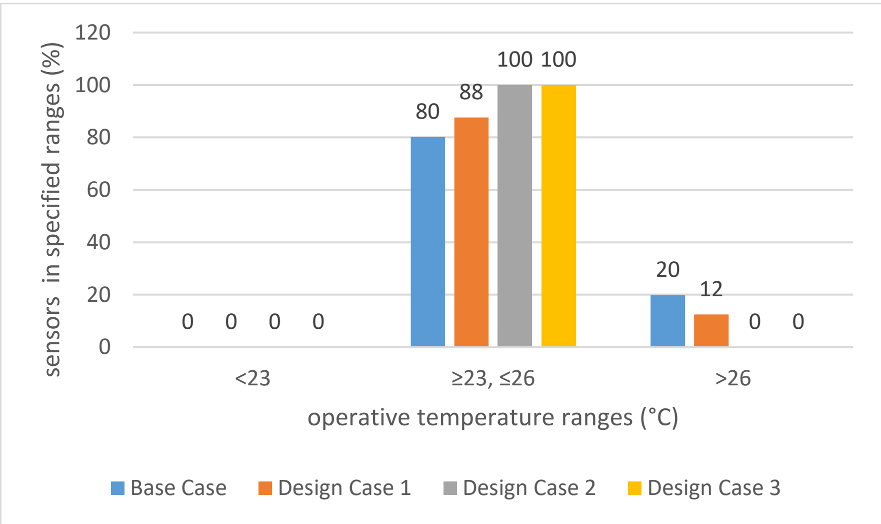

Figure 4.48 The comparison between all cases of the first floor for all operative temperature ranges

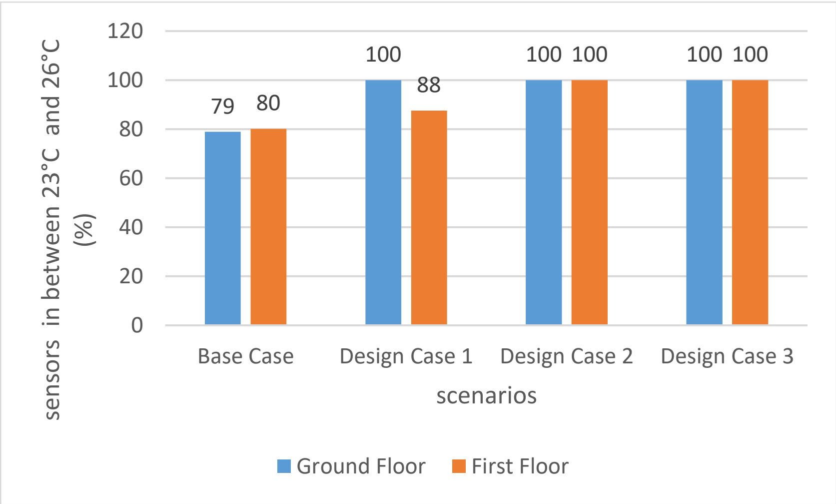

Figure 4.49 The comparison between all scenarios of two floors for the desired operative temperatures

4.4.3 Daylight Factor

According to Figure 4.50, both kinetic morphologies are adequate to provide proper daylight factor results. On the contrary, it can be said fixed shading slightly reduces this result. The darker areas are improved because of fixed shadings; however, the excessive daylight increases. Design case 2 is the most efficient scenario for the ground floor, with an improvement of approximately 53% of the desired daylight factor levels.

When the scenarios of the first floor are investigated, it is observed that with a 2% difference, design case 3 is the most useful scenario in terms of daylight factor, as can be seen in Figure 4.51. It improves the daylight factor results by 45% because of its moveability.

The comparison between floors, presented in Figure 4.52 shows that approximately 61% of the sensors are in the desired level for the ground floor with the integration of design case 2. Similar to illuminance results, kinetic facades are more efficient for the ground dining hall in terms of daylight factor.

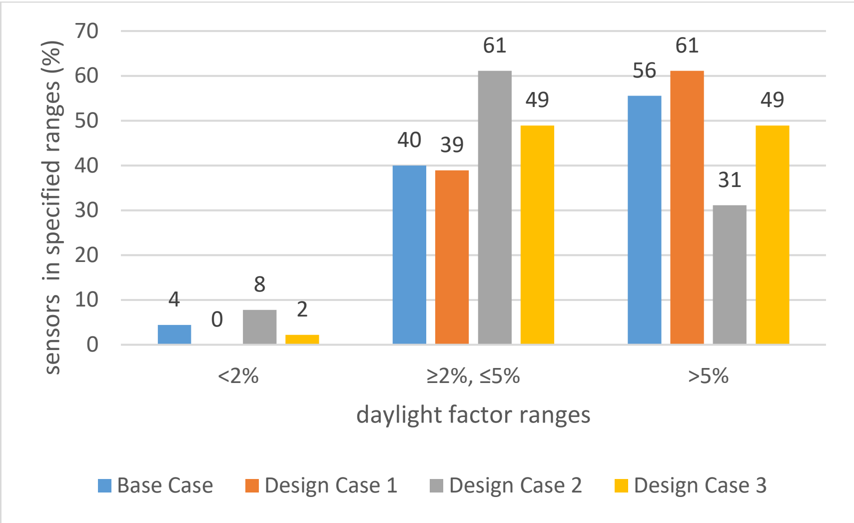

Figure 4.50 The comparison between all cases of the ground floor for all daylight factor ranges

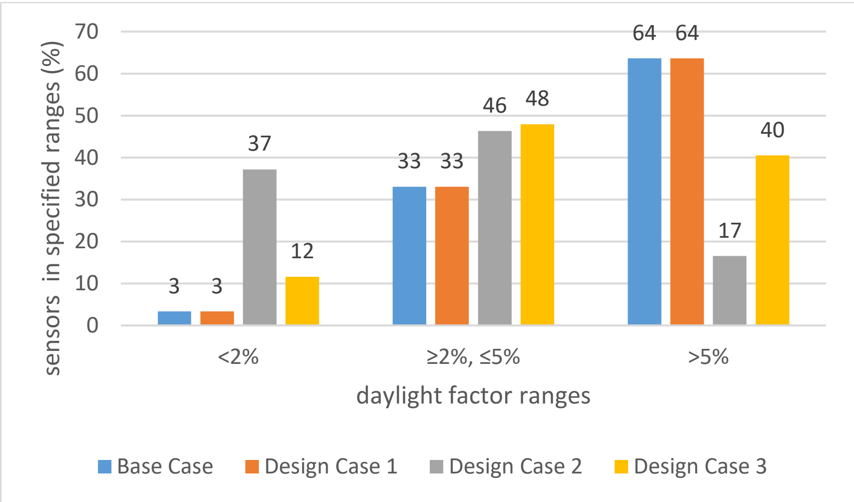

Figure 4.51 The comparison between all cases of the first floor for all daylight factor ranges

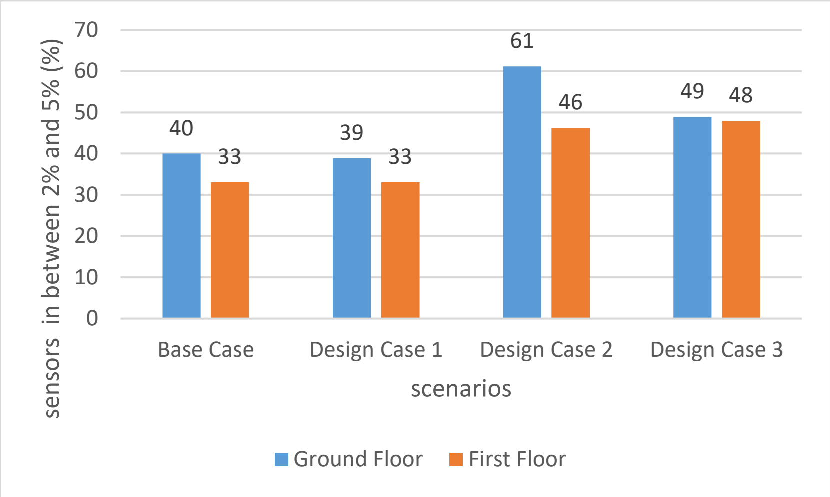

Figure 4.52 The comparison between all scenarios of two floors for the desired daylight factor

4.4.4 UDI

Figure 4.53 presents a UDI comparison for all cases of the ground floor. According to these results, it can be concluded that Design Case 2 is the most effective scenario, with the improvement of an approximate 51% ratio for the ground floor in terms of UDI. Even though the facade optimization is completed for a specific day, but UDI is a result of annual analysis, and design case 2 can still provide optimum conditions for 59% of the sensors for the year. Therefore, it is possible to say since this facade can arrange its movement according to instant needs, it may provide even better results.

Although design case 3 is the best scenario in terms of UDI, for the first floor, there is a slight difference, i.e., 1%, with design case 2, as presented in Figure 4.54. Design case 3 can provide improved UDI conditions by an approximate ratio of 56%. Similar to the situation in the ground floor, it can provide more useful daylight considering its optimization ability.

According to Figure 4.55, UDI results are better for the first floor of all cases as opposed to other metrics. Design case 3 of the first floor has the highest range, around 75%. Hence, as similarly discussed, it is possible to say this can also be enhanced in the actual case since the modules are adaptable.

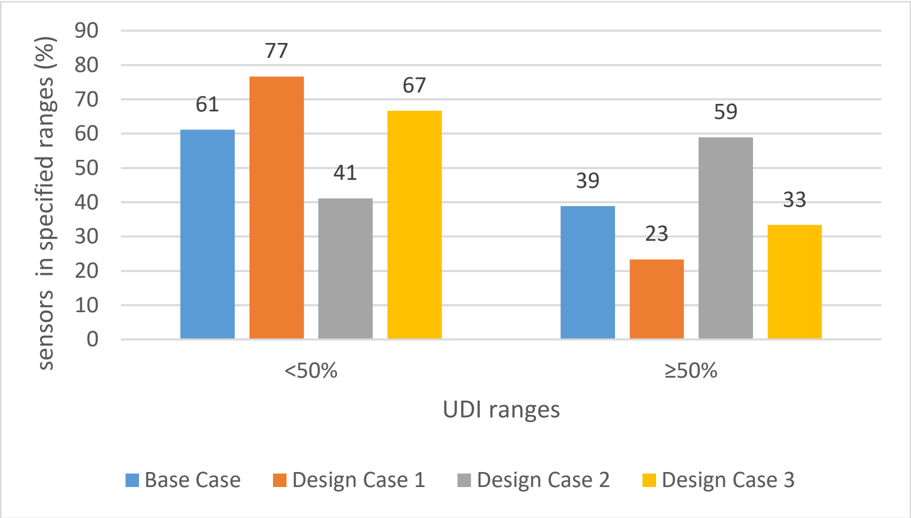

Figure 4.53 The comparison between all cases of the ground floor for all UDI ranges

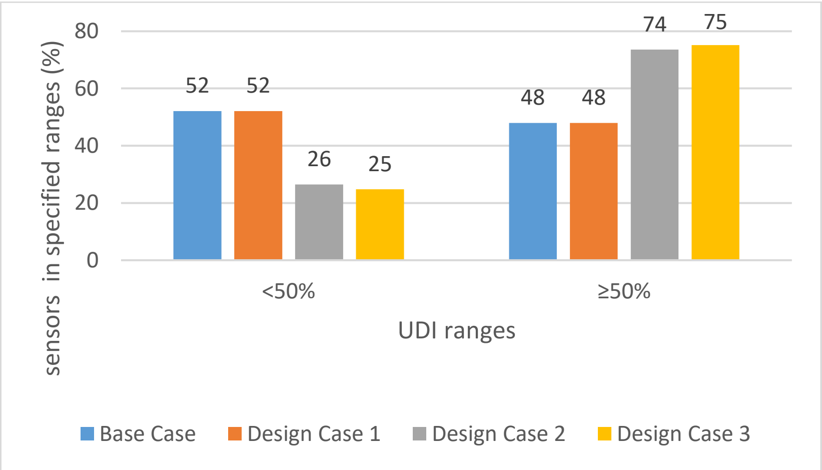

Figure 4.54 The comparison between all cases of the first floor for all UDI ranges

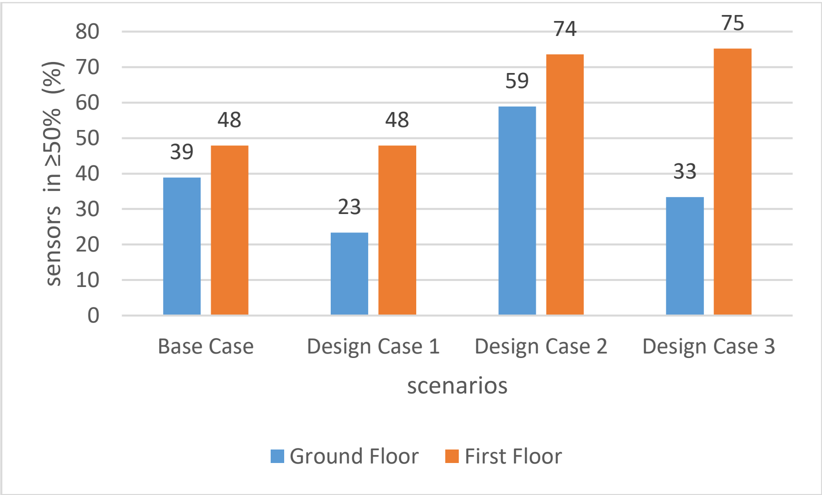

Figure 4.55 The comparison between all scenarios of two floors for the desired UDI

CHAPTER 5

CONCLUSION

Many studies show that the environmental conditions on our planet have been deteriorating rapidly during the past decades, and many sectors have taken action to decelerate this collapse. The building construction sector should also pay attention to the environment since the deterioration caused by the construction cannot be underestimated. Amongst these effects, constructing new buildings have a significant impact, according to the studies in the literature. Therefore, rather than constructing new ones in the case of a need, existing buildings should be evaluated if the conditions can be enhanced.

Building facades have a crucial role in regulating indoor and outdoor conditions. Moreover, many studies in the literature show that kinetic facades are energy-efficient solutions for a building. They can reduce energy consumption and improve user satisfaction, leading to effective space use. Thermal and visual comfort are the two effective parameters for space usage. They may cause a decrease in the efficient space use in public buildings where people can choose seats if thermal or visual discomfort occurs. However, as previously discussed, facades are the key elements that can provide the desired condition levels with their behavior as a regulator between the interior and the exterior environments. Especially considering the technological developments in the last years, kinetic facades with advanced computer technologies have become an effective solution to arrange these conditions.

The objective of this research is to investigate the kinetic facades' effect on thermal and visual comfort in a highly glazed public building. METU Cafeteria Building, located in Ankara, was selected as the case study building since thermal discomfort and excessive daylight was observed.

Actual temperature data was collected by TESTO 405-V1 from all six dining halls of the building. The most uncomfortable section was selected as the focus study, one with two floors, and these floors were simulated to observe the effects of possible facade integrations.

After selecting the focus section, a lux meter, RO1335 by Rotronic, was used to measure the actual illuminance results to calibrate the simulation results since a difference was observed in the simulation results. After the calibration process, simulations were completed for illuminance, operative temperatures, daylight factor, and UDI parameters to obtain the building's daylight and thermal comfort data.

Literature was surveyed to review existing facade morphologies, and two were selected, one from the theoretical and one from the actual case application, for integration into the existing building. Using Galapagos, these facades modules were optimized for a specific date and hour according to the illuminance range for a self-service restaurant, namely between 200 lux and 300 lux. Two different materials were also simulated to see the impact of the reflective and translucent ones. The better one was chosen and applied to all design scenarios of two floors. These scenarios are fixed shadings, kinetic facade with square modules, and kinetic facade with the modules of Al Bahar Towers. The focus study section has glazing facades for three orientations, i.e., west, east, and south. The designed facades were integrated into the west and south facades, not the east facade of the focus study section because the building is being used during lunch hours.

As a result of this study, it is observed that there is no significant difference between ETFE and metal. However, ETFE was selected to provide a view of the outside. Modules adapted from Al Bahar Towers are the most effective scenario for the first floor in every metric, i.e., illuminance, operative temperatures, daylight factor, and UDI parameters, while in terms of daylight criteria, the square modules are the most efficient ones for the ground floor. This may be related to the different dimensions of the two floors. The first floor is larger than the ground floor, and having efficient results near glazing while arranging the same conditions for the inner part can be more challenging. Since the modules adapted from Al Bahar Towers have a more specific movement, these may efficiently arrange the optimized conditions for the larger area.

Considering the simulation results, it can be said that all the measured visual and thermal parameters may be affected by many factors, such as floor height, surrounding vegetation, etc. Overall, it can be concluded that kinetic facades that are adaptable to optimize interior illuminance levels are effective in enhancing visual and thermal comfort in a highly glazed public building in the continental climate of Ankara; however, the design of the morphology or the height of the floors may have an impact on the results.

As previously stated in the literature, installing these facades can cause high costs to the construction. Materials should be selected accordingly to decrease the cost, and the system should be as simple as it can be since the cost of installing complex systems would be higher. The operational cost and the payback time should also be taken into consideration since, in the literature, it is stated that these facades have mostly higher initial costs, but during the operation phase, this cost is covered by the facade’s efficiency. PV panels can be installed in the building to supply the energy of the control mechanism of the kinetic facades, which would be more sustainable.

If the moveable modules were applied to all glazing parts, the efficiency would be increased, but it depends on the occupation needs, such as if the building is used in the morning, the east facade should also be considered for more effective interior condition results.

As the next step of this study, since all these conditions were tested according to the computer simulations in a theoretical approach, these can also be tested with a scaled real model to observe if these facade morphologies have the same thermal and visual performances in the real environment conditions of Ankara.

For further research, these facade interventions can be tested for different section orientations, such as north or east, since this study only covers the south section of the case study building. It can also be tested for different facade orientations, such as north and east. The illuminance range was based on the restaurant requirements; testing with other building types with different illuminance ranges will provide a contribution to observing the difference.

This study covers a facade moving according to illuminance values and its contribution to visual and thermal conditions. A facade that adapts itself according to temperature can be designed to investigate if it can also provide an improvement to visual comfort conditions. Additionally, facade modules can be designed based on the needs of the climatic conditions and facade orientations, considering the horizontal movement for the south and the vertical one for the west.

On the other hand, it can be concluded that these facades can be more efficient for high-rise buildings in hot and humid climates considering the total impact with cost return. Another future study can also focus on this efficiency comparison of the buildings with different heights in different climatic conditions.

REFERENCES

Ahmed, M. M. S., Abdel-Rahman, A. K., Bady, M., & Mahrous, E. (2016). The Thermal Performance of Residential Building Integrated with Adaptive Kinetic Shading System. *International Energy Journal*, *16*(3). http://www.rericjournal.ait.ac.th/index.php/reric/article/view/1452

Alba-Rodríguez, M. D., Martínez-Rocamora, A., González-Vallejo, P., Ferreira-Sánchez, A., & Marrero, M. (2017). Building rehabilitation versus demolition and new construction: Economic and environmental assessment. *Environmental Impact Assessment Review*, *66*, 115–126. https://doi.org/10.1016/j.eiar.2017.06.002

Alotaibi, F. (2015). The Role of Kinetic Envelopes to Improve Energy Performance in Buildings. *Journal of Architectural Engineering Technology*, *04*(03), 1–5. https://doi.org/10.4172/2168-9717.1000149

Altın, M., & Orhon, A. V. (2016). Enerji Korunumunda Adaptif/Uyarlı Cepheler. *8. Ulusal Çatı & Cephe Sempozyumu*.

Ardabili, N. G. (2020). *Parametric Design and Simulation of a Smart Facade for Hot and Humid Climates Using Biomimetics, PCMs and SMAs: A Case Study in Iran.* [Master's Thesis, METU]

Ardente, F., Beccali, M., Cellura, M., & Mistretta, M. (2011). Energy and environmental benefits in public buildings as a result of retrofit actions. In *Renewable and Sustainable Energy Reviews* (Vol. 15, Issue 1, pp. 460–470). https://doi.org/10.1016/j.rser.2010.09.022

ASHRAE Standard 55-2017. (2017). *Thermal Environmental Conditions for Human Occupancy*. https://ashrae.iwrapper.com/ASHRAE_PREVIEW_ONLY_STANDARDS/STD_55_2017

Bakker, L. G., Hoes-van Oeffelen, E. C. M., Loonen, R. C. G. M., & Hensen, J. L.

M. (2014). User satisfaction and interaction with automated dynamic facades: A pilot study. *Building and Environment*, *78*, 44–52. https://doi.org/10.1016/j.buildenv.2014.04.007

Böke, J., Knaack, U., & Hemmerling, M. (2020). Automated adaptive facade functions in practice - Case studies on office buildings. *Automation in Construction*, *113*, 103113. https://doi.org/10.1016/j.autcon.2020.103113

Cimmino, M. C., Miranda, R., Sicignano, E., Ferreira, A. J. M., Skelton, R. E., & Fraternali, F. (2017). Composite solar facades and wind generators with tensegrity architecture. *Composites Part B: Engineering*, *115*, 275–281. https://doi.org/10.1016/J.COMPOSITESB.2016.09.077

Dawit Melaku. (2016). *the Impact of Glass Facade on Users Comfort* [Addis Ababa University]. http://213.55.95.56/handle/123456789/819

Dewidar, K., Mahmoud, A. H., Magdy, N., & Ahmed, S. (2010). The Role of Intelligent Facades in Energy Conservation. *Nternational Conference on Sustainability and the Future: Future Intermediate Sustainable Cities*, *1*, 1–23.

Di Salvo, S. (2018). Kinetic Solutions for Responsive and Communicative Building Skin. *Advanced Materials Research*, *1149*, 86–97. https://doi.org/10.4028/www.scientific.net/amr.1149.86

Elmokadem, A., Ekram, M., Waseef, A., & Nashaat, B. (2018). Kinetic Architecture: Concepts, History and Applications. *International Journal of Science and Research (IJSR)*, *7*(4), 750–758. https://doi.org/10.21275/ART20181560

EN 12464-1. (2002). Light and lighting – Lighting of work places – Part 1 : Indoor work places. In *European Committee for Standardization*.

Enshassi, A., Kochendoerfer, B., & Rizq, E. (2014). An evaluation of environmental impacts of construction projects. *Revista Ingenieria de Construccion*, *29*(3), 234–254. https://doi.org/10.4067/s0718-50732014000300002

Fakourian, F., & Asefi, M. (2019). Environmentally responsive kinetic facade for educational buildings. *Journal of Green Building*, *14*(1), 165–186. https://doi.org/10.3992/1943-4618.14.1.165

Flor, J. F., Liu, X., Sun, Y., Beccarelli, P., Chilton, J., & Wu, Y. (2022). Switching daylight: Performance prediction of climate adaptive ETFE foil facades. *Building and Environment*, *209*, 108650. https://doi.org/10.1016/J.BUILDENV.2021.108650

Formentini, M., & Lenci, S. (2018). An innovative building envelope (kinetic facade) with Shape Memory Alloys used as actuators and sensors. *Automation in Construction*, *85*, 220–231. https://doi.org/10.1016/j.autcon.2017.10.006

Fortmeyer, R., & Linn, C. D. (2014). *Kinetic Architecture: Design for Active Envelopes*. The Images Publishing.

Fox, M., & Kemp, M. (2009). *Interactive Architecture*. Princeton Architectural Press.

Frontczak, M., & Wargocki, P. (2011). Literature survey on how different factors influence human comfort in indoor environments. *Building and Environment*, *46*(4), 922–937. https://doi.org/10.1016/j.buildenv.2010.10.021

Google Earth. (n.d.). *Google Earth*. Retrieved July 27, 2022, from https://earth.google.com/web/

Guan, L. (2011). The Influence of Glass Types on the Performance of Air-Conditioned Office Buildings in Australia. *Advanced Materials Research*, *346*, 34–39. Advanced Materials Research

Hasik, V., Escott, E., Bates, R., Carlisle, S., Faircloth, B., & Bilec, M. M. (2019). Comparative whole-building life cycle assessment of renovation and new construction. *Building and Environment*, *161*, 106218. https://doi.org/10.1016/j.buildenv.2019.106218

Hosseini, S. M., & Heidari, S. (2022). General morphological analysis of Orosi windows and morpho butterfly wing's principles for improving occupant's daylight performance through interactive kinetic facade. *Journal of Building Engineering*, 105027. https://doi.org/10.1016/J.JOBE.2022.105027

Hosseini, S. M., Mohammadi, M., & Guerra-Santin, O. (2019). Interactive kinetic facade: Improving visual comfort based on dynamic daylight and occupant's positions by 2D and 3D shape changes. *Building and Environment*, *165*, 106396. https://doi.org/10.1016/j.buildenv.2019.106396

Hosseini, S. M., Mohammadi, M., Schröder, T., & Guerra-Santin, O. (2020). Integrating interactive kinetic facade design with colored glass to improve daylight performance based on occupants' position. *Journal of Building Engineering*, *31*, 101404. https://doi.org/10.1016/J.JOBE.2020.101404

Hosseini, S. M., Mohammadi, M., Schröder, T., & Guerra-Santin, O. (2021). Bio-inspired interactive kinetic facade: Using dynamic transitory-sensitive area to improve multiple occupants' visual comfort. *Frontiers of Architectural Research*, *10*(4), 821–837. https://doi.org/10.1016/J.FOAR.2021.07.004

ISO 7730. (2005). *Ergonomics of the thermal environment — Analytical determination and interpretation of thermal comfort using calculation of the PMV and PPD indices and local thermal comfort criteria*.

Kalzip. (2009). Solar Reflectance, Thermal Emittance and Solar Reflectance Index (SRI). In *Kalzip Technical Infiormation* (Issue 6). www.kalzip.com

Kensek, K., & Hansanuwat, R. (2011). Environment Control Systems for Sustainable Design: A Methodology for Testing, Simulating and Comparing Kinetic Facade Systems. *Journal of Creative Sustainable Architecture & Built Environmental*, *1*, 27–46.

Khezri, M., & Rasmussen, K. J. R. (2022). Functionalising buckling for structural morphing in kinetic facades: Concepts, strategies and applications. *Thin-Walled Structures*, *180*, 109749. https://doi.org/10.1016/J.TWS.2022.109749

Kong, Z., Utzinger, D. M., Freihoefer, K., & Steege, T. (2018). The impact of interior design on visual discomfort reduction: A field study integrating lighting environments with POE survey. *Building and Environment*, *138*, 135–148. https://doi.org/10.1016/j.buildenv.2018.04.025

Korsavi, S. S., Zomorodian, Z. S., & Tahsildoost, M. (2016). Visual comfort assessment of daylit and sunlit areas: A longitudinal field survey in classrooms in Kashan, Iran. *Energy and Buildings*, *128*, 305–318. https://doi.org/10.1016/j.enbuild.2016.06.091

Le-Thanh, L., Le-Duc, T., Ngo-Minh, H., Nguyen, Q. H., & Nguyen-Xuan, H. (2021). Optimal design of an Origami-inspired kinetic facade by balancing composite motion optimization for improving daylight performance and energy efficiency. *Energy*, *219*. https://doi.org/10.1016/j.energy.2020.119557

Lee, J. Y., Wargocki, P., Chan, Y. H., Chen, L., & Tham, K. W. (2020). How does indoor environmental quality in green refurbished office buildings compare with the one in new certified buildings? *Building and Environment*, *171*, 106677. https://doi.org/10.1016/j.buildenv.2020.106677

Li, X., Zhu, Y., & Zhang, Z. (2010). An LCA-based environmental impact assessment model for construction processes. *Building and Environment*, *45*(3), 766–775. https://doi.org/10.1016/j.buildenv.2009.08.010

Mahmoud, A. H. A., & Elghazi, Y. (2016). Parametric-based designs for kinetic facades to optimize daylight performance: Comparing rotation and translation kinetic motion for hexagonal facade patterns. *Solar Energy*, *126*, 111–127. https://doi.org/10.1016/j.solener.2015.12.039

Marceau, M. L., & VanGeem, M. G. (2008). Solar Reflectance Values of Concrete. *Concrete Lnternational*, *30*(8).

Matin, N. H., & Eydgahi, A. (2019). Technologies used in responsive facade systems: a comparative study. *Intelligent Buildings International*, 1–20. https://doi.org/10.1080/17508975.2019.1577213

Mehdizadeh, F., Ahadi, A. A., Masoumi, H. R., & Maleki, N. (2014). Learning lessons from heritage houses: making balance between optimum daylight and maximum thermal comfort Case Study: Rashidy historic house in hot-humid climate of Bushehr city, Iran. *International Journal of Architectural Engineering & Urban Planning*, *24*(2). https://www.researchgate.net/publication/271444533_Learning_lessons_from_heritage_houses_making_balance_between_optimum_daylight_and_maximum_thermal_comfort_Case_Study_Rashidy_historic_house_in_hot-humid_climate_of_Bushehr_city_Iran

Michael, A., Gregoriou, S., & Kalogirou, S. A. (2018). Environmental assessment of an integrated adaptive system for the improvement of indoor visual comfort of existing buildings. *Renewable Energy*, *115*, 620–633. https://doi.org/10.1016/J.RENENE.2017.07.079

Moloney, J. (2011). Designing kinetics for architectural facades: State change. In *Designing Kinetics for Architectural Facades: State Change*. Taylor and Francis. https://doi.org/10.4324/9780203814703

Müeller, H. F. O. (2013). Daylighting. *Sustainability, Energy and Architecture: Case Studies in Realizing Green Buildings*, 227–255. https://doi.org/10.1016/B978-0-12-397269-9.00009-8

Nabil, A., & Mardaljevic, J. (2005). Useful daylight illuminance: A new paradigm for assessing daylight in buildings. *Lighting Research and Technology*, *37*(1), 41–59. https://doi.org/10.1191/1365782805LI128OA

Nady, R. (2017). Dynamic Facades Environmental Control Systems for Sustainable Design. *Renewable Energy and Sustainable Development (RESD)*, *3*(1), 118–127. https://doi.org/10.21622/RESD.2017.03.1.118

Nagy, Z., Svetozarevic, B., Jayathissa, P., Begle, M., Hofer, J., Lydon, G., Willmann, A., & Schlueter, A. (2016). The Adaptive Solar Facade: From concept to prototypes. *Frontiers of Architectural Research*, *5*(2), 143–156.

https://doi.org/10.1016/J.FOAR.2016.03.002

Nielsen, M. V., Svendsen, S., & Jensen, L. B. (2011). Quantifying the potential of automated dynamic solar shading in office buildings through integrated simulations of energy and daylight. *Solar Energy*, *85*(5), 757–768. https://doi.org/10.1016/j.solener.2011.01.010

ODTÜ Kafeterya Müdürlüğü. (n.d.). *Tarihçe*. https://kafeterya.metu.edu.tr/tarihce

OneBuilding. (n.d.). *Climate.OneBuilding.Org*. http://climate.onebuilding.org/WMO_Region_6_Europe/TUR_Turkey/AN_Ankara/TUR_AN_Ankara_171300_TurTMY.zip

Pesenti, M., Masera, G., Fiorito, F., & Sauchelli, M. (2015). Kinetic Solar Skin: A Responsive Folding Technique. *Energy Procedia*, *70*, 661–672. https://doi.org/10.1016/J.EGYPRO.2015.02.174

Ramzy, N., & Fayed, H. (2011). Kinetic systems in architecture: New approach for environmental control systems and context-sensitive buildings. *Sustainable Cities and Society*, *1*(3), 170–177. https://doi.org/10.1016/j.scs.2011.07.004

Rizi, R. A., & Eltaweel, A. (2021). A user detective adaptive facade towards improving visual and thermal comfort. *Journal of Building Engineering*, *33*, 101554. https://doi.org/10.1016/j.jobe.2020.101554

Schielke, T. (2014). *Light Matters: Mashrabiyas - Translating Tradition into Dynamic Facades*. ArchDaily. https://www.archdaily.com/510226/light-matters-mashrabiyas-translating-tradition-into-dynamic-facades

Schwartz, Y., Raslan, R., & Mumovic, D. (2018). The life cycle carbon footprint of refurbished and new buildings – A systematic review of case studies. In *Renewable and Sustainable Energy Reviews* (Vol. 81, pp. 231–241). https://doi.org/10.1016/j.rser.2017.07.061

Shafaghat, A., & Keyvanfar, A. (2022). Dynamic facades design typologies, technologies, measurement techniques, and physical performances across thermal, optical, ventilation, and electricity generation outlooks. *Renewable and Sustainable Energy Reviews*, *167*, 112647. https://doi.org/10.1016/J.RSER.2022.112647

Shafavi, N. S., Tahsildoost, M., & Zomorodian, Z. S. (2020). Investigation of illuminance-based metrics in predicting occupants' visual comfort (case study: Architecture design studios). *Solar Energy*, *197*, 111–125. https://doi.org/10.1016/J.SOLENER.2019.12.051

Shahin, H. S. M. (2019). Adaptive building envelopes of multistory buildings as an example of high performance building skins. *Alexandria Engineering Journal*, *58*(1), 345–352. https://doi.org/10.1016/j.aej.2018.11.013

Sheikh, M. M. El. (2011). *Intelligent building skins: Parametric-based algorithm for kinetic facades design and daylighting performance integration* [University Of Southern California]. https://www.proquest.com/docview/884901432?pq-origsite=gscholar&fromopenview=true

Sheikh, W. T., & Asghar, Q. (2019). Adaptive biomimetic facades: Enhancing energy efficiency of highly glazed buildings. *Frontiers of Architectural Research*, *8*(3), 319–331. https://doi.org/10.1016/j.foar.2019.06.001

Song, Y., Mao, F., & Liu, Q. (2019). Human Comfort in Indoor Environment: A Review on Assessment Criteria, Data Collection and Data Analysis Methods. *IEEE Access*, *7*, 119774–119786. https://doi.org/10.1109/access.2019.2937320

Soyluk, A., & Sarıcıoğlu, P. (2015). Kinetik Mimarlıkta Cephede Origami ve Akıllı Malzeme Kullanımı. *Mimaran*, *9*(12), 62–66.

T.C. Ankara Valiliği. (n.d.). *Genel İklim Durumu*. http://ankara.gov.tr/iklimi#:~:text=Genel İklim Durumu&text=Kara ikliminin hüküm sürdüğü bu,ve güney kesimlerde farklılık gösterir.

Tabadkani, A., Banihashemi, S., & Hosseini, M. R. (2018). Daylighting and visual comfort of oriental sun responsive skins: A parametric analysis. *Building*

Simulation 2018 11:4, *11*(4), 663–676. https://doi.org/10.1007/S12273-018-0433-0

Tabadkani, A., Roetzel, A., Li, H. X., & Tsangrassoulis, A. (2021). Design approaches and typologies of adaptive facades: A review. In *Automation in Construction* (Vol. 121, p. 103450). Elsevier B.V. https://doi.org/10.1016/j.autcon.2020.103450

Tabadkani, A., Valinejad Shoubi, M., Soflaei, F., & Banihashemi, S. (2019). Integrated parametric design of adaptive facades for user's visual comfort. *Automation in Construction*, *106*, 102857. https://doi.org/10.1016/j.autcon.2019.102857

Teamah, H. M., Kabeel, A. E., & Teamah, M. (2022). Potential retrofits in office buildings located in harsh Northern climate for better energy efficiency, cost effectiveness, and environmental impact. *Process Safety and Environmental Protection*, *162*, 124–133. https://doi.org/10.1016/J.PSEP.2022.03.067

United States Green Building Council. (n.d.). *Daylight*. https://www.usgbc.org/credits/eq8

Wu, W., & Ng, E. (2016). A review of the development of daylighting in schools. *Http://Dx.Doi.Org/10.1191/1477153503li072oa*, *35*(2), 111–124. https://doi.org/10.1191/1477153503LI072OA

Yi, Y. K., Sharston, R., & Barakat, D. (2019). Auxetic Structures and Advanced Daylight Control Systems. *Journal of Facade Design and Engineering*, *7*(1), 63–74. https://doi.org/10.7480/JFDE.2019.1.2620

Zhou, Z., Zhang, S., Wang, C., Zuo, J., He, Q., & Rameezdeen, R. (2016). Achieving energy efficient buildings via retrofitting of existing buildings: A case study. *Journal of Cleaner Production*, *112*, 3605–3615. https://doi.org/10.1016/j.jclepro.2015.09.046

Zolfagharian, S., Nourbakhsh, M., Irizarry, J., Ressang, A., & Gheisari, M. (2012).

Environmental Impacts Assessment on Construction Sites. *Construction Research Congress 2012*, 1750–1759. https://doi.org/10.1061/9780784412329.176

Zuk, W., & Clark, R. H. (1970). *Kinetic Architecture*. Van Nostrand Reinhold Company.

APPENDICES

A. PICTURES OF THE METU CAFETERIA BUILDING

Figure A.1 Exterior view of the south section of the METU Cafeteria Building, pictured by the author

Figure A.2 Exterior view from the west facade of the south section of the METU Cafeteria Building, pictured by the author

Figure A.3 Exterior view of the east section of the METU Cafeteria Building, pictured by the author

Figure A.4 Exterior view of the north section of the METU Cafeteria Building, pictured by the author

Figure A.5 Exterior view of the north section of the METU Cafeteria Building, pictured by the author

Figure A.6 Interior view of the first floor south section of the METU Cafeteria Building, pictured by the author

Figure A.7 Interior view of the ground floor east section of the METU Cafeteria Building, pictured by the author

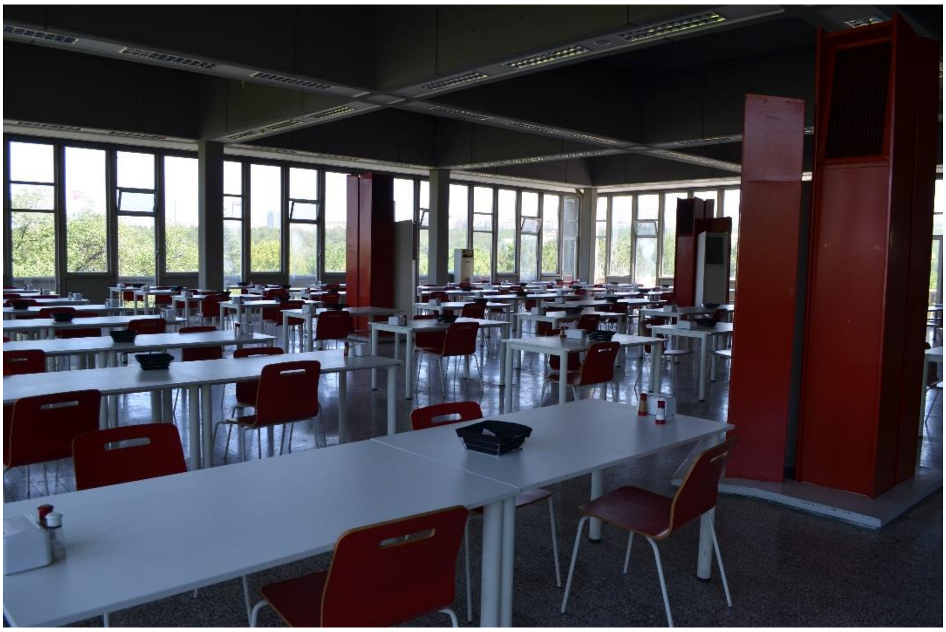

Figure A.8 Interior view of the first floor east section of the METU Cafeteria Building, pictured by the author

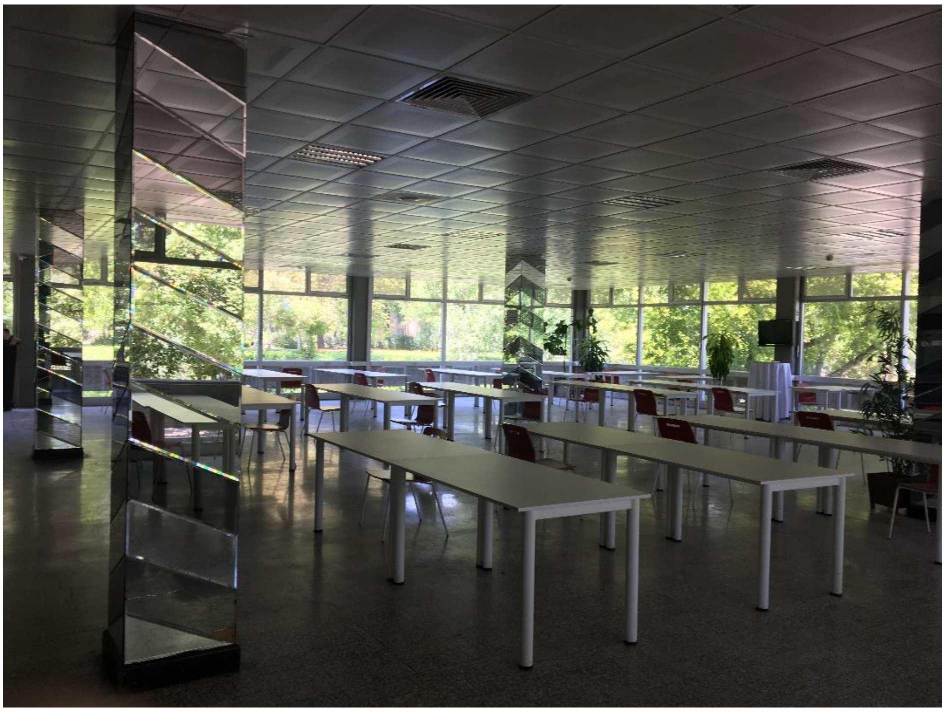

Figure A.9 Interior view of the ground floor north section of the METU Cafeteria Building, pictured by the author

B. DRAWINGS OF THE SOUTH SECTION OF THE METU CAFETERIA BUILDING

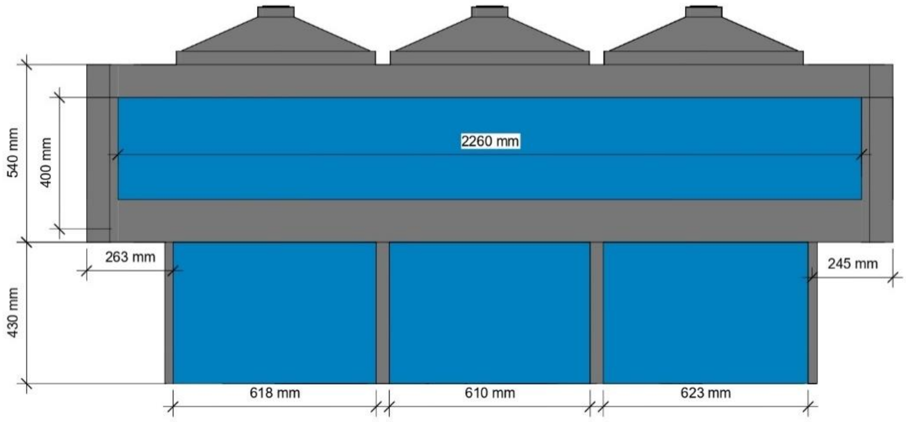

Figure B.1 South facade drawing of the south section of METU Cafeteria Building

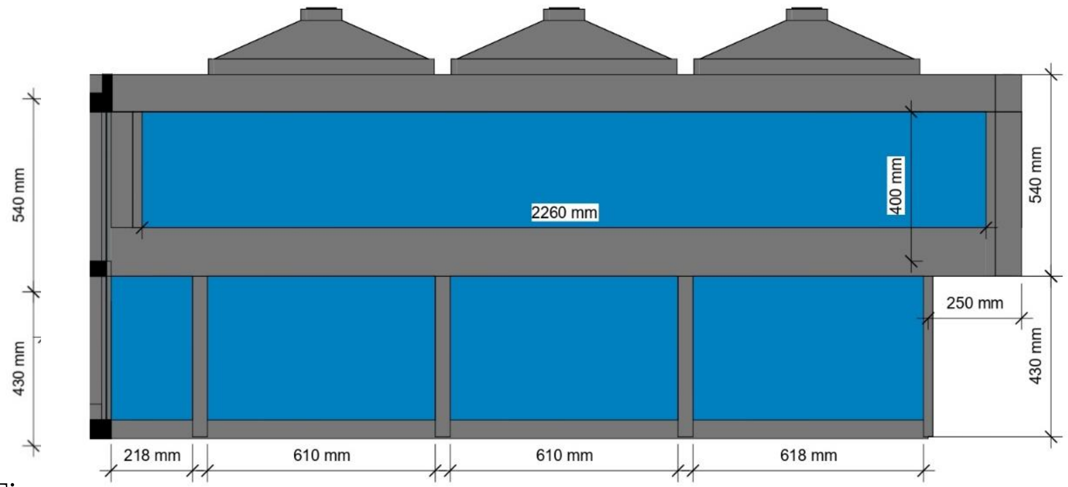

Figu

Figure B.3 West facade drawing of the south section of METU Cafeteria Building

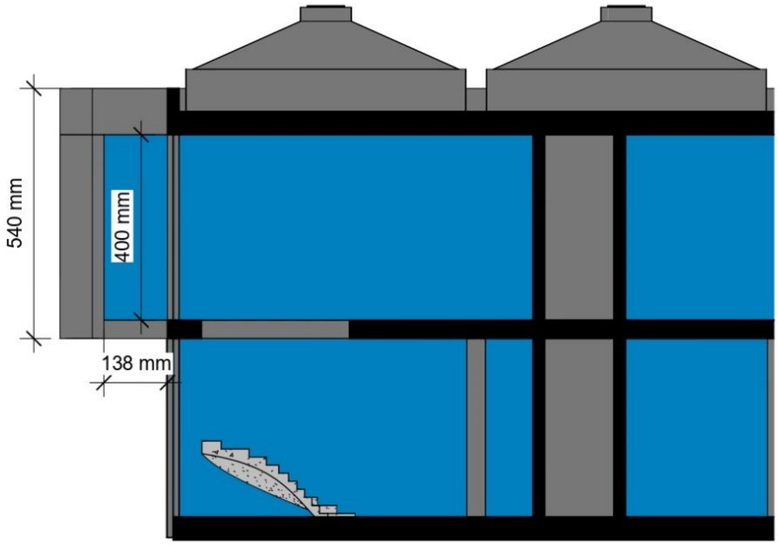

Figure B.4 North facade drawing of the south section of METU Cafeteria Building